THE FUNCTION OF RKIP IN

CLEAR CELL RCC TUMOURIGENESIS

THE FUNCTION OF RKIP IN THE TUMOURIGENESIS OF CLEAR CELL RENAL CELL CARCINOMA

By

BRIANNE HILL, B.Sc. (Hons.)

A Thesis

Submitted to the School of Graduate Studies

In Partial Fulfilment of the Requirements

for the Degree

Master of Science

McMaster University

MASTER OF SCIENCE (2011) McMaster University

(Medical Sciences) Hamilton, Ontario

TITLE: The Function of RKIP in the Tumourigenesis of Clear Cell Renal Cell Carcinoma

AUTHOR: Brianne Hill, B.Sc. (Hons.) (University of Toronto)

SUPERVISOR: Dr. Damu Tang

NUMBER OF PAGES: xiv, 120

ABSTRACT

Despite clear cell renal cell carcinoma (ccRCC) being the most common and one of the most lethal forms of RCC, our understanding of ccRCC tumourigenesis remains limited. To identify factors contributing to ccRCC formation, we have found that raf kinase inhibitor protein (RKIP) is a candidate tumour suppressor of ccRCC. This is consistent with publications implicating that RKIP possesses tumour suppression functions in several human cancers. However, whether RKIP suppresses ccRCC tumorigenesis has yet to be determined. This thesis was therefore undertaken to examine the role of RKIP in the tumourigenesis of ccRCC as well as to gain knowledge about this understudied area of kidney cancer research. Upon examination of more than 600 patients with ccRCC in several independent patient cohorts, levels of RKIP protein are significantly reduced in more than 80% of ccRCC tumours in comparison to the adjacent non-tumour kidney or normal kidney tissues. This observed magnitude of RKIP reduction strongly suggests that RKIP is an important tumour suppressor of ccRCC. Supporting this concept is observations that ectopic expression of RKIP inhibited A498 and 786-O ccRCC cell invasion. Conversely, knockdown of RKIP in A498 and 786-O cells enhanced the invasion ability of those cells. Additionally, the progression of ccRCC into advanced tumour stages and tumour grades is correlated with a reduction in RKIP protein. This reduction of RKIP protein levels is more apparent in metastasized ccRCC tumours in which all tumours were negative for RKIP protein expression in comparison to the matched organ-confined tumours. To date there have been no reports investigating

the role of RKIP in renal cell carcinoma, our results demonstrate a strong relationship between RKIP reduction and progression of this often fatal disease.

ACKOWLEDGMENTS

First off I would like to thank my supervisor, Dr. Damu Tang for agreeing to take me on as a Masters student. Throughout this process, you were always there for me to go to for insight, patience and support. Your ability to always see a positive regardless of the result is very much appreciated and kept me from dwelling on setbacks. I would also like to thank everyone in the Tang lab for their guidance and technical support over the last few years. Thank you to all lab members of the surrounding labs who were always willing to help and answer any of my questions.

Judy, Jason - thank you for your constant support and encouragement over the past three years. Our countless lunches and dinners meant so much to me and kept us sane! I don't know what I would have done without you both going through this experience with me.

I also have to thank my family for none of this could have been possible without them. Thank you for your constant support and encouragement. Mom and Dad - thank you for always being there for me no matter what. I know I may have made things difficult over the years and may have taken out a few bad days on you, but your ability to calm me down and put things into perspective truly amazes me. Even though you might not understand all the 'science' terminology I use, you two are still willing to listen and help work things out. I greatly appreciate everything. The two of you make me strive to be the best I can be. To my sister, Amiee words can't even begin to describe how much you mean to me and everything you do for me on a daily basis. Knowing that I have

someone like you to talk to at anytime means the world to me and I don't know how I would have gotten through the many ups and downs in life without your endless support. Just knowing that you are always there for me is greatly appreciated. From our serious 'I need to sort out my life' chats to a quick email here and there – Thank you!

TABLE OF CONTENTS

LIST OF TABLES

LIST OF FIGURES

Section I: Introduction

Section III: Materials and Methods

Section V. Results

LIST OF ABBREVIATIONS

ANGPTL4	Angiopoietin-like 4
ANK	Adjacent non tumour kidney tissue and normal tissue
ccRCC	Clear cell renal cell carcinoma
EGR1	Early growth response 1
EMT	Epithelial-mesenchymal transition
EPO	Erythropoietin
ERK1/2	Extracellular signal regulated kinase 1 and 2
FBS	Fetal bovine serum
FDA	Food and Drug Administration
GP	Gag-pol expression vector
GPCR	G protein coupled receptor
GRK2	G protein coupled receptor kinase 2
HCNP	Hippocampal cholinergic meurostimulating peptide
HIFα	Hypoxia-inducible factor α
IHC	Immunohistochemisty
IκB	Inhibitor of κB

IKK	I kappa B kinase
IKKα	IκB kinase α
IKKβ	IκB kinase β
LeTx	Anthrax lethal toxin
MAPK	Mitogen activated protein kinase
MAPKK	MAP kinase kinase
MEK	Mitogen activated protein kinase
MKK	Mitogen activated protein kinase kinase
MMP	Matrix metalloproteinases
mTOR	Mammalian target of rapamycin
MUC12	Mucin 12 cell surface assoctiated
NFκB	Nuclear factor kappa B
NID2	Nidogen 2
NIK	NFκB inducing kinase
PBS	Phosphate buffered saline
PAK	p21 activated kinase

PDGF	Platelet-derived growth factor
PEBP	Phosphatidylethanolamine binding protein
PKC	Protein kinase C
POSTN	Periostin
RCC	Renal cell carcinoma
RKIP	Raf kinase inhibitor protein
RTK	Receptor tyrosine kinase
S153	Serine 153
TAK1	TGF-B activated kinase 1
TGF-α	Transforming growth factor α
TMA	Tissue microarray
VHL	von Hippel-Lindau
VEGF	Vascular endothelial growth factor
VSV-G	Vesicular stomatitis virus G protein

I. INTRODUCTION

1.1. Renal Cell Carcinoma

Renal cell carcinoma (RCC) accounts for approximately 3-4% of all cancers with the highest rates found in North Americans and Scandinavians (Rini *et al.,* 2009; Motzer *et al.,* 1996; Jemal *et al.,* 2010). Renal cell carcinoma arises from the epithelium of the renal tubules (Fletcher *et al.,* 2000). The Canadian Cancer Society estimates that in 2010 there will be 4800 new cases of kidney cancer in Canada with 1650 (34.4%) Canadians dying from this disease (Canadian Cancer Society 2010). In Canada, kidney cancer is the 10th most common newly diagnosed cancer and the 13th leading cause of cancer deaths (Canadian Cancer Society, 2010). In the United Sates there is estimated to be 58,240 new cases in 2010 and 13,040 (22.4%) deaths (Jemal *et al.,* 2010), while worldwide estimates are 289,000 new cases per year with 102,000 (35.3%) deaths each year (Rini *et al.,* 2009). The identified risk factors for RCC are smoking, obesity, hypertension and genetics (Cohen and McGovern, 2005; Linehan and Zbar, 2003; Linehan, 2006; Linehan *et al.,* 2007). Genetics is a major risk factor for development of ccRCC and will be discussed in greater detail in the following sections.

RCC is associated with a high rate of metastasis and therefore a high rate of mortality. Once kidney cancer reaches the metastatic disease state it is often fatal (Pantuck *et al.,* 2001). RCC is more common in men than women with incidence rates being twice as high for men (Motzer *et al.,* 1996). Patients diagnosed with early organ confined tumours have a 5 year survival rate of 80-90%, those diagnosed with locally

advanced disease have a 50-60% 5 year survival rate and those individuals diagnosed with metastatic disease have a 5 year survival rate of only 5-10% (Brugarolas *et al.,* 2007). Although early diagnosis is a vital aspect in control of RCC, this is a very challenging task, which is in part due to the lack of warning signs. A high proportion of patients, therefore, present with metastatic disease at diagnosis and metastatic RCCs are, unfortunately, incurable (Motzer *et al.,* 1996; Brugarolas *et al.,* 2007). Additionally, the diverse clinical manifestations of RCC, if present, make it hard for diagnosis (Nelson *et al.,* 2007). The classic signs and symptoms of RCC include flank pain, haematuria and palpable abdominal mass (Nelson *et al.,* 2007). The incidence of RCC cases being diagnosed has been increasing mainly due to improvements in medical imaging especially advances in ultrasound, CT and MRI scans (Drucker *et al.,* 2005). However, most presentations of RCC are found incidentally due to the routine use of abdominal imaging in medical diagnostics (Rini *et al.,* 2009). Even though more and more cases are being diagnosed in their earliest stages, 40 to 45% of patients still present with locally advanced to metastatic RCC (Nelson *et al.,* 2007). Collectively ⅓ of RCC patients will develop metastatic spread with the most common sites being the lungs, lymph nodes, brain, bone and liver (Drucker *et al.,* 2005). Currently, there are no effective options available to treat metastatic RCC and unfortunately the median survival is only 13 months for these patients (Drucker *et al.,* 2005; Motzer *et al.,* 1996; Cohen and McGovern, 2005).

Up until 2005, the only Food and Drug Administration (FDA) approved treatment for RCC was high dose interleukin 2 (Brugarolas *et al.,* 2007). Interferon-α (INFα),

although not approved by the FDA, and interleukin 2 have been the standard of care for those individuals with advanced and metastatic RCC (Grandinetti and Goldspiel, 2007). Interleukin 2 and interferon-α based iummunotherapy offers only modest benefits, extending median survival for 3.8 months and is often associated with severe side effects (Coppin *et al.,* 2005). Since then, other multi-kinase inhibitors and antibodies have been approved for treatment. These include, but are not limited to Sorafenib, Sunitinib, Temsirolimus, and Bevacizumab as first and second line treatment options for patients with advanced RCC (Grandinetti and Goldspiel, 2007; Bracarda *et al.,* 2007; Thompson Coon *et al.,* 2009; Yang *et al.,* 2003). Sorafenib and Sunitinib are small molecule multi-kinase inhibitor drugs which target Ras-Raf/MEK/ERK, vascular endothelial growth factor (VEFG) and hypoxia-inducible factor (HIF) pathways known to be involved in the pathology of RCC (Costa *et al.,* 2007; Grandinetti and Goldspiel, 2007). Temsirolimus inhibits mammalian target of rapamycin (mTOR) a serine/threonine kinase important in regulation of cell proliferation and division (Costa *et al.,* 2007). Bevacizumab is a recombinant monoclonal anti-VEGF antibody which inhibits VEGF from binding to its receptors, preventing angiogenesis and hence tumour growth and proliferation (Thompson Coon *et al.,* 2009; Yang *et al.,* 2003). These new agents specifically target growth factor receptors known to be activated in RCC and are able to extend progression free survival for several months when compared to interferon based treatment (Thompson Coon *et al.,* 2009). However, metastatic RCC still remains incurable despite these recent advances.

RCC consists of multiple subgroups of tumours (Motzer *et al.,* 1996). Its classification is based on tumour location in the nephron and on the cell type that gave rise to the tumour (Drucker *et al.,* 2005). RCC can be divided into 6 sub types (Table 1): clear cell, papillary (chromophillic), chromophobic, oncocytoma, collecting duct and unclassified (Motzer *et al.,* 1996). Clear cell RCC (ccRCC) accounts for 75 to 85% of all RCC cases (Motzer *et al.,* 1996). Clear cell RCC tumours usually arise from epithelial cells of the proximal convoluted tubule and are characterized by a loss of genetic material in chromosome section 3p which contains the von Hippel-Lindau gene (VHL) (Fletcher *et al.,* 2000; Nelson *et al.,* 2007). One histological feature of ccRCC is its clear cytoplasm. This is due to the high lipid content found in the cytoplasm which, during histological preparation the lipids are dissolved leaving behind a clear cytoplasm (Rini *et al.,* 2009). Chromophillic (papillary) RCC accounts for 10-15% of RCC cases. Papillary RCC arises in the distal convoluted tubule and this type of RCC is less likely to metastasize (Nelson *et al.,* 2007). Genetic studies of these tumours reveal chromosomal gains in chromosomes 7 and 17 (Nelson *et al.,* 2007). These gains are usually in the form of tri or tetra chromosome increases. Two subtypes of papillary RCC exist; type 1 and type 2 with type 1 having a better prognosis compared to type 2 (Nelson *et al.*, 2007). Chromophobic RCC accounts for roughly 5% of RCC cases. Chromophobic tumours arise in the renal parenchyma specifically in the type B intercalated cells (Cohen and McGovern, 2005). The genetic hallmark of these tumours is the loss of multiple chromosomes including chromosomes Y, 1, 2, 6, 10, 13, 17 and 21 (Rini *et al.,* 2009). Oncocytoma RCC usually presents as benign tumours and are mainly found because

RCC was suspected and a renal biopsy was performed (Cohen and McGovern, 2005). Collecting duct RCC accounts for less than 1% of all RCC cases (Nelson *et al.,* 2007). These tumours have been found to be aggressive (Nelson *et al.,* 2007).

Table 1: Summary of RCC classification types

Type of RCC	**Percentage of total RCC cases**	**Location**	**Characteristics**
Clear Cell	75-85	Proximal convoluted tubule	Genetic loss in chromosome 3
Papillary (chromophillic)	10-15	Distal convoluted tubule	Chromosomal gains in chromosomes 7 and 17
Chromophobic	5	Renal parenchyma	Loss of multiple chromosomes
Oncocytoma	-	-	Benign tumour
Collecting Duct	1	Collecting duct	Aggressive tumours

Several autosomal dominant and familial syndromes have been linked to the development of RCC such as von Hippel-Lindau, hereditary papillary renal carcinoma, hereditary leiomyomatosis renal cell carcinoma, Birt-Hogg-Dube and tuberous sclerosis (Rini *et al.,* 2009). These syndromes account for 2-3% of RCC cases (Rini *et al.,* 2009). von Hippel-Lindau syndrome is highly penetrant and perhaps the most recognized syndrome. von Hippel-Lindau disease results in the formation of several vascular tumours including clear cell RCC, haemangioblastomas of the CNS and pheochromocytoma (Rini *et al.,* 2009). The von Hippel-Lindau (VHL) gene is a tumour suppressor gene that has been implicated in the development of this disease (Rini *et al.,* 2009). The VHL gene was mapped on chromosome 3 (Rini *et al.,* 2009). von Hippel-Lindau syndrome patients inherit a defect in one of their VHL alleles and patients who

develop vascular tumours acquire a defect in the other VHL allele in that affected organ (Rini *et al.,* 2009). VHL is involved in the cellular pathway that controls gene expression in response to cellular oxygen availability (Bruarolas *et al.,* 2007) though regulation of the hypoxia inducible factor α (HIFα) transcription factor (Bruarolas *et al.,* 2007). VHL protein is part of the ubiqutin ligase complex which tags HIFα for degradation by adding polyubiquitin to the α-subunit (Kondo and Laelin, 2001). Loss of VHL leads to an accumulation of HIFα, which transactivates a variety of growth factors including VEGF, erythropoietin (EPO), transforming growth factor-α (TGF-α) and platelet-derived growth factor (PDGF). These changes collectively promote tumour cell proliferation, survival and angiogenesis (Grandinetti and Goldspiel, 2007). Patients with von Hippel-Lindau syndrome develop ccRCC 40% of the time (Motzer *et al.,* 1996). Interestingly, approximately 60% of sporadic ccRCCs are associated with a defect in both alleles of the VHL gene (Nelson et al., 2007; Cohen and McGovern, 2005; Rini *et al.,* 2009).

1.2. RCC and MAPK Signaling

The mitogen activated protein kinase (MAPK) signaling pathway regulates several different biological processes involved in cell differentiation, proliferation and survival (Zeng *et al.,* 2008). Growth factors activate Ras via receptor tyrosine kinases (RTKs), resulting in a conformational change which opens up a binding pocket for Raf-1 (Karp 2005). Raf-1 is recruited to the plasma membrane where it becomes activated by Ras (Karp 2005). Raf-1, a serine/threonine kinase, subsequently activates a MAP kinase

kinase (MAPKK) MAPK extracellular signal regulated kinase kinase (MEK) (Weinberg 2007). MEK then phosphorylates and activates the extracellular signal-regulated kinases 1 and 2 (ERK1 and ERK2) MAP kinases (MAPK) (Weinberg 2007), resulting in activating downstream events including transcription factors (Karp 2005; Weinberg 2007). Consistent with this pathway being involved in multiple cellular processes, dis-regulation in the pathway contributes to approximately 20-30% of all human cancers (Huang *et al.,* 2008; Reddy *et al.,* 2003; Gollob *et al.,* 2006).

The MEK-ERK cascade has been implicated in tumourigenesis and tumour metastasis. Increases in ERK activation were observed in many human tumours (Huang *et al.,* 2008). These include tumours of the breast, brain, kidney, colon and lung (Sivaraman *et al.,* 1997; Mandell *et al.,* 1998; Hoshino *et al.,* 1999; Salh *et al.,* 1999; Huang *et al.,* 2008). Studies by Oka *et al,* 1995, demonstrated that constitutive activation of the MAPK pathway occurred in the majority of RCC cases. Changes in the components of the MAPK pathway, including phosphorylation of Raf-1 and MEK as well as overexpression of MEK, were detected in more than 50% of RCC cases examined (Oka *et al.,* 1995). Moreover, elevated activation of MAPKs correlates with histological grade of RCC tumours and MAPK activation occurs more frequently in high grade RCCs, suggesting that increased activation of MAPK could be associated with greater malignancy potential (Oka *et al.,* 1995). Recent studies showed that the administration of anthrax lethal toxin (LeTx) was able to decrease RCC growth and prevent tumour vascularisation *in vivo* (Huang *et al.,* 2008). LeTx blocks multiple MAPK signaling pathways through cleavage of the NH_2 termini on MAPK kinases (MKKs) resulting in

loss of kinase function. This loss of kinase activity prevented downstream proteins from being phosphorylated including ERK (Huang *et al.,* 2008). LeTx inhibited RCC growth *in vitro* and RCC tumorigenesis in mice (Huang *et al.,* 2008). Therefore, MKKs are targets in anticancer therapies (Huang *et al.,* 2008). This is attractive, as prevention of MAPK signaling could be blocked regardless of upstream oncogenic activity.

1.3. Raf Kinase Inhibitor Protein (RKIP)

Considering the importance of the Ras/MAPK signaling pathway in multiple biological events, it comes as no surprise that this pathway is under tight regulatory control (Trakul and Rosner, 2005). Raf-1 protein appears to be a good target for this regulation as Raf-1 binding to Ras is the rate limiting step in the activation of this signaling cascade (Trakul *et al.,* 2005). Aiming in finding proteins that inhibit Raf-1 function, a yeast two hybrid screen was used (Yeung *et al.,* 1999). Among the 500,000 clones in the human T-cell cDNA library screened, Raf kinase inhibitor protein (RKIP) or PEBP1 was identified, which belongs to phosphatidylethanolamine binding protein (PEBP) family (Yeung *et al.,* 1999). RKIP was initially purified from bovine brain as a soluble basic cytosolic protein of molecular weight 23kDa with organic anion binding abilities (Bernier *et al.,* 1984). RKIP was later classified as a member of the PEBP family due to its ability to bind phospholipids (Bernier *et al.,* 1986).

RKIP is widely expressed in many tissues during development and exists most abundantly in the testis, brain, epididymis, liver and kidney (Frayne *et al.,* 1998; Frayne

et al., 1999; Zeng *et al.*, 2008). RKIP is highly conserved and has no significant homology to any other protein families (Keller *et al.,* 2004b). Structurally, X-ray crystallography studies revealed that RKIP is characterized by a large central β-sheet and a smaller β-sheet consisting of anti parallel strands which constitute a β-fold and a αβα motif located near the C terminus (Rath *et al.,* 2008; Banfield *et al.,* 1998; Banfield and Brady, 2000). A highly conserved phosphate binding site is found within the large central β-sheet structure (Banfield *et al.,* 1998; Banfield and Brady, 2000). RKIP has two conserved regions (CR1 and CR2) that form part of the ligand binding domain and these conserved regions are unique to PEBP protein family members (Banfield *et al.,* 1998). Residues 2-12 of the N-terminal region of RKIP are identical to the hippocampal cholinergic neurostimulating peptide (HCNP), a natural cleavage peptide (Trakul and Rosner, 2005). This peptide plays a role in neuronal development and differentiation but it remains unclear if RKIP is cleaved to form this peptide (Trakul and Rosner 2005, Zeng *et al.,* 2008).

There is emerging evidence to support a role of RKIP in several multiple signal transduction pathways that manage cell growth, differentiation, apoptosis and migration (Zeng *et al.,* 2008). These pathways include those of MAPK, G protein coupled receptor (GPCR) and NFκB (Zeng *et al.,* 2008). RKIP modulates these events via binding to Raf-1, B-Raf, MEK, G protein-coupled receptor kinase 2 (GRK2), NFκB inducing kinase (NIK), TGF-B activated kinase 1 (TAK1) and I-kappa B kinase (IKK) (Zeng *et al.,* 2008). The phosphorylation state of RKIP and its interacting proteins play a role in determining the pathways that RKIP can regulate (Zeng *et al.,* 2008).

1.4. RKIP and the MAPK Pathway

Deregulation of the Raf/MEK/MAPK signaling pathway contributes to tumorigenesis. One of the potential mechanisms responsible for activation of the MAPK pathway in cancer is to impair RKIP-mediated inhibition of the MAPK pathway. Yeung *et al*, 1999, were the first to demonstrate that RKIP can inhibit MAPK signaling (Fig 1). RKIP binds to Raf-1, which disrupts the physical interaction between Raf-1 and MEK (Yeung *et al.*, 2000). Conversely, compromising RKIP function by using either specific antibodies or antisense RNA resulted in activation of MEK and ERK (Yeung *et al.*, 1999). RKIP also inhibits the activation Raf-1 by blocking the phosphorylation of critical residues (Serine338 and Tyrosine341) on Raf-1, which is performed by p21 activated kinase (PAK) and Src kinases (Trakul and Rosner, 2005; Trakul *et al.*, 2005). RKIP can act on Raf-1 before Raf-1 is recruited to the membrane, which prevents Raf-1 from interacting with PAK thus, inhibiting PAK-mediated phosphorylation of Raf-1 (Trakul and Rosner, 2005; Trakul *et al.*, 2005). RKIP was also found to act like a competitive inhibitor of MEK phosphorylation (Yeung *et al.*, 2000). RKIP is thought to reduce the binding affinity between Raf-1 and MEK via the binding to Raf-1 and MEK (Yeung *et al.*, 2000). This is due to the fact that Raf-1 and MEK have overlapping RKIP binding sites, therefore the binding of RKIP to either of these proteins prevents Raf-1 and MEK from associating with each other and hence the activation of MEK and downstream signaling (Yeung *et al.*, 2000). Raf-1 binds to RKIP through a 24 amino acid region in its N terminus that contains the Ser338 and Tyr341 phosphorylation sites (Park *et al.*, 2006). Phosphorylation at these two residues increased the affinity of this peptide to associate

with RKIP (Park *et al.,* 2006). This implies that phosphorylation of the N terminus of Raf-1 serves as a docking site for RKIP to bind (Park *et al.,* 2006). Rath *et al,* 2008 further showed that it is the conserved phosphoryl-ligand binding pocket of RKIP that binds to Raf-1. Single mutations to the binding pocket reduced RKIP's ability to inhibit Raf-1 activation (Rath *et al.,* 2008). Moreover, this binding pocket binds to the phosphorylated N terminal region on Raf-1 (Rath *et al.,* 2008). Taken together, the above observations outline a model, in which phosphorylation of RKIP by mitogen stimulation results in its dissociation from Raf-1 and the phosphorylation of the N terminal region of Raf-1 reassumes the association (Park *et al.,* 2006).

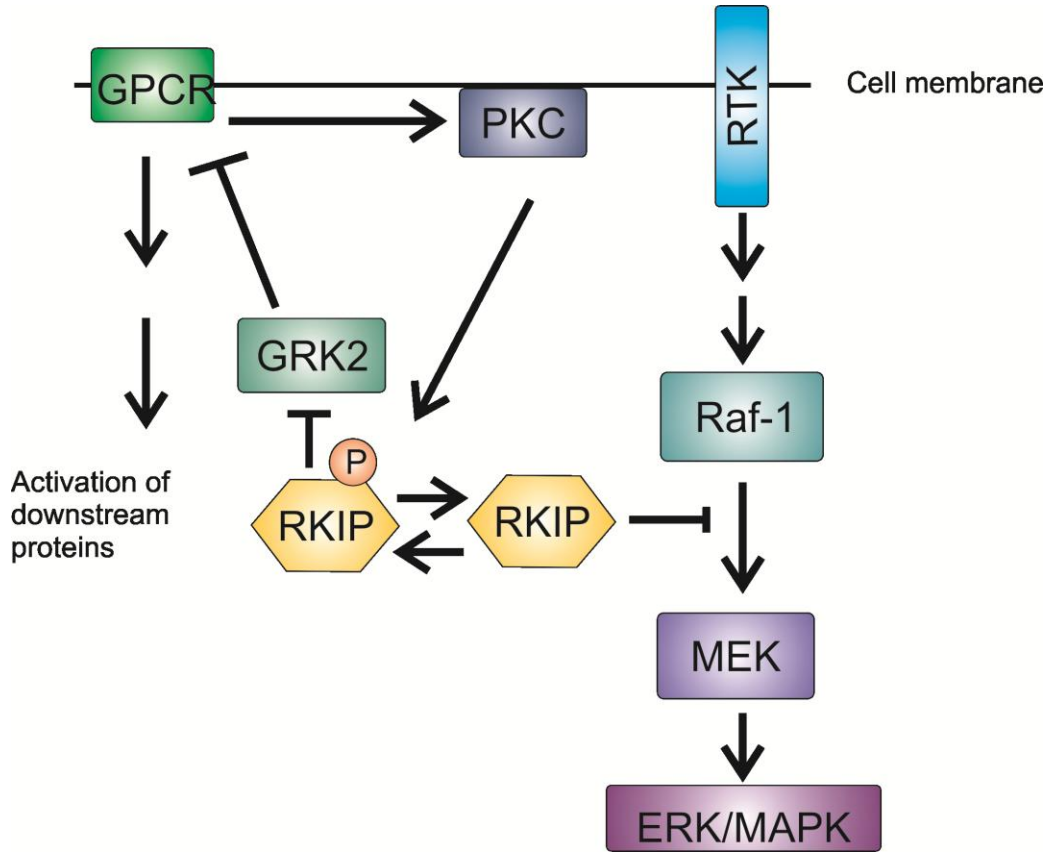

Figure 1: A model shows the regulatory roles of RKIP to the GPCR and MAP kinase pathways. RKIP binding to Raf-1 prevents Raf-1 from activating MEK which in turns inhibits MEK from activating ERK. When RKIP is phosphorylated on S153 by Protein kinase C, it induces a 'switch' in RKIP target binding, causing RKIP to disassociate from Raf-1. This enables RKIP to bind to GRK2, which reduces GRK2 inhibitory function in G-protein coupled receptor signaling.
RTK – receptor tyrosine kinase, MEK- mitogen extracellular kinase, ERK – extracellular signal-related kinase, MAPK – mitogen activated protein kinase, PKC – protein kinase C, GPCR – G-protein coupled receptor, GRK2 – G-protein coupled receptor kinase 2.
Adapted from – Kolch *et al*, 2005.

1.5. RKIP and G-protein Coupled Receptor Signaling

G protein coupled receptors (GPCRs) are involved in the regulation of a variety of vital cellular processes including neurotransmission, hormone and enzyme release, blood pressure regulation and inflammation (Zeng *et al.*, 2008). Stimulation by neurotransmitters, hormones or growth factors causes GPCRs to become activated (Odabaei *et al.*, 2004). This allows the Gα subunit to separate from Gβγ subunits. These two subunits can now stimulate other downstream effectors (Odabaei *et al.*, 2004). In order to prevent uncontrolled cell signaling this pathway needs to be under tight regulatory control. G-protein coupled receptor kinase 2 (GRK-2) is a critical negative feedback inhibitor of this pathway (Fig 1) (Keller *et al.*, 2004a). GRK-2 shuts down GPCR signaling by phosphorylating activated GPCRs resulting in internalization of these receptors (Keller *et al.*, 2004a, Zeng *et al.*, 2008). RKIP has been found to act as an inhibitor of GRK-2 action through its binding to the N terminal region on GRK-2 (Lorenz *et al.*, 2003). RKIP can be phosphorylated on Serine153 by protein kinase C. This induces a 'switch' in RKIP target binding (Granovsky and Rosner 2008). Phosphorylation of Serine153 causes RKIP to be released from Raf-1 enabling RKIP to bind to GRK-2, potentiating G-protein signaling (Fig 1) (Zeng *et al.*, 2008). This switch of RKIP from Raf-1 to GRK-2 demonstrates cross talk between two different signaling pathways with RKIP being the mediator of this cross talk (Odabaei *et al.*, 2004).

1.6. RKIP and NFκB Signaling

The Nuclear factor kappa B (NFκB) transcription factor family are involved in controlling the activation of immune receptors, cytokines, cell proliferation and survival in response to activating stimuli (Odabaei *et al.,* 2004; Tang *et al.,* 2010). RKIP has been shown to interact with the NFκB core kinase complex specifically TGF-β activated kinase (TAK1), NFκB inducing kinase (NIK), IκB kinase-α (IKKα) and IκB kinase-β (IKKβ) (Klysik *et al.,* 2008; Tang *et al.,* 2010). TAK1 and NIK are upstream regulators of the IKK complex. IKKα and IKKβ are the kinase subunits of IKK complex (Tang *et al.,* 2010). Recently it was shown that RKIP is able to interact with TRAF6, another upstream activator of the IKK complex, leading to the observation that RKIP acts more like a scaffold protein because of its ability to interact with many different components in the NFκB pathway (Tang *et al.,* 2010). Previously it was thought that RKIP inhibited NFκB signaling through the binding of RKIP to TAK1 and NIK preventing IKK from activating IκB (Fig 2) (Klysik *et al.,* 2008). This caused NFκB to remain sequestered to IκB preventing NFκB from relocating to the nucleus where it can activate many different target genes (Klysik *et al.,* 2008). Tang *et al,* 2010 propose that by acting as a scaffolding protein, RKIP interacts with many different components of the NFκB pathway allowing for the formation of the IKK complex which in turn leads to the phosphorylation and degradation of IκB, releasing NFκB. Surprisingly, it has been demonstrated that RKIP actually has an overall inhibitory effect on the NFκB pathway, possibly caused by RKIP enhancing a negative regulatory feedback loop in which RKIP induces the rapid synthesis and expression of NFκB activation inhibitors (Tang *et al.,*

2010). Much more research is needed to further elucidate RKIP`s exact role in inhibiting this pathway.

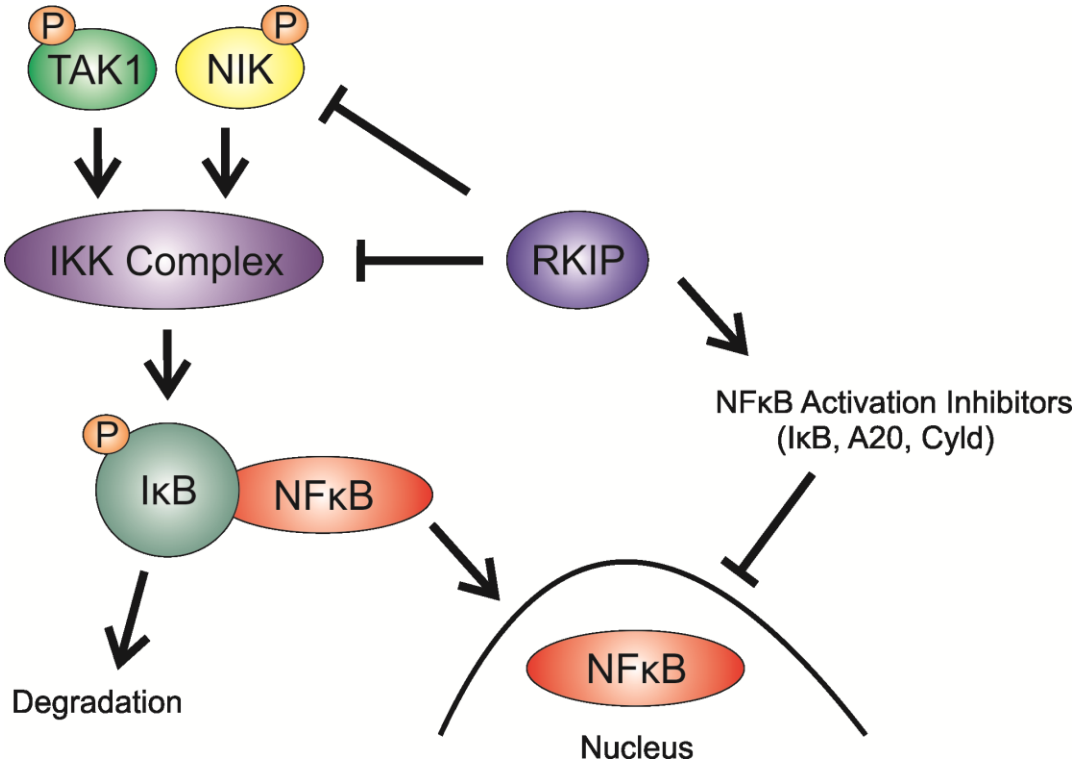

Figure 2: A model showing RKIP-mediated inhibition of NFκB signaling. Klysik *et al*, 2008 proposed that RKIP inhibits NFκB signaling through its binding TAK1 and NIK. This causes NFκB to remain sequestered to IκB preventing NFκB from relocating to the nucleus where it can activate many different target genes. Whereas, Tang *et al*, 2010 propose that by acting as a scaffolding protein, RKIP interacts with many different components of the NFκB pathway. This attenuates the IKK complex-mediated phosphorylation and degradation of IκB, and thereby compromising the release of NFκB from IκB. NFκB – Nuclear factor kappa B, IκB – Inhibitor of κB, IKK – IκB kinase, NIK – NFκB inducing kinase, TAK1 – TGF-β activated kinase. Adapted from – Klysik *et al*, 2008.

1.7. RKIP and the Cell Cycle

RKIP has also been shown to play a role in the regulation of the cell cycle. One key step in the cell cycle is the attachment of kinetochores to chromosomes to ensure proper separation of chromosomes into daughter cells (Zeng *et al.*, 2008). The MAPK pathway plays a role in cell cycle regulation, which underlies the involvement of RKIP in cell cycle regulation (Zeng *et al.*, 2008). During mitosis, RKIP locates at centrosomes and kinetochores (Eves *et al.*, 2006). Hyperactivation of the Raf-1/MEK signaling pathway due to decreased RKIP levels leads to the inhibition of Aurora B kinase. This causes the spindle checkpoint to be bypassed leading to aberrant chromosome segregation and acceleration of mitosis progression (Eves *et al.*, 2006). Consistent with compromising the spindle checkpoint, reduction in RKIP contributes to chromosomal loss (Al-Mulla *et al.*, 2008). Furthermore, RKIP promoter methylation was observed in human cancers (Al-Mulla *et al.*, 2008), which may contribute to genome instability, a hallmark of cancer.

1.8. RKIP as a Metastasis Suppressor Gene

RKIP plays a role in inhibition of cancer metastasis. In an effort to identify candidate genes associated with prostate cancer metastasis, microarray profiling gene expression between LNCaP line and its metastatic derivative C4-2B line revealed reduction of the RKIP transcript in C4-2B cells (Fu *et al.*, 2002; Keller, 2004; Keller *et al.*, 2004b). Further analysis of prostate tissue, primary prostate cancer and metastatic

prostate cancer detected RKIP protein in both non-cancerous and primary cancer tissue whereas RKIP was not detected in prostate metastases (Fu *et al.,* 2003). The expression levels of RKIP were highest for prostate glands, decreased with increasing Gleason scores in cancerous tissue and were not present in metastases (Keller, 2004; Keller *et al.,* 2005). Furthermore, decreased RKIP expression was associated with increased activation of both MEK and ERK (Fu *et al.,* 2003). Reduction of RKIP was also observed in other types of human cancers, including melanoma (Park *et al.,* 2005; Schuierer *et al.,* 2004), insulinomas (Zhang *et al.,* 2004), breast cancer (Hagan *et al.,* 2005), hepatocellular carcinoma (Schuierer *et al.,* 2006; Lee *et al.,* 2006a), anaplastic thyroid cancer (Akaishi *et al.,* 2006) and colorectal cancer (Al-Mulla *et al.,* 2006; Minoo *et al.,* 2007; Zlobec *et al.,* 2008a; Zlobec *et al.,* 2008b; Zeng *et al.,* 2008).

Consistent with the observed correlation between reduction of RKIP with prostate cancer metastasis *in vitro* and *in vivo*, modulation of RKIP was reported to impact prostate cancer metastasis *in vitro* and *in vivo* (Keller *et al.,* 2004a; Keller *et al.,* 2004b). In immunocompromised mice, RKIP overexpression in tumour xenografts resulted in decreased metastasis formation with no effect on primary tumour growth in human prostate, breast and ovarian cancers (Fu *et al.,* 2003, Dangi-Garimella *et al.,* 2009; Li *et al.,* 2008). RKIP overexpression was found to decrease cell invasion and the formation of metastases at distant sites (Fu *et al.,* 2003). Prostate cancers that displayed low RKIP levels were strongly associated with cancer recurrence (Fu *et al.,* 2006). RKIP levels are inversely correlated with the metastasis formation in melanoma (Schuierer *et al.,* 2004), breast cancer (Hagan *et al.,* 2005; Dangi-Garimella *et al.,* 2009), colorectal cancer (Al-

Mulla *et al.,* 2006; Minoo *et al.,* 2007; Zlobec *et al.,* 2008a; Zlobec *et al.,* 2008b), ovarian cancer (Li *et al.,* 2008), and nasopharyngeal cancer (Chen *et al.,* 2008). Taken together, these observations strongly support RKIP being a metastasis suppressor. In line with this notion, RKIP is a prognostic marker in colorectal cancer (Zeng *et al.,* 2008), prostate cancer (Fu *et al.,* 2006), gastrointestinal stromal tumours (Beshir *et al.,* 2010) and intestinal-type gastric adenocarcinoma (Chatterjee *et al.,* 2008).

RKIP may suppress cancer metastasis by inhibiting the epithelial-mesenchymal transition (EMT). EMT is characterized by a loss in cell-cell adhesion and an increase in cell mobility. In order for this to occur several key events take place including loss of intercellular cohesion (loss of cell-cell junctions), disruption of the basement membrane and extracellular matrix, cytoskeleton rearrangement and migration into the stromal compartment (Yilmaz and Christofori, 2009; Guarino *et al.,* 2007). Mounting evidence reveals that the epithelial-mesenchymal transition plays an essential role in metastasis (Guarino *et al.,* 2007). Inhibition of MAPK by RKIP leads to decreased transcription of *Myc* and *Lin28*, resulting in enhanced *let-7* expression. This prevents HMGA2 from activating pro-invasive and pro-metastatic genes including Snail. (Dangi-Garimella *et al,* 2009). Snail is a key transcription factor involved in the initiation of EMT (Beach *et al.,* 2008; Baritaki *et al.,* 2009; Guarino *et al.,* 2007) and Snail is able to repress RKIP transcription (Beach *et al.,* 2008; Barbera *et al.,* 2004; Baritaki *et al.,* 2009; Wu and Bonavida, 2009). Moreover, studies have demonstrated that RKIP inhibits the NFκB pathway. NFκB is involved in the upregulation of Snail expression and in promoting the

formation of metastasis (Wu and Bonavida, 2009; Tang *et al.*, 2010; Baritaki *et al.*, 2009; Yeung *et al.*, 2001).

Recently studies have defined which RKIP regulated signaling pathways (Raf-1/MEK/ERK or NFκB) are involved in cancer invasion (Beshir *et al.*, 2010). By using specific inhibitors, U0126 for the MEK and DHMEQ for NFκB pathway, it was found that only when the NFκB pathway was inhibited did it have any significant effect on the invasion rate of cancer cells (Beshir *et al.*, 2010). Additionally, knockdown of RKIP in cell lines displaying a low metastatic potential increased their in invasion capacities (Beshir *et al.*, 2010). Conversely, overexpression of RKIP in cancer cell lines having a high metastatic potential decreased their invasion abilities *in vitro* and their abilities to form metastases in mice (Beshir *et al.*, 2010). It was also found that knockdown of RKIP resulted in increased expression of matrix metalloproteinases (MMPs), specifically MMP-1 and MMP-2 (Beshir *et al.*, 2010). MMPs are extracellular matrix degrading enzymes implicated in invasion and metastasis (Deryugina and Quigley, 2006). Taken together these observations suggest an interesting feedback loop between Snail, RKIP and the NFκB pathway. In this model, 1) Snail inhibits RKIP expression; 2) RKIP inhibits the NFκB pathway; 3) NFκB up-regulates Snail transcription factor. Based on this model, it is proposed that in the normal state (low snail, high RKIP) there is less repression of RKIP transcription by Snail, which allows for RKIP to inhibit the NFκB pathway. This would keep Snail at low levels. On the other hand, under an aberrant state, reduced levels of RKIP will enable up-regulation of Snail to occur via attenuation of RKIP-mediated inhibition of the NFκB pathway (Beshir *et al.*, 2010).

1.9. Summary and Current Insights from this Research

Clear cell renal cell carcinoma (ccRCC) is associated with high rate of metastasis with approximately ⅓ of patients developing metastasis over the course of the disease (Drucker *et al.,* 2005). This leads to a high rate of mortality associated with the disease (Jermal *et al.*, 2008). However, the exact pathological causes of RCC remain unclear. One of the abnormalities contributing to ccRCC is activation of the MAPK pathway. In an effort to identify factors that plays a role in the pathogenesis of ccRCC, we have demonstrated that one of these novel factors is RKIP.

While RKIP has been reported to be a metastasis suppressor of several types of human cancers, including prostate, breast, melanoma and colorectal cancers and gastrointestinal stroma tumours (Fu *et al.,* 2003; Keller *et al.,* 2005; Chatterjee *et al.,* 2004; Hagan *et al.,* 2005; Schuierer *et al.,* 2004; Al-Mulla *et al.,* 2006; Martinho *et al.,* 2009), the involvement of RKIP in ccRCC remains to be examined. In our examination of more than 600 patients with ccRCC in several independent patient cohorts, levels of the RKIP protein are significantly reduced in approximately 80% of ccRCC tumours in comparison to the adjacent non-tumour kidney or normal kidney tissues. Consistent with ccRCC being originated from the epithelial cells of proximal tubules, RKIP is largely expressed in these cells in the kidney. The observed magnitude of RKIP reduction strongly suggests that RKIP is an important tumour suppressor of ccRCC. Supporting this concept are our observations that 1) ectopic expression of RKIP inhibited A498 ccRCC cells invasion, 2) knockdown of RKIP in A498 cells enhanced the invasion ability

of A498 cells, 3) progression of ccRCC from tumour grade 2 to grade 3 and tumour stage T2N0M0 to T3N0M0 associates with further reduction in the RKIP protein, and 4) further RKIP reduction was also observed in metastasized ccRCC tumours in comparison to the matched organ-confined tumours. Taken together, our research reveals that RKIP is a potentially dominant tumour suppressor of ccRCC. While VHL is a dominant tumour suppressor of ccRCC, loss of VHL is not sufficient to induce ccRCC (Neumann and Zbar, 1997). In light with our research, it will be very intriguing to examine whether loss of two dominant tumour suppressors, VHL and RKIP, will be sufficient to result in ccRCC.

II. HYPOTHESIS

Existing evidence strongly suggests that RKIP is a metastasis suppressor. Decreases in RKIP were observed in numerous cancers, especially in metastatic diseases including those of prostate, breast and colorectal cancers (Fu *et al.,* 2003; Keller *et al.,* 2005; Hagan *et al.,* 2005; Al-Mulla *et al.,* 2006). However, whether RKIP also inhibits ccRCC tumorigenesis remains to be reported.

Our preliminary research has found reduction of RKIP in ccRCC tumours in comparison to the adjacent non-kidney tumour tissues in a limited number of ccRCC patients. A major role of RKIP is inhibiting Raf-1-mediated activation of MEK and abnormal activation of the Raf-1-MEK-ERK pathway plays a major role in ccRCC tumorigenesis. Taken together, the central hypothesis of this research is that RKIP is a tumour suppressor of ccRCC. To examine this hypothesis, our major objectives include:

A. To examine the relationship between RKIP reduction and ccRCC development.
B. To examine the effect of modulation of RKIP on ccRCC tumourigenesis *in vitro* and *in vivo*.

III. MATERIALS AND METHODS

3.1. Reagents

Ampicillin, calcium chloride ($CaCl_2$), crystal violet dimethyl sulfoxide (DMSO), ethidium bromide, EDTA, aprotinin, leupeptin, phenylmethylsulfonyl fluoride (PMSF), β-glycerophosphate, soldium fluoride, soldium orthovanade (Na_3VO_4), Triton X-100, Tween 20, β-mecaptoethanol, puromycin potassium dihydrogen orthophosphate (KH_2PO_4), dipotassium hydrogen orthophosphate (K_2HPO_4), potassium acetate, potassium chloride, sodium dihydrogen orthophosphate (NaH_2PO_4), disodium hydrogen orthophosphate (Na_2HPO_4), Bromophenol blue, ammonium per sulphate (APS), and GenElute Plasmid Miniprep kit were purchased from Sigma, Oakville, ON. Agarose, bovine serum albumin (BSA), Tris, glycine, sodium dodecyl sulphate (SDS), sodium citrate, sodium chloride (NaCl), TEMED were purchased from Bioshop Burlington, ON. Hygromycin B, and trypsin-EDTA were purchased from Invitrogen, Carlsbad, CA. 30% Acrylamide/Bis solution was purchased from Bio-Rad, Mississauga, ON. Methanol and isopropyl alcohol were purchased from Caledon Laboratories, Georgetown, ON and Reagent Alcohol was purchased from Fisher Scientific, Ottawa, ON. Anhydrous Ethyl Alcohol was purchased from Commercial Alcohols, Brampton, ON. Ultraclean 15 DNA purification kit was purchased from MoBio Laboratories Carlsbad, CA.

3.2. Cell Lines and Antibodies

3.2.1. Cell Lines

The following cell lines were purchased from the American Type Culture Collection (ATCC); 786-O, 293T and A498. All cells were cultured according to specified conditions. The culture conditions for 786-O, A498, and 293T cells are RPMI-1640 media, Minimum Essential Medium (MEM), and Dulbecco's Modified Eagle Medium (DMEM), respectively, supplemented with 10% fetal bovine serum (FBS) (Sigma, Oakville, ON) and 1% penicillin/streptomycin (Invitrogen, Carlsbad, CA). Cells were grown in their respective media at 37°C and 5% CO_2 in a tissue culture incubator.

3.2.2. Antibodies

Antibodies used for western blotting and immunohistochemistry include rabbit anti-RKIP (Santa Cruz Biotechnology, Santa Cruz, CA), goat anti-β-actin (Santa Cruz Biotechnology, Santa Cruz, CA), mouse anti-FLAG (Sigma, Oakville, ON), rabbit anti-ERK (Cell Signaling, Danvers MA), rabbit anti-pERK (Cell Signaling, Danvers MA), rabbit anti-pRKIP (Santa Cruz Biotechnology, Santa Cruz, CA), mouse anti-N-cadherin (Sigma, Oakville, ON) and mouse anti-vimentin (Santa Cruz Biotechnology, Santa Cruz, CA) . Secondary antibodies for western blot were purchased from Amersham (anti-rabbit and anti-mouse) and Santa Cruz Biotechnology (anti-goat). Secondary antibodies for immunohistochemistry were purchased from Vector Laboratories (Burlingame, CA).

3.3. Plasmids

Vesicular stomatitis virus G (VSV-G) and gag-pol (GP) expressing plasmids were purchased from Agilent Technologies (Mississauga, ON). pCDNA 3.0 plasmid was purchased from Clontech (Mountain View, CA). The pRIH1 plasmid was constructed in our laboratory for RNAi purposes (He *et al.*, 2011). The pBabe plasmid was a gift from Dr. Tak Mak at the University of Toronto.

3.3.1. Generation of pBabe/RKIP C-terminal Flag Tagged Plasmid

C-terminal FLAG-tagged RKIP (RKIP-FLAG) was subcloned into the pBabe retroviral vector from the pcDNA 3.0/C-FLAG RKIP plasmid previously constructed in our laboratory. pBabe was linearized using the EcoR1 restriction enzyme (Invitrogen, Carlsbad, CA). This was followed by ethanol precipitation, conversion of EcoR1-cleaved ends to blunt ends, and dephosphorylation of the blunted ends to prevent self ligation. The RKIP-FLAG insert was released from the pcDNA 3.0/C-FLAG RKIP using EcoR1 and Nhe1 (Invitrogen), followed by converting the EcoR1- and Nhe1-prepared ends into blunt ends. This insert was then ligated, using the rapid DNA ligation kit (Roche, Mississauga, ON), to the prepared pBabe vector to produce pBabe/RKIP-FLAG construct. Confirmation of positive clones was determined by calcium phosphate transfection of pBabe/RKIP-FLAG into 293T cells and western blot analysis for FLAG protein expression.

3.3.2. Short Hairpin RNA

The pRIHI plasmid is a retroviral vector constructed in our laboratory driven by the H1 promoter used to generate short hairpin RNA structures. RNAi fragments are produced when sense and anti-sense strands are complementary to each other producing a hairpin structure which is then processed into 21 base pair double stranded RNAi fragment (Kim and Rossi, 2007). The RKIP targeting sequence used was 5'– GTGGGATGGTCTTGATTCA –3'.

3.4. Gene Expression in Mammalian Cells

3.4.1. Retroviral Mediated Gene Expression

To overexpress (ectopically) or knockdown targets of interest into the cell using the retroviral methodology, 293T cells were used to package retroviral particles using a gag-pol expression vector (GP) and an envelope-expressing vector (VSV-G, vesicular stomatitis virus G protein) (Agilent Technologies, Mississauga, ON). Briefly 293T cells were seeded one day ahead and then transfected with 10 µg of each of the following vectors; pVPack-VSV-G, pVPack-GP and respective retroviral vector containing gene of interest or empty vector were added to 50 µL of 2.5M $CaCl_2$ and H_2O for a total volume of 500 µl in a 13 mL round bottom tube. Between each addition of vector the solution was mixed with a vortex. The solution was then added drop wise using a glass pipette to 500 µL of 2X Hepes Buffered Saline (HeBS, 0.28 M NaCl, 0.05 M hepes, 1.5 mM

$Na_2HPO_4 \cdot 7\ H_2O$, pH 7.1) with shaking. The solution was then mixed using a vortex for 30 seconds. Following incubation for 20 minutes at room temperature, the transfection mixture was added drop-wise using a glass pipette to a 293T plate containing 9 mL of complete DMEM complete media and incubated at 37°C, 5% CO_2 for 12 hours. The media was then changed to fresh complete media. After 48 hours, the supernatant containing retroviral particles was collected and filtered through a 0.45 µm filter. Approximately 2-3 mL of supernatant was incubated with A498 or 786-O cells, which were split 24 hours prior to infection, in a tissue culture incubator for 1 hour with rotation every 20 minutes to evenly distribute the virus. The viral-containing medium was then replaced with complete medium for 24-48 hours. Cells were then selected for by addition of designated antibiotics specific for retrovirus. The concentration and specific antibiotic concentration used was: pBabe – puromycin (1 µg/mL) and pRIHI – hygromycin (0.5 mg/mL).

3.5. Cell and Kidney Tissue Protein Analysis

3.5.1. Cell Lysate Preparation

Cell lysates were prepared by washing cells twice with cold phosphate buffered saline (PBS, 1.36 M NaCl, 14.7 mM KH_2PO_4, 80 mM Na_2HPO_4, 26.8 mM KCl, pH 7.4). Cells were then scraped off the tissue culture plate, centrifuged (2000 RPM, 4°C, 5min) and lysed in a cell lysis buffer containing 50 mM Tris-HCl (pH 7.4-7.5), 150 mM NaCl, 5 mM EDTA, 1% triton X-100, 10% glycerol, 1 mM NaF, 1 mM β-glycerophosphate, 100

μM sodium orthovanadate (Na_3VO_4), 1 mM PMSF, 2 μg/mL leupeptin and 10 μg/mL aprotinin for 30 minutes on ice. Samples were then centrifuged (13,000 RPM, 4°C, 5 min). The supernatant was collected and protein concentration was determined using the Bradford method (Bio-Rad, Mississauga, ON) and measuring absorbance at 595 nm using the Ultrospec 2100 pro spectrophotometer (Biochrom Ltd, Cambridge, England). Samples were stored at -80°C until use.

3.5.2. Preparation of Lysates from Kidney Tissue

Human kidney tissue samples previously frozen in liquid nitrogen were removed and approximately 20mg of tissue was homogenized into a fine powder using a mortar and pestle in liquid nitrogen. Lysates were then prepared as described above.

3.5.3. Western Blotting

A total of 50 μg protein from cell or tissue lysate was diluted in 5XPSB (protein sample buffer, 0.1mM Tris pH 6.8, 5% SDS, 50% glycerol, 2% β-mercaptoethanol, 0.02% bromophenol blue) and ddH_2O to a final concentration of 1XPSB. The samples were then denatured by boiling for 3 minutes and then separated on a 12.5% SDS-polyacrylamide gel at 50 mA. Membranes were incubated in transfer buffer (25 mM Tris-HCl, 192 mM glycine, 20% methanol) prior to use. Proteins were then transferred onto an Amersham hybond ECL nitrocellulose membrane (Amersham, Bair d'Urfe, QC) for 75 minutes at 260 mA. Membranes were then blocked with 5% non-fat dry milk powder in Tris Buffered Saline and 0.1% Tween 20 (1XTBS-T) for 1 hour at room temperature. After blocking, membranes were incubated with gentle shaking overnight at

4°C or for 1 hour at room temperature with anti-RKIP (1:500), anti-phosphoRKIP (1:500), anti-ERK (1:1000), anti-phosphoERK (1:1000), anti-FLAG (1:1000), anti-N-cadherin (1:1000) or anti-Vimentin (1:500). Membranes were subsequently washed with 1XTBS-T and incubated with secondary antibody (1:3000) for 1 hour at room temperature with gentle shaking. Membranes were then washed with 1XTBS-T and protein signals were detected using the ECL western blotting kit (Amersham) followed by exposure onto Kodak X-OMAT X-ray film (Perkin Elmer, Waltham, MA). Membranes were washed briefly to remove any traces of the ECL reagent and then incubated with anti-actin (1:1000) for 1 hour at room temperature with gentle shaking. Membranes were then processed by washing, incubating with a secondary antibody, and developing signals as described above.

3.6. 5-Aza-2'-deoxycytidine Dosing of A498 and 786-O Cells

A498 and 786-O cells were seeded the day before so that cells would be 80-90% confluent in 24 hours. Cells were then either mock treated with H_2O or treated with 2 μM 5-Aza-2′-deoxycytidine (5-aza-dC, Sigma) for 48 hours. Cells were then either lysed for protein analysis or RNA was extracted for qRT-PCR analysis according to methods outlined previously and below.

3.7. Immunohistochemistry

3.7.1. Tissue Microarray Slides

Tissue microarray (TMA) slides were purchased from US Biomax, Rockville, MD. The Slides purchased included KD 806, KD 951, KD 2085, KD 2088 and KD 6161. TMA slides were first baked at 55°C in an oven for 1-2 hours to melt the layer of paraffin covering the tissue cores. The slides were then deparaffinized and rehydrated by incubating in xylene, 100% ethanol (EtOH), 90% EtOH and 70% EtOH according to the following schedule; 3 incubations of 10, 10 and 5 minutes respectively in xylene followed by one incubation of 5 minutes in 100% EtOH, then one incubation of 5 minutes in 90% EtOH and lastly 2 incubations of 5 and 2.5 minutes respectively in 70% EtOH. The TMA slides were then rinsed and washed with ddH_2O on the shaker (120 RPM). To quench endogenous peroxidise, slides were incubated in 3% hydrogen peroxide (H_2O_2) diluted in H_2O for 10 minutes. Slides were then washed with 1XPBS on shaker at 120 RPM and incubated in antigen retrieval buffer (Sodium Citrate Buffer; 10 mM sodium citrate, 0.05% tween, pH 6.0) for 30 minutes in a food steamer. Slides were then washed with 1XPBS and incubated with blocking buffer (1.5% normal goat serum in 1XPBS) for 1 hour at room temperature in a humidity chamber. Excess blocking buffer was removed and slides were incubated in primary antibody (RKIP 1:500, Santa Cruz) diluted in blocking buffer in the humidity chamber at 4°C overnight. This was followed by washing the slides with 1XPBS and incubating the slides with anti-rabbit biotinylated secondary antibody (1:200, Vectastain ABC kit, Vector Laboratories) for 1 hour at room

temperature in the humidity chamber. During this incubation ABC reagent was prepared according to manufacturer's instructions (Vectastain ABC kit, Vector laboratories). Briefly 20 µL of reagent A was added to 1 mL of blocking buffer, followed by addition of 20 µL of reagent B to the solution. Upon completion of the incubation with the secondary antibody, slides were washed and incubated with ABC reagent for 45 minutes at room temperature. Slides were then washed and DAB solution was added to the slides. DAB solution was prepared according the manufactures instructions (Vector Laboratories). Briefly, to 2.5 mL of ddH_2O the following solutions were sequentially added to the mixture: 1 drop of buffer solution, 2 drops of DAB reagent, and 1 drop of hydrogen peroxide solution. DAB solution was removed off the slides with ddH_2O and incubated in ddH_2O for 5 minutes. Slides were counterstained with Haematoxtylin (Sigma) and washed with H_2O. Slides were incubated in H_2O for 5 minutes and then dehydrated by incubating in 70% EtOH for 5 minutes and in 100% EtOH for 5 minutes followed by two incubations in xylene for 3 minutes each. Coverslips were then added to the slides using Cytoseal mounting medium (Richard Allan Scientific, Kalamazoo, MI). Stained slides were scanned using ScanScope (Aperio Technologies, Vista, CA) a service provided by the Advanced Optical Microscopy facility in Toronto, ON. ImageScope software (Aperio Technologies, Vista, CA) was used to analyze the scanned images. ImageScope software scored the staining intensity of the tissue cores into four categories, strong positive, positive, weak positive and negative staining. A mock-up image showing how ImageScope software scores the stained tissue cores is shown in figure 3. These scores were then used to calculate the H-Score according to the following formula;

$$H - Score = (\%\ weak\ x\ 1 + \%\ positive\ x\ 2 + \%\ strong\ x\ 3 + 1)x\ 100$$

Where %(weak, positive, or strong) = total intensity of (weak, positive, or strong)/total intensity (weak + positive + strong + negative) (He *et al.*, 2010). H-Scores greater than 260 were considered positive for staining and H-Scores less than 260 were considered negative for staining. Each cancerous tissue core was in duplicate and all cores were manually examined. Tissue cores were excluded from analysis if the tissue was scratched or missing majority of the sample.

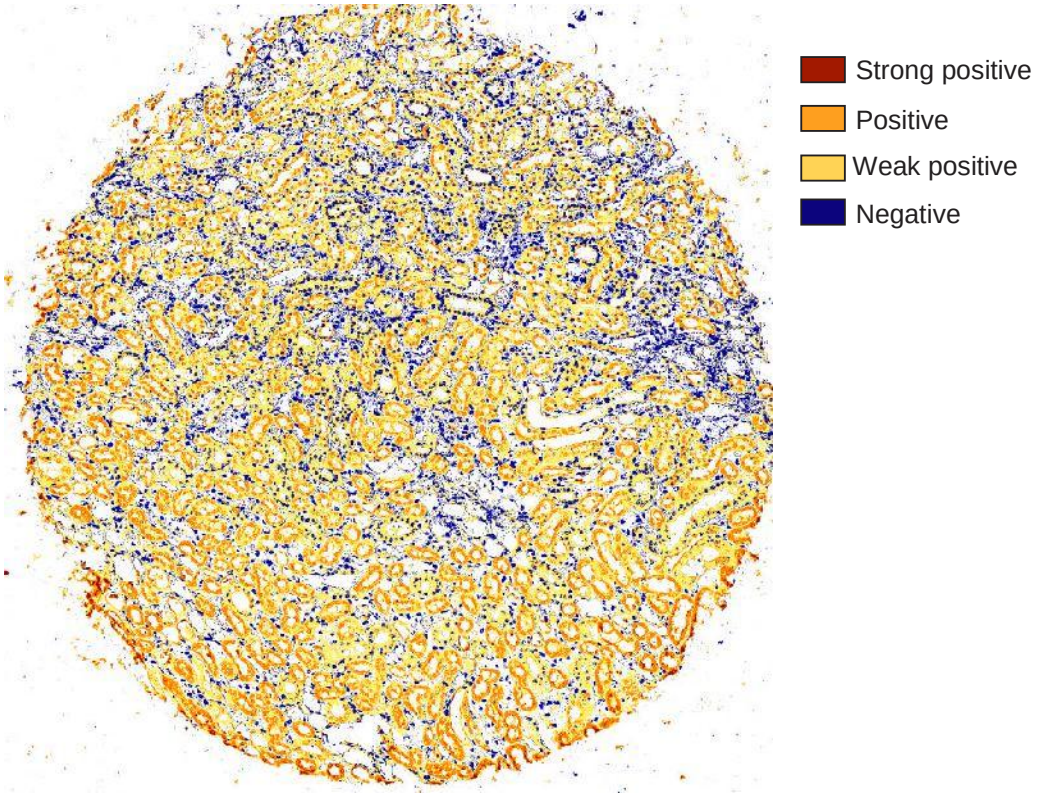

Figure 3: Mock-up Normal tissue Core. ImageScope software scores stained tissue cores based on intensity of staining. The four categories are strong positive (red), positive (orange), weak positive (yellow) and negative (blue). The percent of cells stained in each category is used to calculate the H-Score.

3.8. RNA Isolation and qRT-PCR

3.8.1. RNA Isolation from Cells

Total RNA was isolated from cells using Trizol reagent (Invitrogen) according to manufacturer's instruction. Briefly, cells were lysed by adding Trizol reagent directly to cell culture plate, followed by addition of chloroform and then centrifuged (12,000g, 4°C) for 15 minutes to allow for phase separation. The aqueous phase was removed and isopropyl alcohol was added to precipitate RNA and then centrifuged (12,000g, 4°C) for 10 minutes. The resulting RNA pellet was washed with 75% EtOH (7500g, 4°C) for 5 minutes, air dried and then resuspended in DEPC H_2O. RNA concentration was measured at 260nm using the Ultrospec 2100 pro spectrophotometer (Biochrom Ltd, Cambridge, England). RNA was stored at -80°C until use.

3.8.2. RNA Isolation from Tissue

Total RNA was isolated from Kidney tissue and cancerous tissues using the Protein and RNA Isolation System (PARIS) kit (Applied Biosystems) according to manufacturer's instructions. Approximately 60-80 mg of tissue was homogenized in approximately 600 µL ice cold cell disruption buffer using an automatic homogenizer. Homogenized mixtures were then centrifuged (10,000g, 4°C) for 10 minutes to remove any contaminants and 2X lysis/binding solution was added followed by addition of equal amounts of 100% EtOH. The solution was homogenized by passing through a needle and syringe 5-6 times. The sample solution was then loaded into a filter column and centrifuged (10,000g, 4°C) for 30 seconds. The flow through liquid was discarded and

the filter was washed first with wash solution 1 and then twice with wash solution 2/3 with centrifugations in between each wash step for 30 seconds each. Filter columns were then centrifuged (10,000g, 4°C) for 1 minute without any wash solution to remove any excess liquid. RNA was eluted from the filter by addition of warmed (95°C) elution solution to the filter column and then centrifuging (10,000g) for 1 minute. RNA concentration was measured using NanoVue Plus Spectrophotometer (General Electric Healthcare, Mississauga, ON). RNA concentration was determined based on the average concentration of two independent trials of 2 µL of sample. RNA was stored at -80°C until use.

3.8.3. cDNA Synthesis

RNA was reverse transcribed into cDNA using the High Capacity cDNA Reverse Transcription kit (Applied Biosystems). All cDNA synthesis reactions were performed on the Eppendorf Mastercycler gradient machine (Eppendorf, Mississauga, ON). According to the manufacturer's protocol, 2 µg of RNA was added to a 0.2 µL PCR tube containing 2.0 µL 10x RT buffer, 0.8 µL 25x dNTP Mix, 2.0 µL 10x RT Random Primers, 1.0 µL Multiscribe Reverse Transcriptase and nuclease free H_2O for a final volume of 20 µL. The PCR tube was then incubated at 25ºC for 10min, 42ºC for 1h and 85ºC for 5min. Resulting cDNA was then diluted 1:4 in nuclease free H_2O and stored at -80°C until use.

3.8.4. Quantitative Real-Time PCR (qRT-PCR)

RNA samples were analyzed for RKIP, VEGFA and β-actin mRNA abundance. Primer sequences are listed in Table 2. Primers were synthesized at McMaster University's Institute for Molecular Biology and Biotechnology facility (MOBIX, Hamilton, ON). All qRT-PCR reactions were performed using the 7500 Real Time PCR system and 7500 system sequence detection software (SDS) version 1.2.2 software (Applied Biosystems). Each PCR reaction was performed in a 25 µL reaction volume consisting of 12.5 µL Power SYBR Green PCR Master Mix (Applied Biosystems), 2 µL diluted cDNA, 0.5 µL of 10 µM forward primer, 0.5 µL of 10 µM reverse primer and 9.5 µL UltraPure™ Distilled Water. A master mixture was assembled in a 1.5 mL microcentrifuge tube placed on ice. Each sample was performed in triplicate with 25 µL of the master mix added to a single well of a MicroAmp Optical 96-Well Reaction Plate (Applied Biosystems). MicroAmp Optical 8-Cap Strips (Applied Biosystems) were applied to each column of the 96-well plate. The plate was then centrifuged at 3,500rpm for 1min at 4ºC and placed into the 7500 Real Time PCR System (Applied Biosystems). Target gene analysis was performed using the manufacturer's software with SYBR programmed as the Detector and ROX as the Passive Reference. Fluorescence emission data was collected during the second step of the third stage of the program: (stage 1) 50°C for 2 minutes; (stage 2) 95°C for 10 minutes; (stage 3) 40 cycles, 95°C for 15 seconds, then 60°C for 1 minute; (stage 4) 1 cycle, 95°C for 15 seconds, 60°C for 1 minute, 95°C for 15 seconds. The Dissociation Stage was used to monitor primer dimer formation. RKIP and VEGFA gene expression was determined using the average of the

triplicate critical threshold (C_T) values in the $2^{-\Delta\Delta CT}$ equation, with all target gene expression being relative to β-Actin expression. VEGFA was used as a tumour associated marker to verify tumour tissue. Tumour tissue is known to be highly vascularised. Therefore tumour tissue which did not have increased levels of VEGFA compared to its adjacent normal tissue was not included in the data set.

Table 2: Quantitative Real-Time PCR primer sequences for RKIP, VEGFA and β-Actin genes

Gene	Primer Sequence	Reference
RKIP (Human)	forward – 5'-AGACCCACCAGCATTTCGTG-3'	Zaravino *et al,* 2008
	reverse – 5'-GCTGATGTCATTGCCCTTCA-3'	
VEGF (Human)	forward – 5'-AAGGAGGAGGGCAGAATCAT-3'	Thijssen *et al,* 2004
	reverse – 5'-CCAGGCCCTCGTCATTG-3'	
β-Actin (Human)	forward – 5'CCCTGAAGTACCCCATCGAG-3'	Sloan *et al,* 2009
	reverse – 5'-CAGATTTTCTCCATGTCGTCCC-3'	

3.8.5. RNA Microarray Analysis

Total RNA was extracted from respective cells according to previous outlined methods. Isolated RNA was then sent to the University Health network Microarray Center (UHNMAC) (Toronto, ON) for processing. Affymetrix Human Gene 1.0 ST microarrays were purchased through UHNMAC. All procedures and raw preliminarily data was performed at the UHNMAC.

3.9. Invasion Assay

To assess the invasion potential of cells, inserts containing an 8 µm pore membrane coated with Matrigel were purchased from BD Biosciences (Becton Dickson, Franklin Lakes, NJ). Control inserts containing only the membrane were also purchased (BD, Franklin Lakes, NJ). Control and Matrigel inserts were placed in a 24-well plate with serum free media and allowed to rehydrate at for 2 hours at 37°C and 5% CO_2. Following incubation, 750 µL fresh media containing 10% serum was added to the wells of the plate (the lower chamber) and $2.5x10^4$ cells were placed in the upper chamber (insert) with 500 µL serum-free media. Plates were incubated at 37°C and 5% CO_2 for 22 hours. Non-invading cells from the upper surface were removed using cotton swabs. Cells that were able to migrate through the membrane to the underside of the membrane (bottom of membrane) were fixed with fixative solution for 10 minutes and then stained with crystal violet stain for 10 minutes for visualization purposes. Membranes were then placed on glass slides, cover slipped and photographed using a microscope. For each slide, five photographs were taken for a true representation of the cell numbers throughout the membrane. Cells were counted using Image J software (National Institutes of Health, USA). Invasion potential was determined based on the number of cells that could invade through the Matrigel insert membrane compared to the number of cells that could migrate through the control insert membrane. The following formula was used to determine percent invasion:

$$\%\ invasion = \frac{Number\ of\ cells\ migrating\ through\ matrigel\ membrane}{Number\ of\ cells\ migrating\ through\ control\ membrane}\ x\ 100$$

3.10. Cell Proliferation Assay

To measure the growth rate, respective cells were seeded at a density of 10^4 per well in 6-well plates. Every 24 hours cells were trypsinized and cell counts were determined through microscopic counting for seven days. Triplicate wells were counted each day.

3.11. Generation of A498 Cell-derived Xenograft Tumours

A498 cells overexpressing RKIP (RKIP), empty vector (EV), short hairpin control (CTRL ShRNA) and short hairpin RKIP (RKIP ShRNA) were injected subcutaneous into the flank of NOD/SCID mice (The Jackson Laboratory, Bar Harbor, Maine) with each group containing 5 mice. $3x10^6$ of designated A498 cells were resuspended into a MEM/Matrigel mixture (1:1 volume). 0.1 mL of this cell solution was injected subcutaneous into the flanks of 6 week old mice. Tumour formation was monitored and measured weekly using calipers. When tumours reached 1-2 grams or 5% of normal body weight, mice were sacrificed and tumours collected. Tumour volume was calculated according to the following formula $L \times W^2 \times 0.52$, where L and W are the longest and shortest diameters respectively (He *et al,* 2011). All animal work was performed according to protocols approved by the McMaster University Animal Research Ethics Board. A498 EV and A498 RKIP groups were sacrificed at 8 weeks. A498 CTRL ShRNA and A498 RKIP ShRNA groups were sacrificed at 11 weeks.

3.11.1. Tumour Tissue Collection

Tumours were carefully isolated from mice at time of sacrifice. Tumour tissues were first photographed and then tumour tissue was cut in half where one half was fixed with 10% formalin (VWR, West Chester, PA) and the other half was frozen at -80°C for future use. Tissue was fixed for 24 hours and then the formalin solution was changed to 70% ethanol. The tumour tissue was then sent to the McMaster University Center for Gene Therapeutics – Core Histology Research Services (Hamilton, ON) where the tissue blocks were embedded in paraffin and slides were cut.

3.11.2. Hematoxylin and Eosin (H&E) Staining

The slides were then deparaffinized and rehydrated by incubating in xylene, 100% ethanol (EtOH), and 70% EtOH according to the following schedule; 3 incubations in xylene for 5 minutes each followed by one incubation in 100% EtOH for 5 minutes, and then one incubation in 70% EtOH for 5 minutes. The slides were then rinsed and washed with ddH_2O. Slides were then incubated in hematoxylin (Sigma) for 10 minutes and washed in room temperature H_2O for 5 minutes. Slides were subsequently incubated in Tris buffer pH 7.6 for 1 minute, washed in room temperature H_2O for 1 minute, and quickly dipped in 1% acid alcohol (1% HCl in 70% EtOH) 4 times. Slides were then washed in room temperature H_2O for 1 minute, placed in Tris buffer pH 7.6 for 1 minute, washed in room temperature H_2O, and then rinsed in ddH_2O. Slides were then incubated in 0.5% Eosin (Sigma) for 5 minutes and washed by dipping in room temperature H_2O 30 times followed by a rinse in ddH_2O. Slides were dehydrated by incubating in 70% EtOH

for 5 minutes, in 100% EtOH for 5 minutes, and twice in xylene for 3 minutes each. Slides were mounted using Cytoseal mounting medium (Richard Allan Scientific, Kalamazoo, MI) and visualized under a microscope. Images were subsequently taken.

3.12. Tissue Collection

Kidney cancer tissue and its adjacent normal tissue were collected at St. Joseph's Hospital in Hamilton, Ontario, Canada with consent from patients and under approval of the Research Ethics Board. The tissue collected was either fixed in 10% formalin, embedded in paraffin or snapped frozen in liquid nitrogen for future use.

3.13. Statistical Analysis

All data are presented as mean ± standard error (SE). Statistical analysis was carried out using the statistical program SPSS Statistics 17.0 for Windows. Two-tailed Student's T-Test was used to analyze protein expression differences in normal and cancerous tissue. Two-tailed Students T-Test was also performed to evaluate differences in mock and treatment cell lines. To test invasion ability a two-tailed Students T-Test was performed. To evaluate differences in tumour volume and cell proliferation rate, Two-tailed Student's T-Test was performed. Spearman's Rank Order Correlation was used to test relationships between RKIP protein expression and tumour stage and tumour grade progression. One way analysis of variance (ANOVA) was performed to evaluate

effect of tumour stage, tumour grade and metastasis on H-Score. Tukey's post hoc test was performed to test pair wise differences in the above groups. A p-value <0.05 was considered statistically significant.

IV. RESULTS

4.1. Reduction of RKIP in ccRCC

Clear cell RCC is the major type of RCC accounting for 75 to 85% of all cases and is also one of the most lethal forms of RCC (Motzer *et al.,* 1996; Lopez-Beltran *et al.,* 2009). However, our understanding on what causes the pathogenesis of ccRCC remains limited. In an effort to identify novel factors that are involved in ccRCC oncogenesis, previous research from Dr. Tang's laboratory has examined a limited number of patients for protein expression in their ccRCC tissues and the adjacent non tumour kidney (ANK) by 2D electrophoresis. This research led to the identification of a reduction of RKIP in primary ccRCC tissues (unpublished observation). This was an intriguing observation as RKIP is a candidate tumour suppressor for many human cancers including ovarian cancer (Wang *et al.,* 2008), melanoma (Park *et al.,* 2005; Schuierer *et al.,* 2004) breast cancer (Hagan *et al.,* 2005) and hepatocellular carcinoma (Schuierer *et al.,* 2006; Lee *et al.,* 2006a). At the same time, whether RKIP plays a role in ccRCC tumorigenesis remains undetermined.

To investigate whether RKIP is a potential tumour suppressor for ccRCC, I have examined whether RKIP is indeed reduced in ccRCC in a large cohort of ccRCC patients. Primary RCC and ANK tissues were collected from 81 patients at St. Joseph's Hospital in Hamilton, Ontario. Majority of the patients presented with clear cell RCC (50) followed by papillary RCC (13) and oncocytoma (4) (Table 3).

Table 3: Summary of Patient Data

Type of RCC	Number of Patients
Clear Cell	50
Papillary	13
Oncocytoma	4
Chromophobe RCC	3
Hybrid-clear and papillary	1
Sarcomatiod Chromophobe	1
Mucinous tubular and spindle cell carcinoma	1
Clear cell with multicystic change	1
Oncoytoma/papillary RCC cannot be determined	1
Papillary, Oxophillic	1
Sarcomatiod RCC	1
Unknown	4
Total	81

To determine RKIP expression, tissue lysates were prepared from the tumour and ANK tissues for all 81 patients. Western blot analysis clearly revealed the reduction of RKIP in ccRCC compared with ANK (Fig 4). To quantify RKIP levels in ccRCC and in ANK tissues, the protein expression of individual samples was normalized to actin expression. RKIP protein expression was significantly decreased ($p<0.001$) in cancer tissue as opposed to the adjacent non-tumour kidney tissues, when all 81 patients were considered (Fig 5). Consistent with the vast majority of patients (50) in the data set, presenting with ccRCC (Table 3), RKIP protein expression was also significantly lower ($p<0.001$) in cancerous tissues compared to adjacent normal tissue (Fig 5).

Since RKIP can inhibit ERK activation (Yeung *et al.,* 1999; Odabaei *et al.,* 2004), we have also examined the active form of ERK (phosphorylation of threonine 202 and tyrosine 204 residues) and ERK in 81 RCC patients by western blot (Fig 4). After

normalization of ERK or active ERK to actin, cancerous tissues and ANK tissues express comparable levels of ERK ($p = 0.541$) and active ERK ($p = 0.442$) in the total of 81 patients and in the ccRCC patients (Fig 6A). When the ratio of pERK (active form) was compared to total ERK in the ANK and ccRCC tissues, it was found that pERK remains the same in both tissues ($p = 0.756$) (Fig 6B).

Based on reports, RKIP can be phosphorylated at serine153 (S153) (Granovsky and Rosner, 2008). This phosphorylation not only abolishes RKIP's ability to inhibit Raf-1 but also enables RKIP to activate G protein signaling (Zeng *et al.*, 2008). To examine whether, in addition to reduction of RKIP in ccRCC, RKIP S153 phosphorylation status may also be altered in ccRCC, we observed that RKIP S153 phosphorylation was greatly reduced ($p<0.001$) in ccRCC compared to ANK tissues (Fig 4). However, as RKIP protein is also substantially reduced, the observed reduction of RKIP S153 in ccRCC might be caused by the reduction of RKIP protein. To examine this possibility, the levels of S153 phosphorylated RKIP (pRKIP) was normalized to the levels of RKIP protein in both ANK and RCC tissues. Two-tailed Student's T-Test showed that the normalized pRKIP remains the same in both tissues ($p = 0.100$) (data not shown). Taken together, the above observations demonstrate that RKIP is reduced in ccRCC but its phosphorylation at S153 is not changed and thus reduction of RKIP may not enhance ERK activation. Except for ccRCC, the other subtypes of RCC (papillary and oncocytoma) did not have enough patients in the data set for statistical analysis to be performed, therefore the focus of this project was on patients with ccRCC.

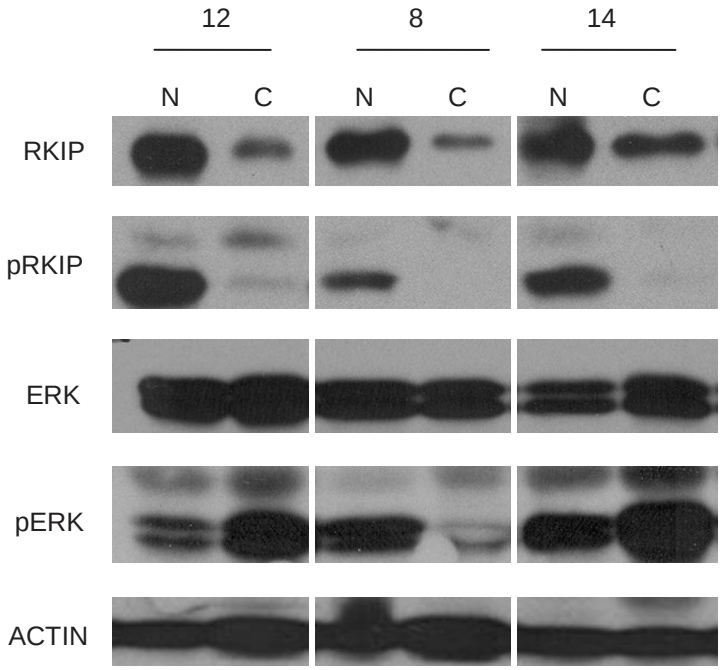

Figure 4: Representative western blot analysis of 3 ccRCC patients (12, 8 and 14). RKIP, pRKIP, ERK and pERK protein expression levels are shown in cancerous tissue (C) and its adjacent normal tissue (N).

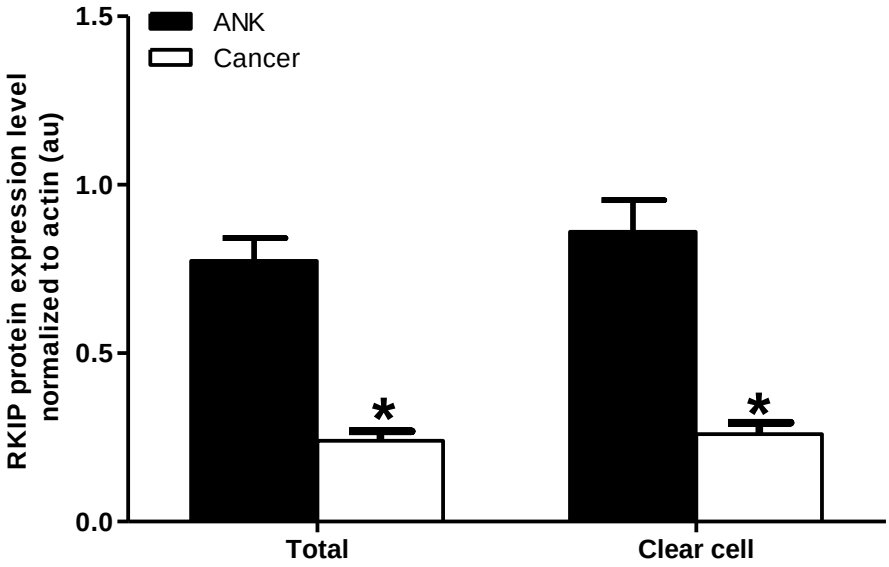

Figure 5: Reduction of RKIP in RCC. RKIP protein in normal and cancerous tissue was normalized to actin. Data are presented as RKIP expression in RCC verse ANK (Total) or in ccRCC population. All data are presented as mean ± SE. * Significant difference between normal and cancer levels ($p<0.001$).

A

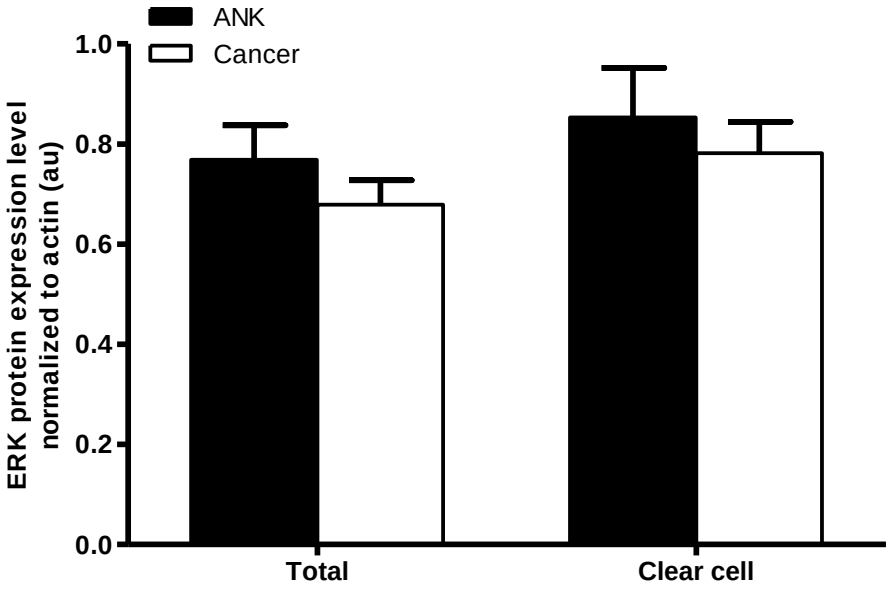

B

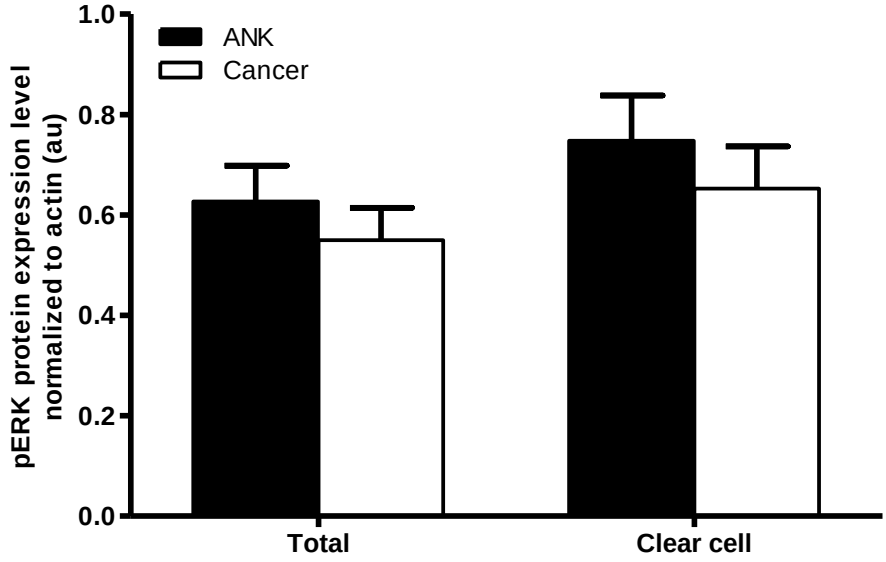

Figure 6: ERK activation is not enhanced in RCC. ERK (A) and pERK (B) protein expression levels in normal and cancerous tissue in all samples run (total) and upon further subdivision of individuals presenting with clear cell RCC. All data are presented as mean ± SE.

While ccRCC largely consists of cancerous cells, ANK contains multiple structures, including glomerulus and tubules (proximal and distal tubules). As ccRCC is widely regarded to arise from the proximal tubule epithelial cells (Neumann and Zbar, 1997; Maher and Kaelin, 1997; Choyke *et al.*, 2003), it is possible that RKIP may not be predominantly expressed in this cell population, which may result in the observed reduction of RKIP in ccRCC. To exclude this possibility, we determined the localization of RKIP in normal kidney tissues. Immunohistochemical (IHC) staining clearly detected RKIP in tubules but not in the glomerulus (Fig 7A). Among tubules, RKIP was predominantly detected in proximal tubular epithelial cells in comparison with distal tubular epithelial cells (Fig 7B). Furthermore, in comparison to proximal tubular epithelial cells in ANK (Fig 7B), ccRCC cancerous cells expressed substantially reduced RKIP (Fig 7C). The differential RKIP expression in ANK and ccRCC did not result from individual IHC procedures, as both ANK and ccRCC tissues were mounted on the same slides. Taken together, the above results demonstrate specific reduction of RKIP in ccRCC in comparison with the proximal tubular epithelial cells of ANK.

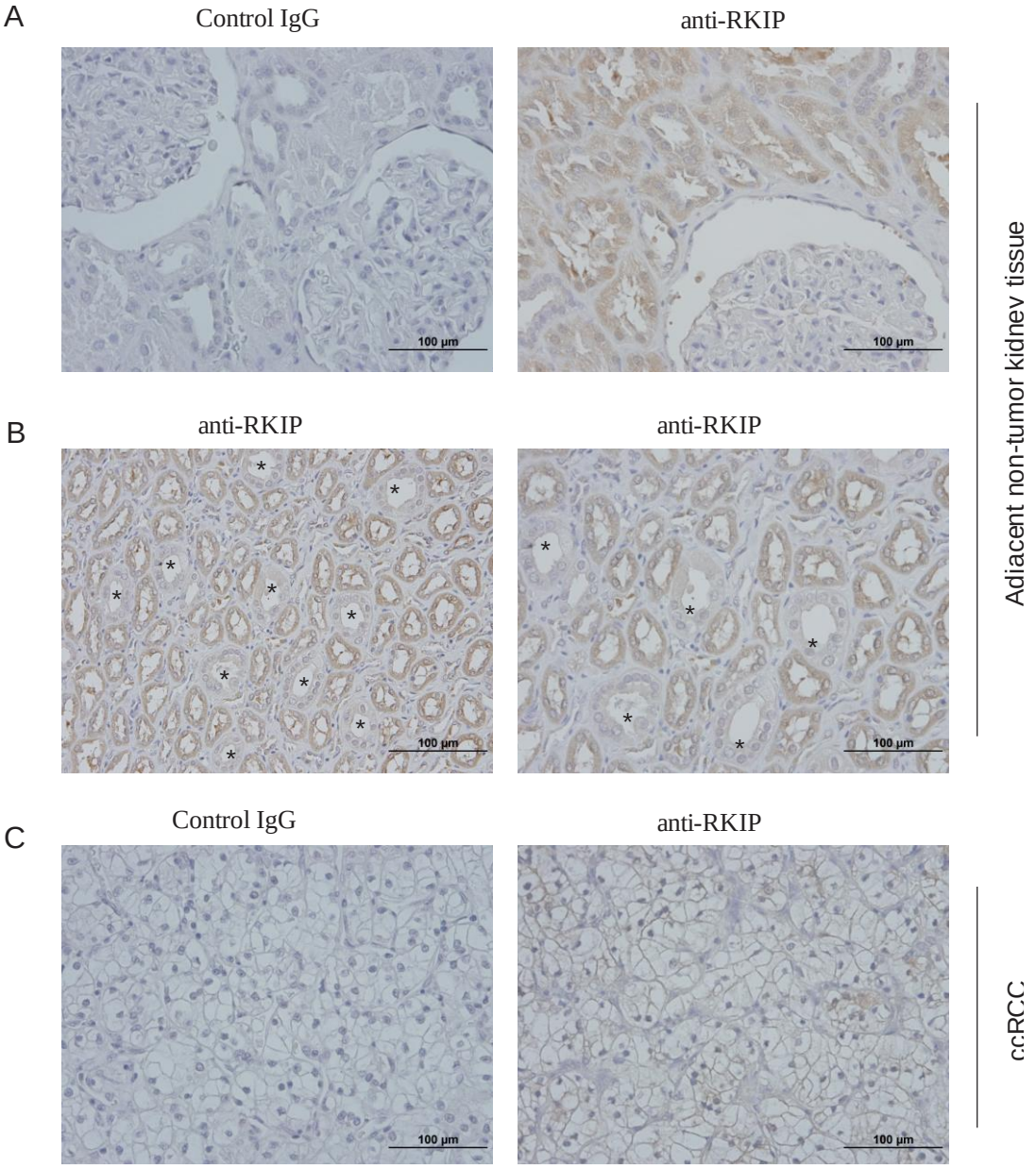

Figure 7: Immunohistochemistry (IHC) staining for RKIP in the adjacent non-tumour kidney tissue and in ccRCC. Both the non-tumour tissue and ccRCC were from the same patient and were mounted on the same slide. A), B) IHC staining of the adjacent non-tumour kidney tissues with anti-RKIP or control IgG. *: Distal tubules. C) ccRCC was stained with control IgG or anti-RKIP as indicated. Anti-RKIP was used at a dilution of 1:500. Images on the left were taken under 40X magnification and images on the right were taken under 60X magnification.

4.2. Reduction of RKIP is a common feature during ccRCC tumorigenesis and correlates with ccRCC progression

Based on our current knowledge, VHL (von Hippel-Lindau) is the dominant tumour suppressor of ccRCC, as mutation of VHL was observed in 70-80% of ccRCC (Kim and Kaelin, 2004; Razorenova *et al.*, 2011). It has also been reported that loss of a single VHL allele occurs in up to 97% of ccRCC tumours (Gnarra *et al.,* 1994; Foster *et al.,* 1994). Furthermore, the VHL pathway or events affected by VHL is being heavily targeted in developing therapies for patients with ccRCC (Grandinetti and Goldspiel, 2007; Yang *et al.*, 2003; Thompson Coon *et al.*, 2009; Bracarda *et al.*, 2007). To examine the magnitude of RKIP reduction during ccRCC tumourigenesis, we were able to show that among the 50 ccRCC patients in our patient cohort, the vast majority, 90% (45/50) of them expressed lower levels of RKIP than the ANK tissues (Fig 8A, Table 4). In line with publications (Kim and Kaelin, 2004; Razorenova *et al.*, 2011; Gnarra *et al.*, 1994; Foster *et al.,* 1994), we found reduction of VHL in 88% (44/50) of ccRCC patients in our cohort (Fig 8B). In 78% (39/50) of ccRCC patients both RKIP and VHL protein levels were reduced in comparison to ANK tissue and in the VHL reduced subpopulation RKIP was also found to be reduced in 89% (39/44) of these cases. These observations imply an intriguing possibility that RKIP, in addition to VHL, may be the second dominant tumour suppressor of ccRCC. Additional research is needed to elucidate the relationship between VHL and RKIP reduction as there are no current investigations ongoing.

A

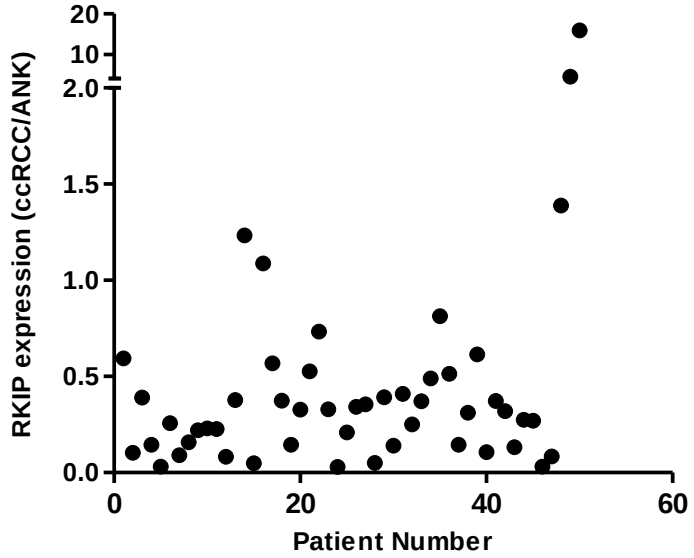

B

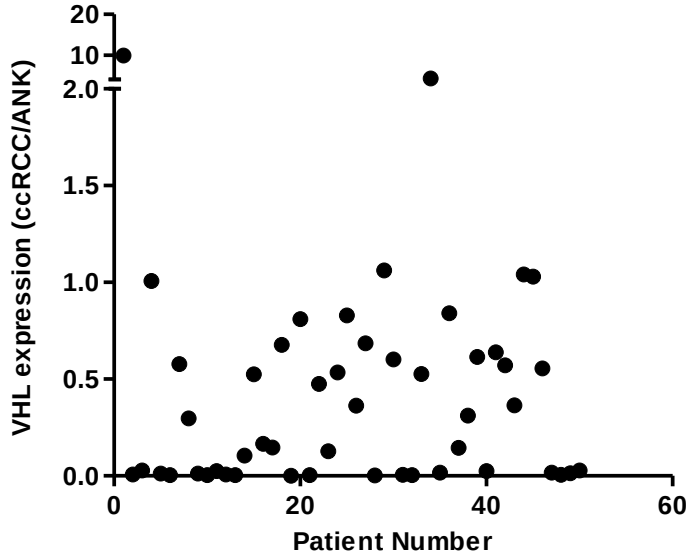

Figure 8: Reduction of RKIP (A) and VHL (B) in ccRCC. RKIP and VHL expression in ccRCC and its ANK tissues for all 50 patients were determined. RKIP or VHL expression was normalized against actin. The levels of normalized RKIP or VHL expression in ccRCCs relative to the normalized RKIP or VHL expression in the adjacent non-tumour kidney tissues.

Table 4: Patient's clinical information and their associated RKIP expression

Patients	Pathology	Age	Gender	Fuhrman	Metastasis	Tumor size	N.K	RCC	C/N
1$	ccRCC	54	M	3	No	5.5 cm	0.127717	0.07581	0.593
2#	ccRCC	65	M	4	Yes -lung	8 cm	0.674501	0.070167	0.104
3	ccRCC	54	F	4	Yes		1.741366	0.678187	0.389
4	ccRCC	54	M	1	No	3.6 cm	0.446428	0.064784	0.145
5#	ccRCC	48	M	3	No	6 cm	0.705356	0.02246	0.031
6	ccRCC	75	F	3	No	11 cm	0.169396	0.043553	0.257
7	ccRCC	38	M	2	No	2.9 cm	1.45	0.130922	0.090
8#	ccRCC	63	M	2	No	11.5 cm	2.370187	0.193881	0.081
9	ccRCC	77	M	2	No	6.5 cm	0.960128	0.151572	0.157
10	ccRCC	63	M	3	No	4.5 cm	1.30682	0.287429	0.219
11	ccRCC	70	F	1	No	4 cm	1.456749	0.334355	0.229
12	ccRCC	63	M	3	No	3.5 cm	1.382522	0.313858	0.227
13	ccRCC	58	M	2	No	2 cm	1.445312	0.546285	0.377
14¥	ccRCC	58	M	2	No	5.4 cm	0.486487	0.599981	**1.233**
15	ccRCC	51	M	1	No	4.5 cm	1.806974	0.087541	0.048
16¥	ccRCC	54	F	1	No	6.2 cm	0.63797	0.693541	**1.087**
17$	ccRCC	77	F	2	No	5.5 cm	1.269767	0.72066	0.567
18	ccRCC	48	M	3	No	13.5 cm	1.270234	0.475082	0.374
19	ccRCC	45	M	3	No	4.5 cm	1.043326	0.150719	0.144
20	ccRCC	41	F	1	No	6.2 cm	2.168121	0.711055	0.327
21$	ccRCC	68	M	3	No	6 cm	1.740729	0.916528	0.526
22	ccRCC	57	M	3	Yes	9 cm	0.564783	0.41376	0.732
23	ccRCC	55	M	4	No	13 cm	1.572677	0.519176	0.330
24#	ccRCC	76	M	2	Yes -bone	6.2 cm	1.596312	0.046612	0.029
25	ccRCC	68	F	2	No	3.5 cm	2.689019	0.560247	0.208
26	ccRCC	59	M	2	No	5.5 cm	0.818924	0.279611	0.341
27	ccRCC	49	F	2	No	5 cm	1.193792	0.42416	0.355

28[#]	ccRCC	43	M	2	No	3 cm	1.825573	0.092531	0.050
29	ccRCC	68	M	3	No	4.5 cm	0.458977	0.179648	0.391
30	ccRCC	50	M	1	No	1.7 cm	0.446257	0.062582	0.140
31	ccRCC	83	F	2	No	8 cm	0.699453	0.286779	0.410
32	ccRCC						0.767934	0.192831	0.251
33	ccRCC	56	F	3	No	3 cm	0.364325	0.135054	0.370
34	ccRCC	71	M	3	No	12.5 cm	0.175649	0.08613	0.490
35[¥]	ccRCC	67	F	2	No	3.2 cm	0.1326	0.107878	0.813
36[$]	ccRCC	62	M	3	No	3 cm	0.153308	0.078777	0.513
37	ccRCC		F	2	No	2 cm	0.40706	0.059358	0.145
38	ccRCC	91	F	2	No	2.7 cm	0.457912	0.14268	0.311
39	ccRCC	72	F	2	No	3.5 cm	0.496548	0.305436	0.615
40	ccRCC	48	F	2	No	1 cm	0.720965	0.077126	0.106
41	ccRCC	62	M	3	No	3.5 cm	0.138263	0.051452	0.372
42	ccRCC	75	M	2	No	6 cm	0.032308	0.010309	0.319
43	ccRCC	74	M	2	No	3.5cm	0.427803	0.05628	0.131
44	ccRCC	45	F	1	No	2.5 cm	0.348807	0.096062	0.275
45	ccRCC	48	M	1		5 cm	0.274534	0.07416	0.270
46	ccRCC	62	M	2	No		0.710442	0.022004	0.030
47	ccRCC	53	F	1	No	5.6 cm	0.574011	0.04837	0.084
48[¥]	ccRCC	61	M	1	No	5.5 cm	0.229504	0.318556	1.388
49[¥]	ccRCC	46	M	2	No	3.5 cm	0.032964	0.149353	4.53
50[¥]	ccRCC	49	F	1	No	4 cm	0.052059	0.828449	15.914

[#]: The ratios (ccRCC/ANK) of RKIP expression ≤ 0.1
[$]: The ratios (ccRCC/ANK) of RKIP expression = 0.5-0.6
[¥]: The ratios (ccRCC/ANK) of RKIP expression ≥ 0.8

To test the above possibility, we have examined RKIP expression in a large independent cohort of ccRCC patients. A set of tissue microarray (TMA) slides were purchased (US BioMax), which consisted of 45 normal kidney tissues, 501 cases (patients) of ccRCC, and a small number of other types of RCC (Table 5). This set of ccRCC contains sufficient number of cases in different stages of ccRCC development in terms of tumour stages and grades (Tables 6, 7). This large group of patients will therefore allow examination of the magnitude of RKIP reduction and the relationship of RKIP reduction to ccRCC progression.

To address these issues, immunohistochemical (IHC) staining was performed on these TMA slides to determine RKIP protein expression. TMA slides contained 616 tissue cores consisting of normal and cancer tissue from patients with ccRCC (Table 8). Each cancerous tissue core was in duplicate and all cores were manually examined. Tissue cores were excluded if the tissue was scratched or missing majority of the sample. As expected, strong RKIP staining was commonly observed in the tubules of the normal kidney and RKIP levels were substantially reduced in ccRCC (Fig 9).

IHC staining was scanned and quantified by converting IHC intensities to H-Scores according to published systems, in which H-Scores greater than 260 and less than 260 were considered positive and negative for RKIP staining, respectively (He *et al.*, 2010). Although H-Scores less than 260 were considered negative for RKIP staining there is still some RKIP staining present.

Table 5: Summary of Pathology Data

Pathology	Number of tissue cores
Normal	45
Clear cell RCC	501
Papillary	12
Carcinoma Sarcomatodes	16
Transition cell carcinoma	40
Chromophobe carcinoma	1
Collecting duct	1

Table 6: Tumour Stage Data

Tumour Stage	Number of Tissue Cores
T1N0M0	254
T2N0M0	183
T3N0M0	97
T4N0M0	6

Table 7: Tumour Grade Data

Tumour Grade	Number of Tissue Cores
1	277
2	194
3	15

Table 8: Summary of TMA Slide Data

Total number of cases	616
Normal cases	45
RCC cases	571
RCC cases without distant metastasis	556
Primary RCC cases with distant metastasis	15
Metastasis in other organs	8

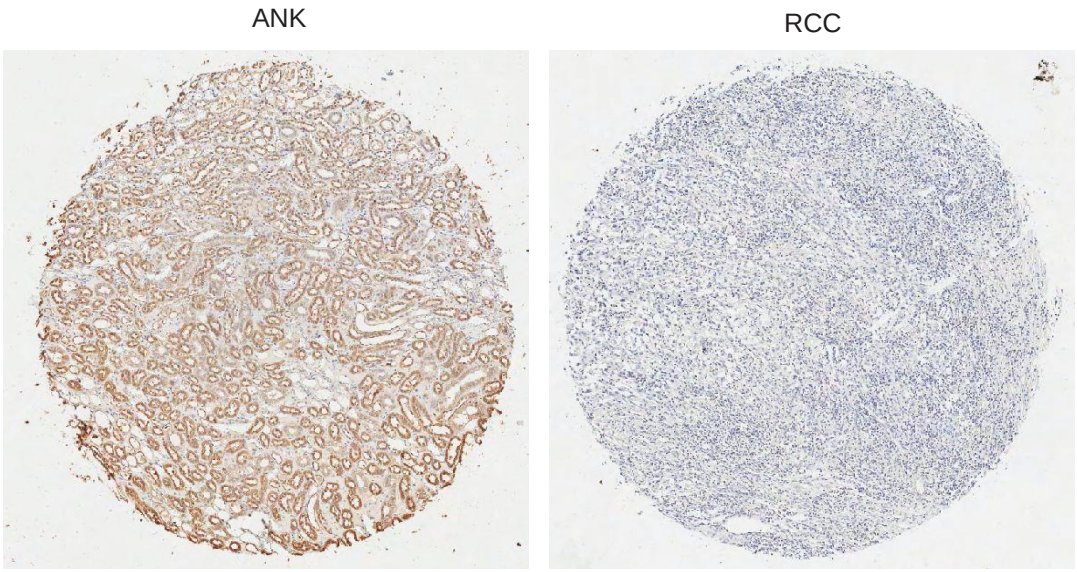

Figure 9: Representative immunohistochemical staining of normal and ccRCC kidney tissue on tissue microarray slides (TMA). Tissue cores were stained with anti-RKIP at a dilution of 1:500. Images were scanned at 20X magnification using ScanScope software.

As it was expected, majority of normal kidney tissue cores stained positive for RKIP with 93.3% of cores being positive (42 out of 45 tissues) (Fig 10). Conversely, significantly less ccRCC tissues stained positive for RKIP at just 19.3% (110 out of 571 tissue cores) (Fig 10). When the ccRCC tissue cores were further analyzed based on the Tumour-Node-Metastasis (TNM) tumour stage scale, it shows that the percentage of RKIP positive tissues was 20.9%, 22.9%, 11.3% and 0% for the tumours of T1N0M0, T2N0M0, T3N0M0 and T4N0M0 stages, respectively (Fig 11A). When analyzing tumour progression according to tumour grade, the percentage of RKIP positive tissues was 28.3%, 12.4% and 13.3% for tumour grade 1, 2 and 3 respectively (Fig 11B).

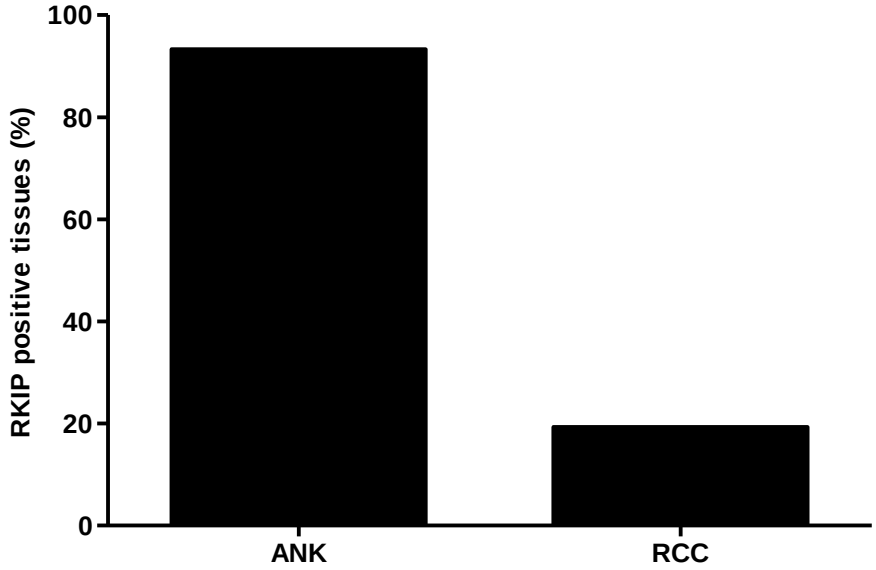

Figure 10: Percentage of tissue cores that stained positive for RKIP protein in normal adjacent (ANK) and RCC tissues. A H-Score > 260 was considered positive. 93.3 % of ANK tissues and 19.3% of RCC tissues were positive for RKIP protein.

A

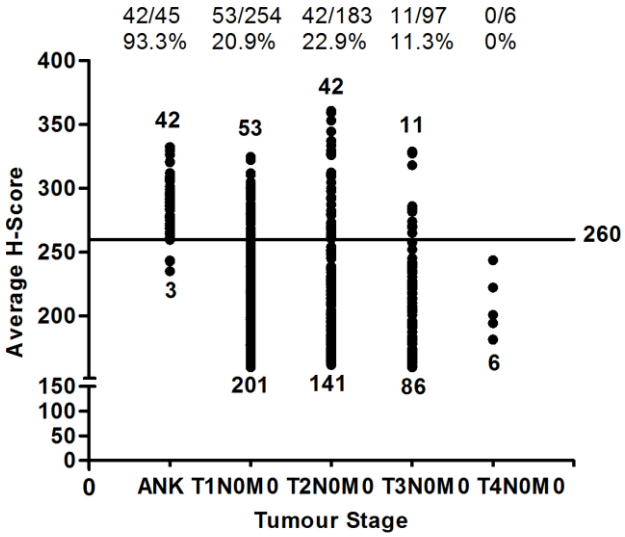

B

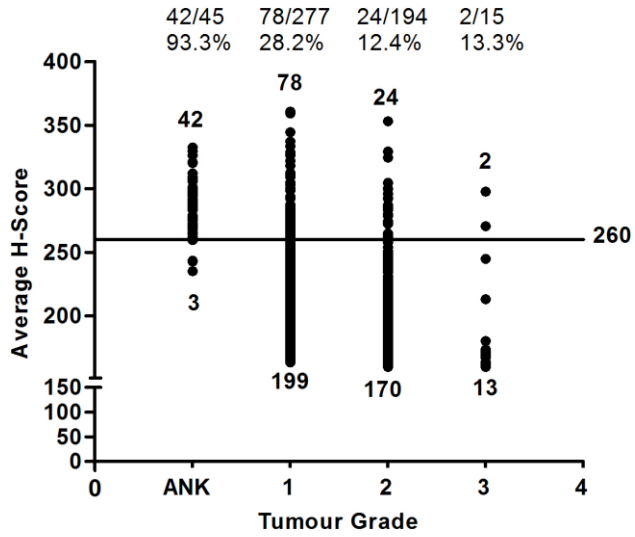

Figure 11: Percentage of RKIP positive tissue cores in normal tissue (ANK), and in ccRCC tissues divided based on tumour stage (T1N0M0, T2N0M0, T3N0M0, and T4N0M0) and tumour grade (1-3). A H-Score > 260 was considered positive for RKIP protein. Numbers above and below represent the number of tissue cores either positive or negative for RKIP staining. Percentages are listed at the top of each subgroup. Percent of RKIP positive tissues based on tumour stage (A) and tumour grade (B).

The TNM tumour stage scale describes the severity of a person's cancer based on the extent of the primary tumour and whether the cancer has spread to a distant site within the body (Thiery, 2002). The TNM tumour stage scale is based on the size of the primary tumour (T), the status of nearby (regional) lymph nodes (whether the cancer has spread to the lymph nodes) (N), and the presence of distant metastasis (M) (Thiery, 2002). Tumour grade classifies tumours based on how closely the cells resemble normal cells (Thiery, 2002). Specifically for RCC, the Fuhrman grade scale was adapted. This grade scale is based on the appearance of the nuclei of cancer cells and how different they are from normal nuclei (Fuhrman *et al.*, 1982).

The intensity of RKIP (H-Score) staining was also examined. The average H-Score was determined for normal kidney and adjacent kidney (ANK) tissue and for RCC tissues with T1N0M0, T2N0M0, T3N0M0 and T4N0M0 tumour stage (Fig 12). The average H-Score for ANK tissue was 284.28 ± 3.39, whereas, the average H-Score for T1N0M0, T2N0M0, T3N0M0 and T4N0M0 was 221.943 ± 2.51, 223.500 ± 3.50, 209.295 ± 4.05 and 203.932 ± 10.04, respectively (Fig 12). The H-Scores for T1N0M0, T2N0M0, T3N0M0 and T4N0M0 tissues were significantly lower ($p<0.001$) than the H-Score for ANK tissue (Fig 12). While RKIP was expressed in comparable levels between T1N0M0 and T2N0M0, the levels of RKIP were significantly reduced when ccRCC progressed to T3N0M0 ($p = 0.040$) (Fig 12). It should be noted that the sample size for T4N0M0 tissues was quite small (n=6) so there might not have been enough cases to reach significance. A Spearman's Rank Order correlation was used to determine the relationship between RKIP protein reduction and tumour stage progression. There is a

significant negative correlation (r_s = -0.272, p<0.01) present in which RKIP protein expression is reduced in advanced tumour stages. To confirm this relationship, we have combined T1N0M0 and T2N0M0 tumours into early stage tumours and T3N0M0 and T4N0M0 tumours into advanced stage tumours. The average H-Score for early and advanced stage RCC were 222.60 ± 2.06 and 208.98 ± 3.85 respectively (Fig 13). The abundance of RKIP protein in advanced stage RCC was significantly lower (p = 0.008) then the amount of RKIP protein found in early stage RCC (Fig 13). Collectively, these results support a relationship between RKIP reduction and ccRCC progression.

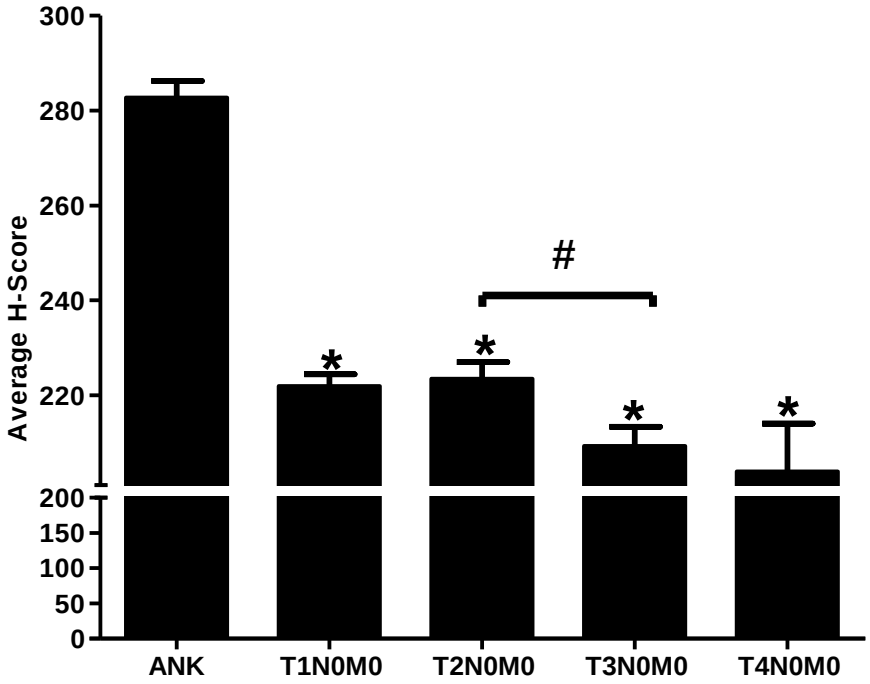

Figure 12: Average H-Score of ANK, T1N0M0, T2N0M0, T3N0M0 and T4N0M0 tissue cores. All data are presented as mean ± SE. * represents a significant difference of H-Score between ANK and T1N0M0, T2N0M0, T3N0M0 and T4N0M0 ($p<0.001$). # represents a significant difference of H-Score between T2N0M0 and T3N0M0 ($p = 0.040$).

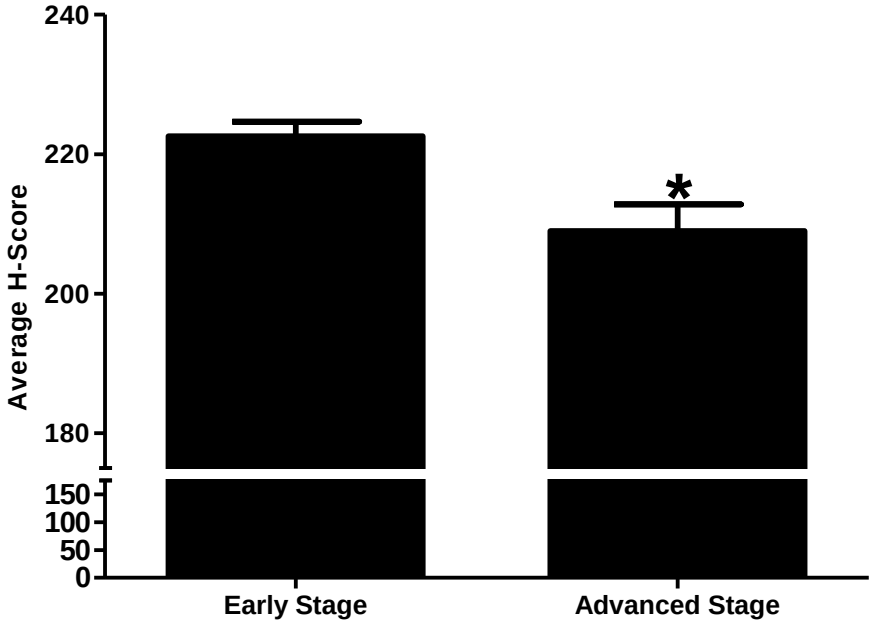

Figure 13: Average H-Score of early stage ccRCC (T1N0M0 and T2N0M0) and advanced stage ccRCC (T3N0M0 and T4N0M0) tissue cores. All data are presented as mean ± SE. * represents a significant difference between early stage and advanced stage ccRCC ($p = 0.008$).

To confirm this relationship, we were able to show that the average H-Score for ANK tissue was 284.28 ± 3.39, whereas the average H-Score for grades 1, 2, and 3 ccRCC tumours was 233.716 ± 2.55, 210.883 ± 2.74, and 192.353 ± 11.29, respectively (Fig 14). The H-Scores for tumour grades 1, 2, and 3 tissues were significantly lower ($p<0.001$) than the H-Score for ANK tissue. It was also found that grade 2 and 3 tissues had significantly lower ($p = 0.001$) amounts of RKIP protein then grade 1 tissues (Fig 13). Spearman's Rank Order correlation test revealed that there is a significant negative correlation between tumour grade progression and RKIP protein reduction ($r_s = -0.379$, $p<0.01$). Taken together, these observations demonstrate that reduction of RKIP correlates with ccRCC progression.

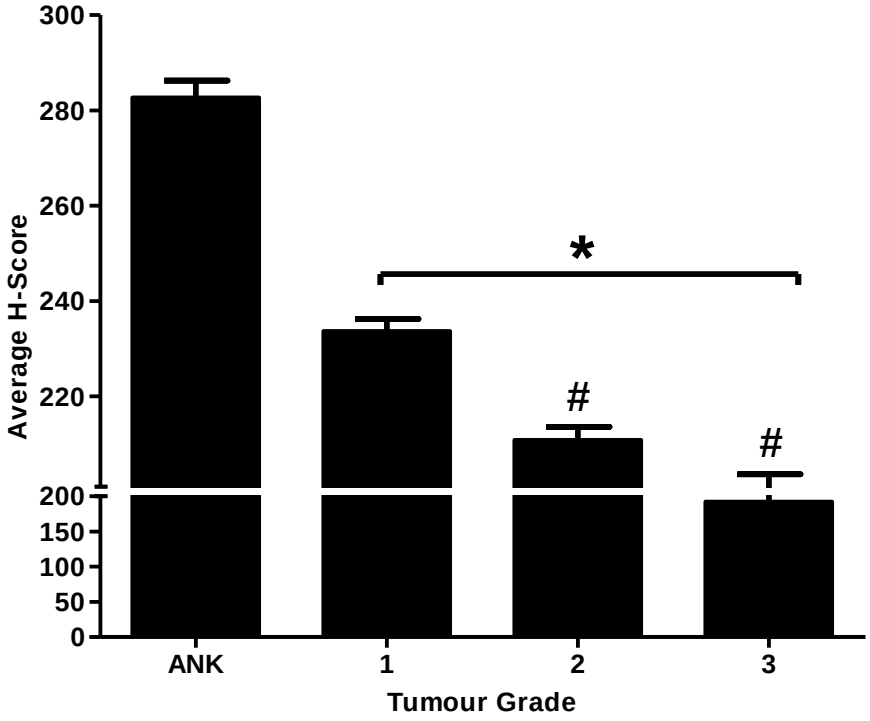

Figure 14: Average H-Score of ANK, grade 1, grade 2 and grade 3 tissue cores. All data are presented as mean ± SE. * represents a significant difference of H-core between ANK and grade 1, 2, and 3 (p<0.001). # represents a significant difference of H-Score between grade 1 and grade 2 and 3 (p = 0.001).

4.3. Potential association of RKIP reduction with ccRCC metastasis

Reduction of RKIP has been reported in metastatic prostate, breast, melanoma, colorectal cancers and gastrointestinal stromal tumours (Fu *et al.*, 2003; Keller *et al.*, 2005; Chatterjee *et al.*, 2004, Hagan *et al.*, 2005; Schuierer *et al.*, 2004; Al-Mulla *et al.*, 2006; Martinho *et al.*, 2009; Zlobec *et al.*, 2008a; Zlobec *et al.*, 2008b). Additionally, RKIP has been shown to have an effect on metastasis and invasion with reduced RKIP

levels being inversely proportional to invasion ability (Beshir *et al.*, 2010). To examine whether reduction of RKIP occurs in metastatic ccRCCs, the RCC tissues were also grouped according to metastatic ability (Fig 15). The TMA slides contained 571 ccRCC cases with 556 of those being organ (kidney)-confined ccRCC with no evidence of metastasis and 15 cases of primary ccRCC kidney tissue with evidence of metastasis (Table 8). In addition, the TMA slides also contained 8 cases of tissue harvested from metastatic sites (Table 8). The tissue from organs with RCC derived metastasis included the adrenal gland, bone, lymph node, lung, thyroid, intestine and spleen. The average H-Score for ANK, ccRCC cases without distant metastasis, ccRCC cases with distant metastasis and organ metastases were 284.28 ± 3.39, 219.87 ± 1.80, 203.82 ± 10.41 and 181.20 ± 6.26, respectively. Normal tissue was found to have significantly higher levels ($p< 0.001$) of RKIP then ccRCC cases without distant metastasis, ccRCC cases with distant metastasis and those that metastasized to other organs. Also those organ tissues with ccRCC derived metastasis had lower ($p = 0.022$) RKIP staining then ccRCC tissues with no presence of metastasis (Fig 15). All organ metastasized tissue was considered negative for RKIP staining. In 75% of cases (6/8 tissue cores) the H-Score in the organ metastases was lower than then H-Score in the matched RCC tissue (Fig 16). In line with other reports of RKIP expression in prostate cancer, breast cancer and melanoma (Fu *et al.*, 2003; Keller *et al.*, 2004a; Keller, 2004; Hagan *et al.*, 2005; Schuierer *et al.*, 2004), our results exhibit similar results with the highest levels of RKIP protein being detected in adjacent non- tumour kidney tissue, decreased with increasing tumour stage or tumour grade with no RKIP being detected in RCC derived organ metastasis.

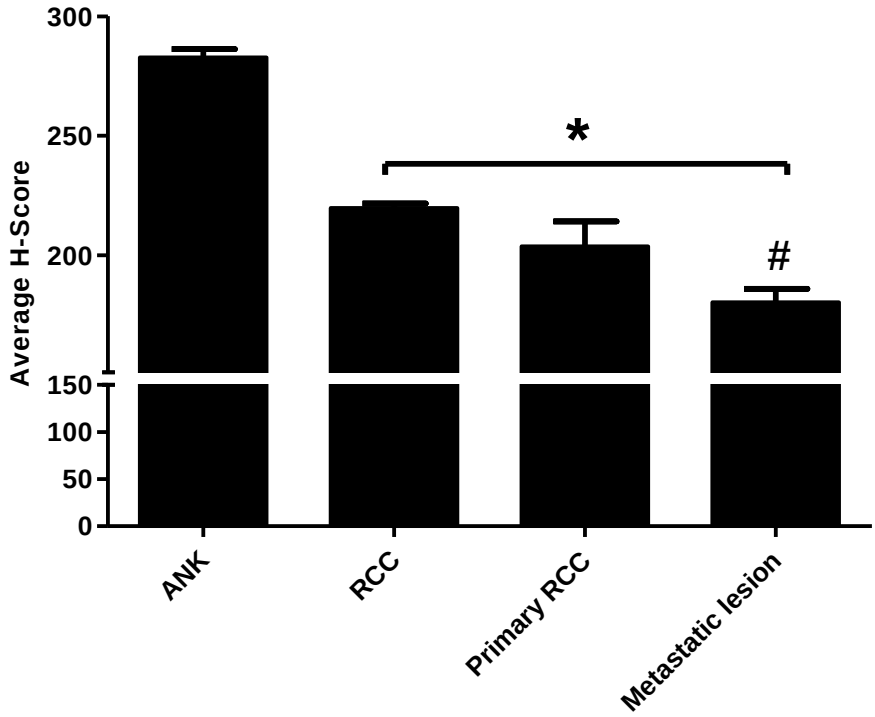

Figure 15: Average H-Score of ANK, RCC cases, primary RCC tissue with evidence of metastasis (n=15) and metastatic lesion tissue (n=8). All data are presented as mean ± SE. * represents a significant difference of H-Score between ANK and RCC, RCC with distant metastasis and organ metastases *(p*<0.001). # represents a significant difference of H-Score between RCC and organ metastases (*p* = 0.022).

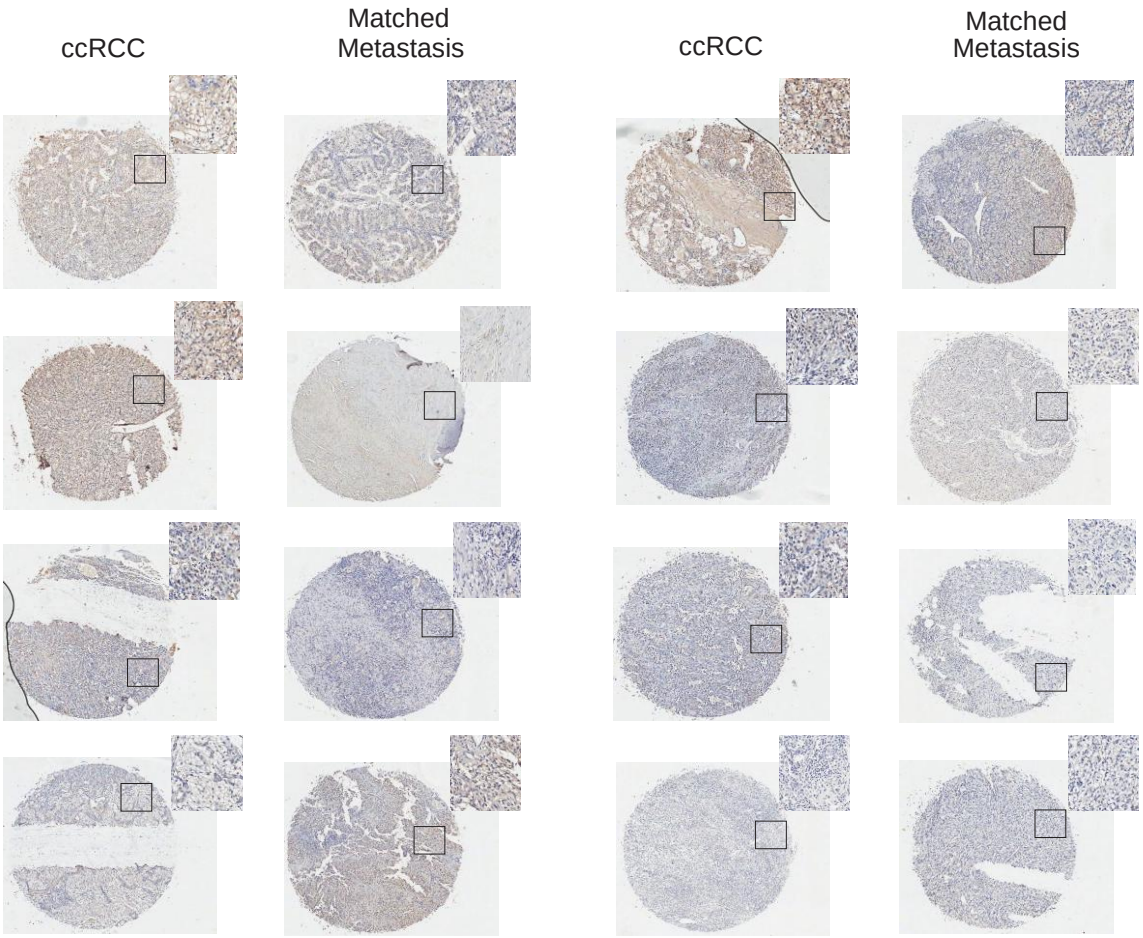

Figure 16: RKIP staining observed local ccRCC tissues with their matched organ metastasized tissue. Each ccRCC tissue represents an individual case with their matched organ metastasized tissue. Tissue cores were stained with anti-RKIP at a dilution of 1:500. Images were scanned at 20X magnification using ScanScope software. Highlighted regions were magnified 20 fold for visualization purposes.

One TMA slide contained follow-up patient data for 116 months. It was found that those pateints who died from ccRCC cancer had decreased amounts of RKIP protein (H-Score = 208.98 ± 2.06) then those pateints who were alive after 116 months (H-Score = 222.60 ± 2.06) (results not shown). Although this did not reach significance (p = 0.223) because of the small size of patients with follow-up information, there is a trend present in which lower levels of RKIP result in a poor prognosis. Taken together,

evidence indicates that RKIP is further reduced in metastasized ccRCC. These results confirm the metastatic process in ccRCC involes a reduction or loss of RKIP expression and form a case for RKIP to be a potential novel prognostic marker in ccRCC. However, further experiments will be needed to address this issue using a large patient population.

4.4. The levels of RKIP mRNA correlate with RKIP levels in ccRCC

To investigate the mechanisms responsible for the observed reduction of RKIP in ccRCC, we have examined the levels of RKIP mRNA using real time PCR. While ANK tissues consist of multiple cell types derived from glomeruli and distal tubules, RKIP is predominantly expressed in proximal tubule epithelial cells (Fig 7B). As there is no bona fide markers available specific for the proximal tubular epithelial cells, in which ccRCC is originated, it is impossible to compare the abundance of RKIP mRNA in the proximal tubular epithelial cells with that in ccRCC. However, we noticed that the RKIP protein levels in ccRCC vary significantly (Table 4). Therefore, we have examined whether the levels of RKIP mRNA correlates with the abundance of RKIP protein in individual ccRCCs. We first grouped ccRCCs into three levels, based on the ratios of RKIP protein between ccRCC/ANK (Table 4) and extracted RNA from three groups of patients whose RKIP protein expression between cancer/ANK was low (≤ 0.1), medium (0.5-0.6) or high (≥ 0.8) (Table 4). Semi-quantitative real time PCR (qRT-PCR) was performed on representative tissues from each group. Actin was used as an internal control and VEGF-A was used as a tumour associated marker to confirm the tissue mRNA that was

extracted was in fact from tumour tissue (Fig 17). RKIP gene expression in cancer tissue followed the same trend as what was observed in RKIP protein expression. RKIP mRNA abundance was significantly higher in both the cancer medium (p = 0.046) and high (p = 0.011) protein expression group then in the cancer low protein expression group (Fig 18). RKIP mRNA abundance was also higher (p=0.061) in the cancer high protein expression group when compared to the medium protein expression group.

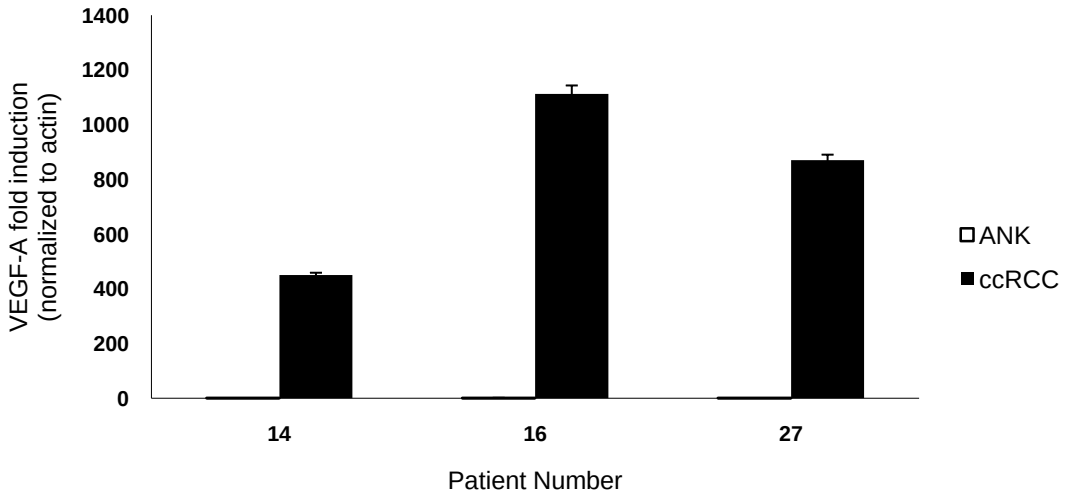

Figure 17: Representative individual samples of VEGF-A mRNA fold induction in patients 14, 16 and 27. VEGF-A was used as a tumour associated marker to verify tumour tissue in our data set. Samples with no increase of VEGF-A in ccRCC sample compared to normal were removed from the data set. VEGF-A fold induction was normalized to actin.

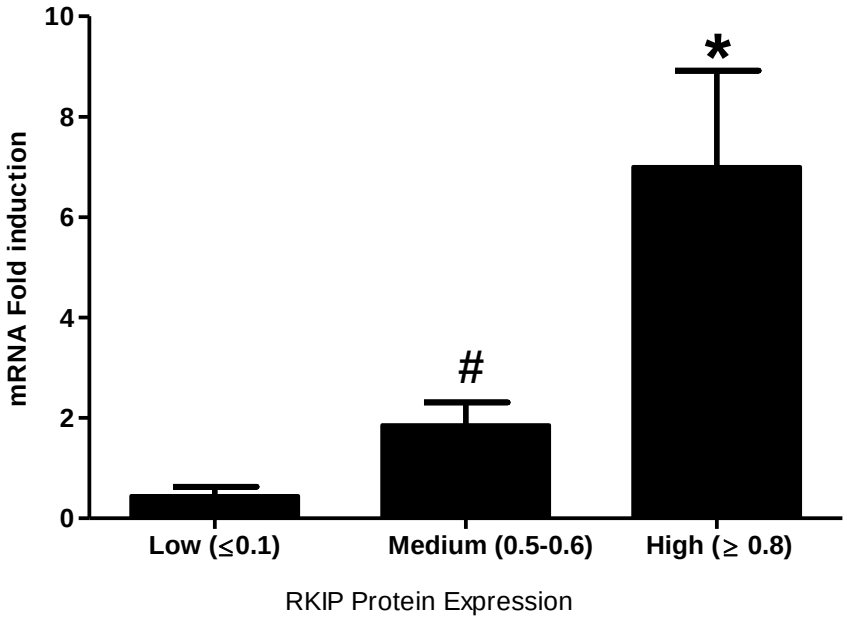

Figure 18: RKIP mRNA abundance at low, medium and high RKIP protein expression groups in ccRCC tissues. All data are presented as mean ± SE. Each group contained three representative samples. * represents significant difference between cancer low protein expression and cancer high protein expression groups ($p = 0.011$). # represents significant difference between cancer low protein expression and cancer medium protein expression groups ($p = 0046$).

The observed correlation of RKIP mRNA levels and RKIP protein abundance in ccRCC suggests that transcription may play a role in RKIP expression. Evidence supporting this scenario has reported RKIP promoter methylation in colorectal cancer (Al-Mulla *et al.,* 2008) but not in prostate cancer (Beach *et al.,* 2008). To investigate whether promoter methylation plays a role in RKIP reduction in ccRCC, we were able to show that in comparison to human proximal tubular epithelial HK2 cells, RKIP protein was modestly and significantly reduced in 786-O and A498 ccRCC cells, respectively (Fig 19). Therefore, if promoter methylation contributes to RKIP reduction, decreases in

promoter methylation should impact RKIP protein expression more in A498 cells than in 786-O cells. Indeed, in the presence of a DNA methyltransferase inhibitor 5-aza-2'-deoxycytidine (5-aza-dC), RKIP expression was enhanced only in A498 cells at both mRNA and protein levels ($p = 0.0234$) (Figs 20, 21). Taken together, the above observations support the concept that promoter methylation contributes to reduction in RKIP in ccRCC.

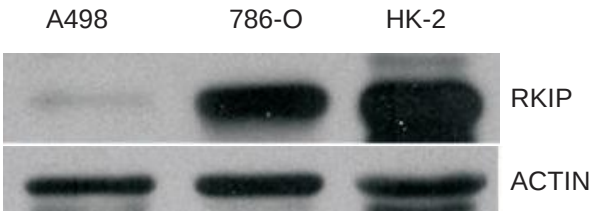

Figure 19: Reduction of RKIP in RCC cell lines. Human proximal tubular epithelial cells (HK-2) and RCC cell lines (786-O and A498) were examined by western blot for the expression of RKIP and actin. Experiments were repeated twice and a representative was shown.

A

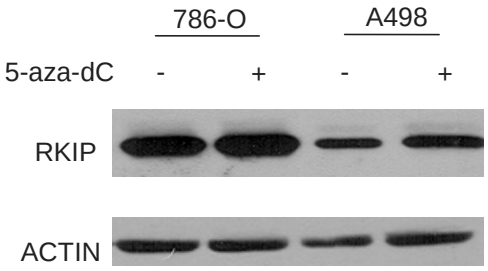

B

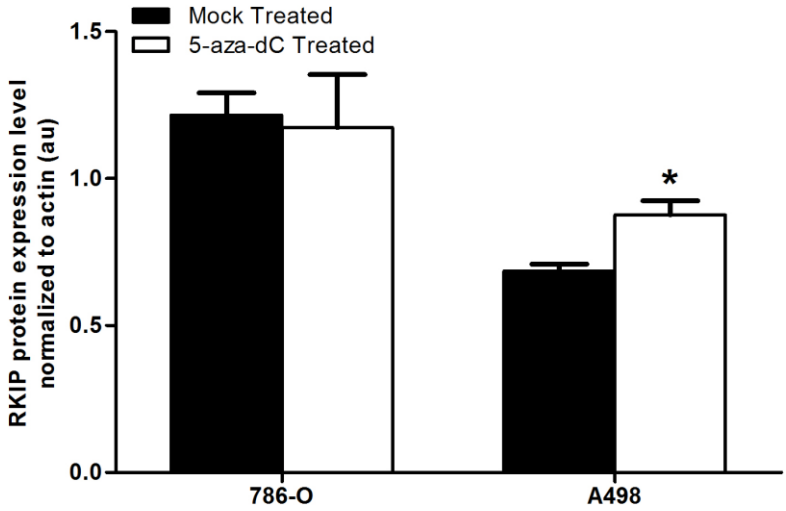

Figure 20: Representative western blot analysis (A) of RKIP protein expression levels in 786-O and A498 cell lines either mock treated or treated with 5-aza-dC for 48 hours. Experiments were repeated three times and a representative was shown. (B) Protein levels were normalized to actin. All data are presented as mean ± SE. * Represents significant difference between A498 mocked treated and A498 5-aza-dC treated cells (p = 0.0234).

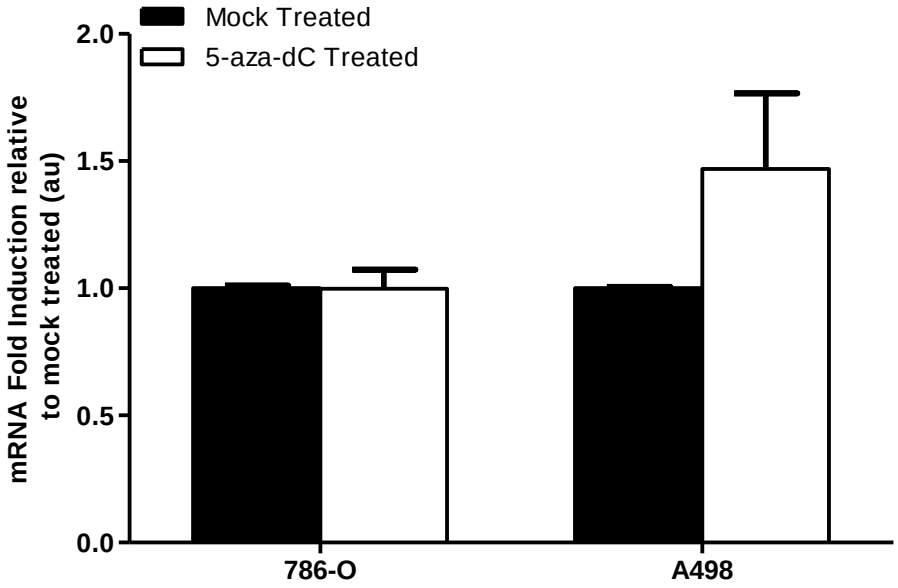

Figure 21: RKIP mRNA abundance in 786-O and A498 cell lines either mock treated or treated with 5-aza-dC for 48 hours. Experiments were repeated in triplicate. All data are presented as mean ± SE.

4.5. RKIP inhibits ccRCC invasion *in vitro*

Specific reduction of RKIP in ccRCC suggests that RKIP may inhibit ccRCC tumourigenesis. To examine this possibility, we have stably overexpressed RKIP in A498 and 786-O cells (Fig 22). In comparison to empty vector (EV) cells, ectopic RKIP did not affect the proliferation of A498 and 786-O cells (Fig 22). Additionally, knockdown of RKIP in both lines (Figs 23, 24) also had no effect on their proliferation (Fig 25). These observations are consistent with reported findings that modulation of RKIP did not affect the proliferation of breast, prostate and ovarian cancer cells (Fu *et al.*, 2003; Dangi-Garimella *et al.*, 2009; Li *et al.*, 2008).

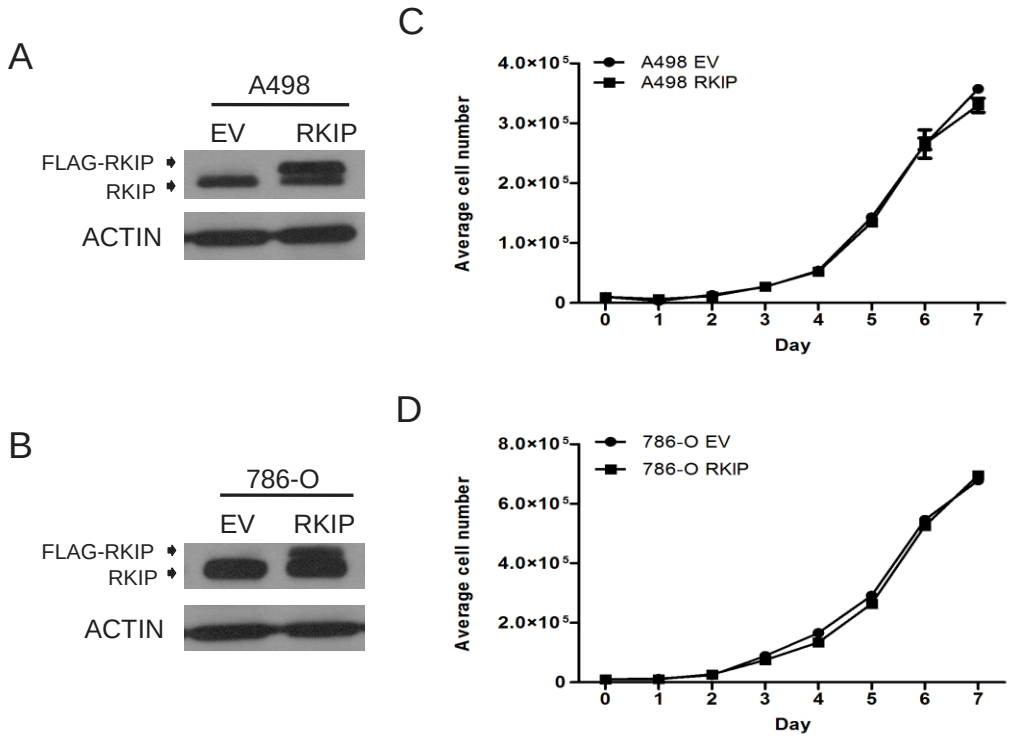

Figure 22: Western blot analysis showing endogenous expression of RKIP as well as FLAG tagged RKIP in A498 (A) and 786-O (B) cells. Experiments were repeated twice and a representative was shown. Cell proliferation assay of ectopic RKIP in A498 (C) and 786-O (D) cells over a seven day time course. Cells were seeded at a density of 10^4 and cell counts were made every 24 hours in triplicate. All data is presented as mean ± SE.

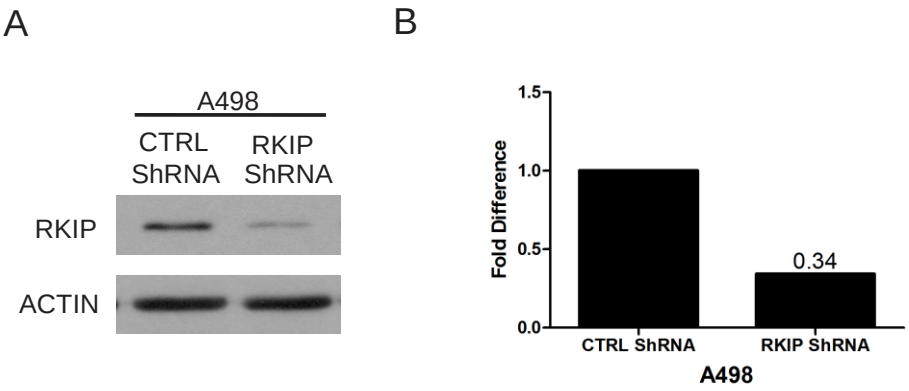

Figure 23: (A) Western blot analysis showing knockdown of RKIP in A498 cells. Experiments were repeated twice and a representative was shown. (B) Densitometry analysis of RKIP knockdown in A498 cells. RKIP protein expression was knocked down 66% relative to control cells.

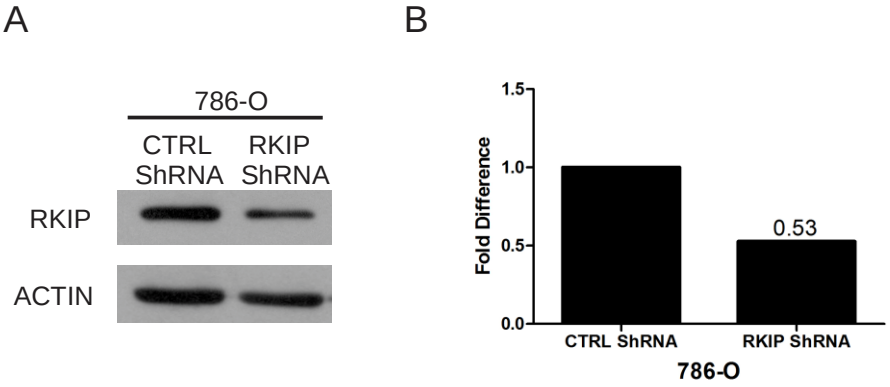

Figure 24: (A) Western blot analysis showing knockdown of RKIP in 786-O cells. Experiments were repeated twice and a representative was shown. (B) Densitometry analysis of RKIP knockdown in 786-O cells. RKIP protein expression was knocked down 47% relative to control cells.

A

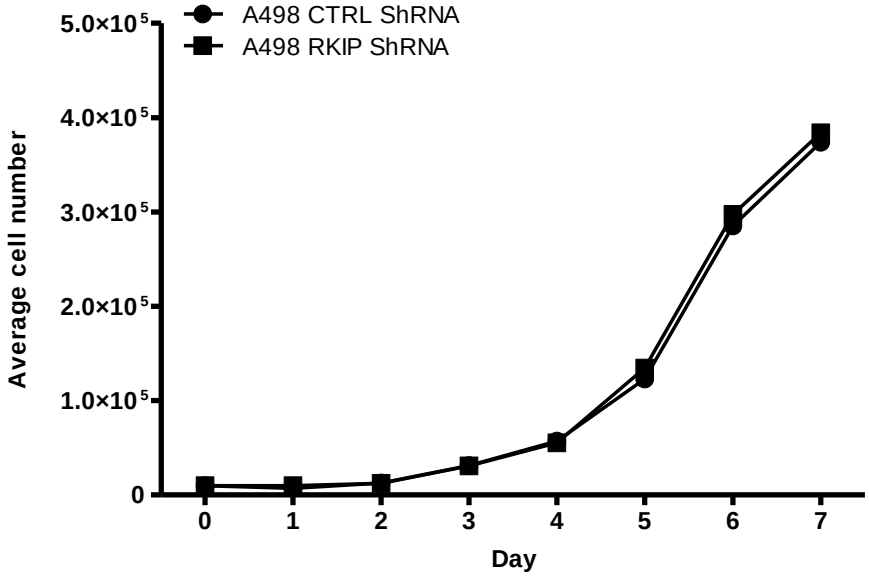

B

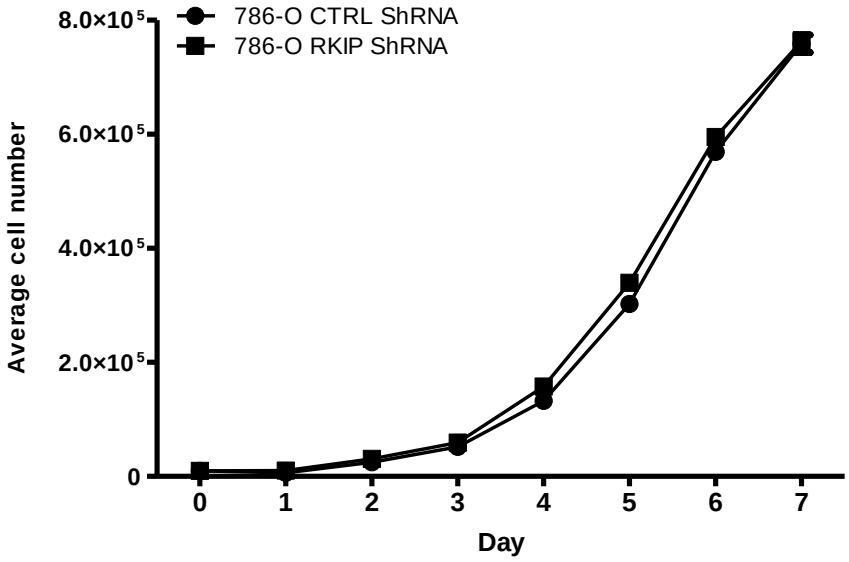

Figure 25: Cell proliferation assay of knockdown RKIP in A498 (A) and 786-O (B) cells over a seven day time course. Cells were seeded at a density of 10^4 and cell counts were made every 24 hours in triplicate. All data is presented as mean ± SE.

RKIP has been reported to inhibit cancer metastasis (Hagan *et al.,* 2005; Schuierer *et al.,* 2004, Minoo *et al.,* 2007, Li *et al.,* 2008). Metastatic ccRCC is often fatal for the majority of patients who develop the disease with 5 year survival rates of only 5-10% (Pantuck *et al.,* 2001; Brugarolas *et al.,* 2007). As cell's *in vitro* invasion ability correlates with their capacity of metastasis, we have determined whether modulation of RKIP impacts the invasion abilities of A498 and 786-O cells. Ectopic RKIP reduced A498 ($p = 0.0071$) and 786-O ($p = 0.0494$) cell's invasion abilities (Figs 26, 27). Conversely, knockdown of RKIP in both cell lines enhanced A498 ($p = 0.0023$) and 786-O ($p = 0.0013$) cell's invasion capacities (Figs 28, 29).

To further investigate RKIP-mediated inhibition of ccRCC cells, we observed that overexpression of RKIP and knockdown of RKIP slightly reduced ($p = 0.169$) and enhanced ($p = 0.008$) N-cadherin expression in A498 cells, respectively (Figs 30, 31). Ectopic RKIP significantly reduced ($p = 0.048$) vimentin expression, while knockdown of RKIP dramatically enhanced ($p = 0.001$) vimentin expression in A498 cells (Figs 30, 31). High levels of N-cadherin and vimentin are well known to associate with EMT (epithelial to mesenchymal transition) (Lee *et al.,* 2006b; Mendez *et al.,* 2010; Nieman *et al.,* 1999) and EMT plays the critical role in cancer metastasis (Guarino *et al.,* 2007; Steeg, 2006; Thiery, 2002; Leber and Efferth, 2009). Taken together, our observation that RKIP reduces the expression of both proteins suggests that RKIP may inhibit EMT in ccRCC.

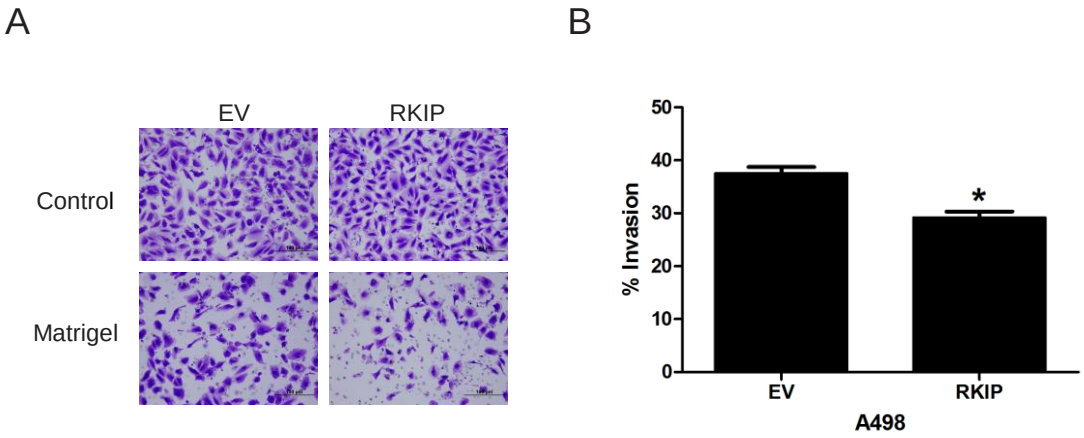

Figure 26: (A) Representative images of A498 EV and A498 RKIP invasion potential though either control or Matrigel membranes. Cells were stained with crystal violet and images were taken at 20X magnification. (B) Invasion potential of A498 EV and A498 RKIP cells. Experiments were repeated three times. All data is presented as mean ± SE. * represents significant difference between A498 EV and A498 RKIP invasion capacity (p = 0.0071).

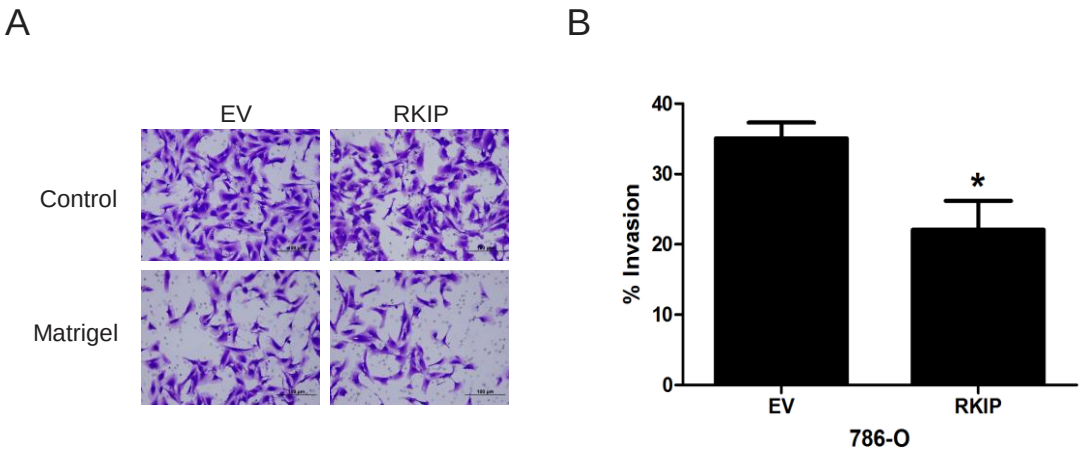

Figure 27: (A) Representative images of 786-O EV and 786-O RKIP invasion potential though either control or Matrigel membranes. Cells were stained with crystal violet and images were taken at 20X magnification. (B) Invasion potential of 786-O EV and 786-O RKIP overexpression cells. Experiments were repeated three times All data is presented as mean ± SE. * represents significant difference between 786-O EV and 786-O RKIP invasion capacity (p = 0.0494).

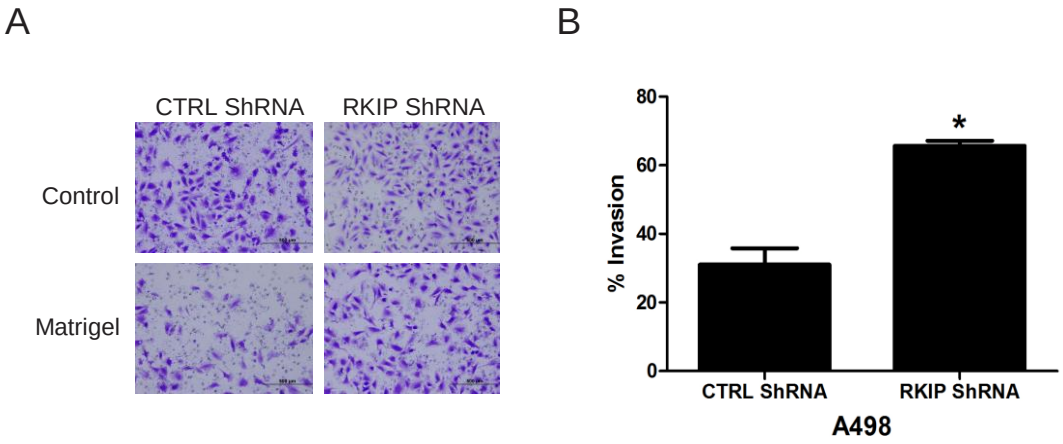

Figure 28: (A) Representative images of A498 CTRL ShRNA and A498 RKIP ShRNA invasion potential though either control or Matrigel membranes. Cells were stained with crystal violet and images were taken at 20X magnification. (B) Invasion potential of A498 CTRL ShRNA and RKIP ShRNA knockdown cells. Experiments were repeated three times. All data is presented as mean ± SE. * represents significant difference between A498 CTRL ShRNA and A498 RKIP ShRNA invasion capacity (p = 0.0023).

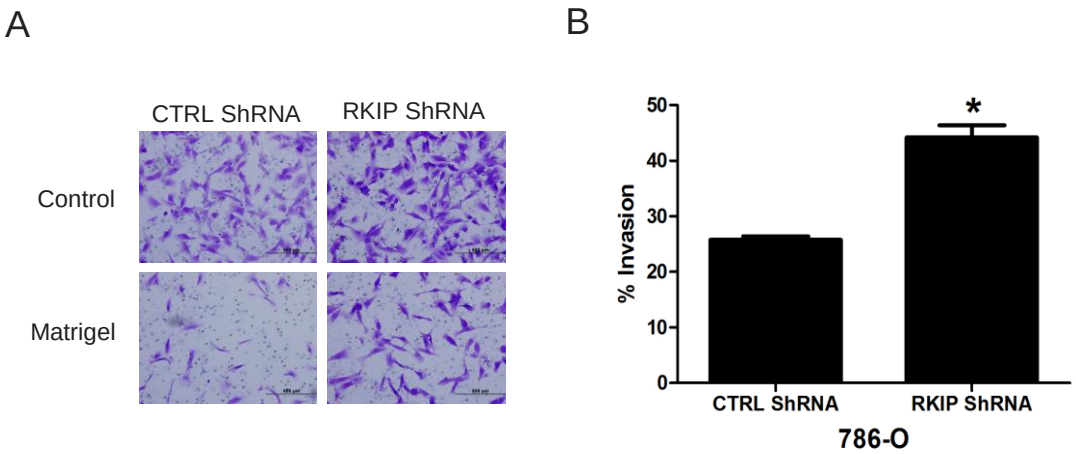

Figure 29: (A) Representative images of 786-O CTRL ShRNA and 786-O RKIP ShRNA invasion potential though either control or Matrigel membranes. Cells were stained with crystal violet and images were taken at 20X magnification. (B) Invasion potential of 786-O CTRL ShRNA and 786-O RKIP ShRNA knockdown cells. Experiments were repeated three times. All data is presented as mean ± SE. * represents significant difference between 786-O CTRL ShRNA and 786-O RKIP ShRNA invasion capacity (p = 0.0013).

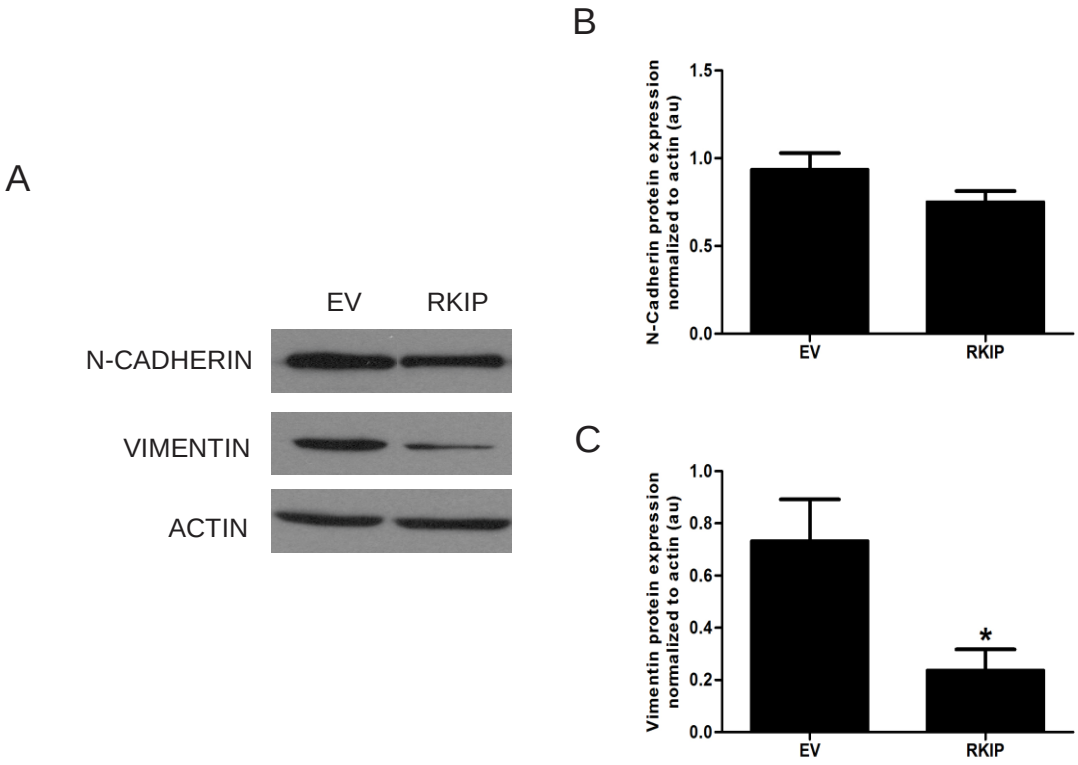

Figure 30: Epithelial-Mesenchymal transition (EMT) markers. (A) Representative western blot of N-cadherin, vimentin and actin protein expression in A498 control cells (EV) and A498 cells overexpressing RKIP (RKIP). Experiments were repeated three times and a representative was shown. Protein expression of N-cadherin (B) and vimentin (C) in A498 EV and A498 RKIP cells. All data is presented as mean ± SE. * represents a significant difference between A498 EV and A498 RKIP vimentin protein expression ($p = 0.048$).

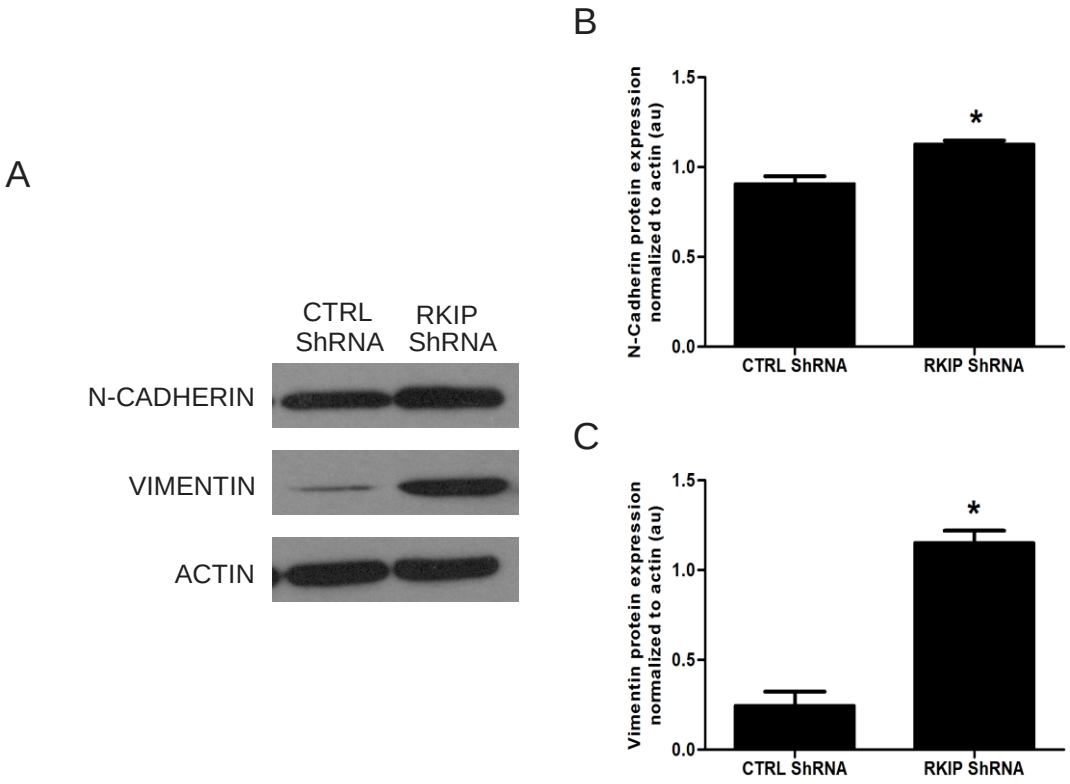

Figure 31: Epithelial-Mesenchymal transition (EMT) markers. (A) Representative western blot of N-Cadherin, Vimentin and Actin protein expression in A498 control cells (CTRL ShRNA) and A498 cells with knocked down RKIP expression (RKIP ShRNA). Experiments were repeated three times and a representative was shown. Protein expression of N-Cadherin (B) and vimentin (C) in A498 CTRL ShRNA and A498 RKIP ShRNA cells. All data is presented as mean ± SE.
* represents significant difference between A498 CTRL ShRNA and A498 RKIP ShRNA N-Cadherin ($p = 0.008$) and vimentin protein expression ($p = 0.001$).

4.6. RKIP does not inhibit A498 cells-derived xenograft tumours in NOD/SCID mice

RKIP has been reported to have no effect on primary tumour formation but effect the formation of metastasis in immunocompromised mice (Fu *et al.*, 2003; Dangi-Garimella *et al.*, 2009). To examine the impact of RKIP modulation on xenograft tumour formation, NOD/SCID mice were subcutaneously implanted with $3x10^6$ A498 EV, RKIP,

CTRL ShRNA, or RKIP ShRNA cells on one side of their flanks only. Tumour volume was calculated based on length and width tumour measurements performed weekly according to the following formula; $L \times W^2 \times 0.52$, where *L* and *W* are the longest and shortest diameters respectively (He *et al,* 2011). The expression of ectopic RKIP in xenograft tumours was confirmed (Fig 32A). In comparison with A498 EV cells, ectopic RKIP did not affect A498 cells forming xenograft tumours (Fig 32B). Furthermore, knockdown of RKIP also was found to have no effect on A498 cell's ability of forming xenograft tumours (Fig 33B), although RKIP was still knockdown in the xenograft tumours (Fig 33A). Taken together, our observations are in line with reports showing that RKIP does not affect primary tumour growth proliferation rate (Fu *et al.*, 2003; Keller, 2004).

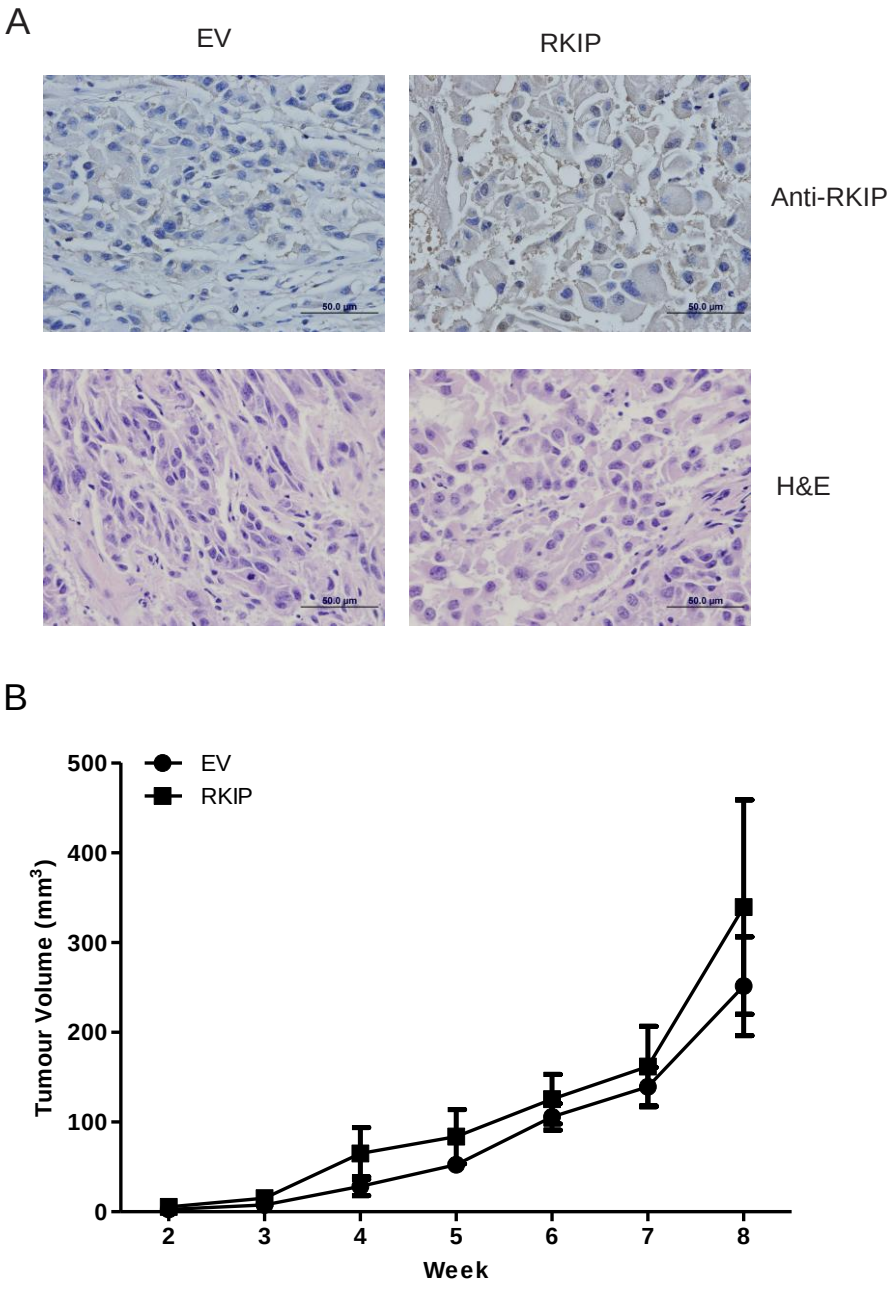

Figure 32: Subcutaneous injection of A498 EV and A498 RKIP cells into NOD/SCID mice. (A) RKIP IHC and H&E staining on tumour sections isolated from mice. Images were taken at 60X magnification. (B) Tumour volume was calculated weekly based on the following formula; $L \times W^2 \times 0.52$, where L and W are the length and width accordingly. Each group contained five mice. All data is presented as mean ± SE.

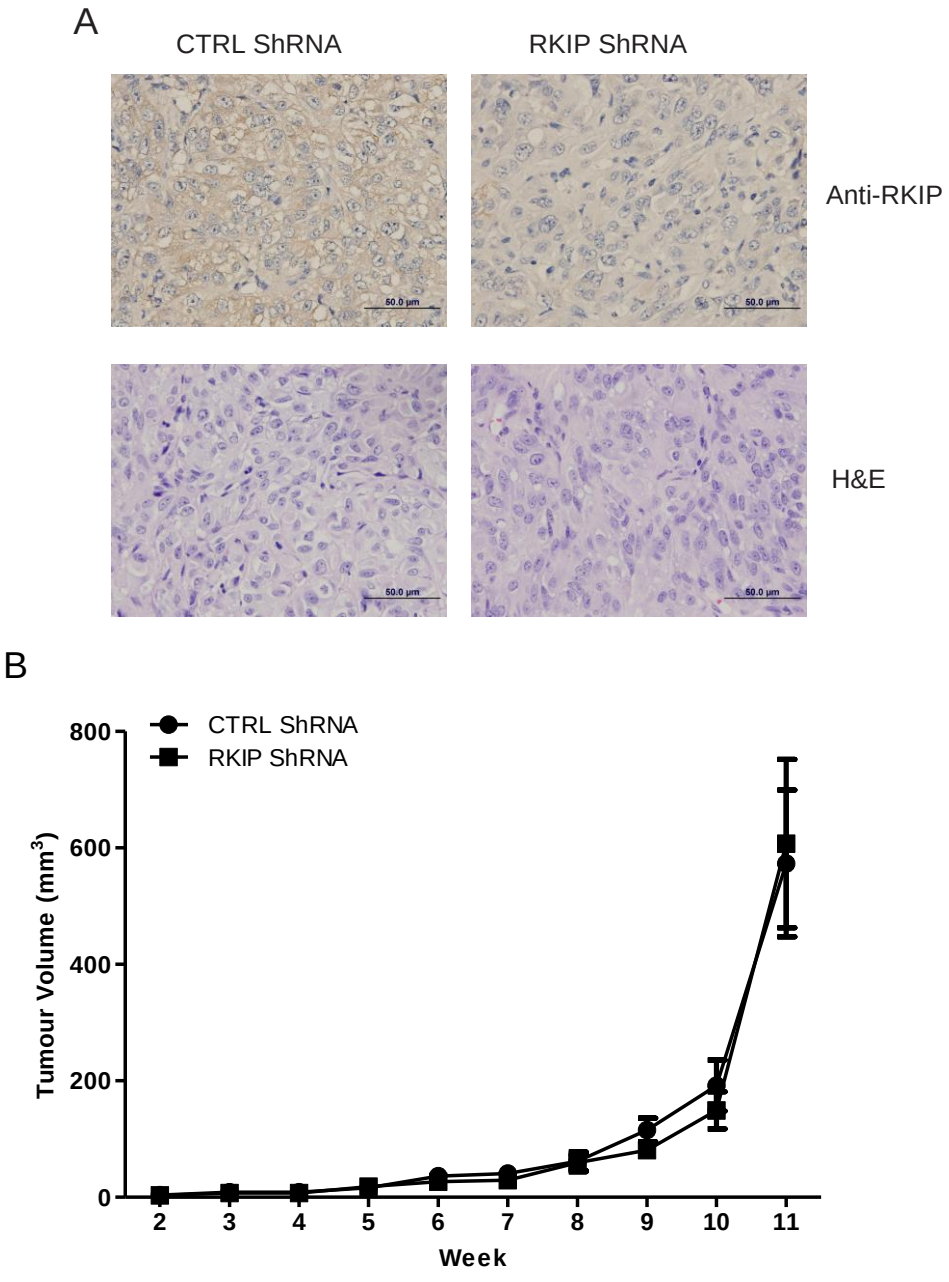

Figure 33: Subcutaneous injection of A498 CTRL ShRNA and A498 RKIP ShRNA cells into NOD/SCID mice. (A) RKIP IHC and H&E staining on tumour sections isolated from mice. Images were taken at 60X magnification. (B) Tumour volume was calculated weekly based on the following formula; L x W^2 x 0.52, where L and W are the length and width accordingly. Each group contained five mice. All data is presented as mean ± SE.

4.7. RNA Microarray analysis on A498 cells

To help understand possible mechanisms behind RKIP reduction found in ccRCC, the Affymetrix Human Gene 1.0 ST microarray was purchased to evaluate any changes in gene expression in A498 cells when RKIP is knocked down. The microarray slide contained over 28,869 genes with 764,885 distinct probes. All raw analysis was performed at the University Health Network Microarray Center located in Toronto, ON. After filtering, which removes any probes that did not show any expression in any of the samples, there were 23,392 distinct probes remaining. It was observed that 59 genes changed their expression (Table 9) by at least 1.5 fold in RKIP ShRNA cells compared to CTRL ShRNA cells (Fig 33, Table 9). It was found that RKIP mRNA was reduced 1.65 fold in knockdown cells compared to control A498 cells. A heat map showing changes in gene regulation was generated for all 59 genes and for the 10 top genes (Figs 34, 35). The Ingenuity Systems Pathway Analysis software (Ingenuity Systems, Redwood City, CA) was used to generate insights based on raw microarray data. The top biological functions found to change in RKIP knockdown cells compared to control A498 cells are: cell to cell signaling and interaction, cellular movements and inflammatory response/disease. These top biological functions are consistent with our *in vitro* results as it has been demonstrated that RKIP knockdown A498 cells are more invasive and have increased mobility.

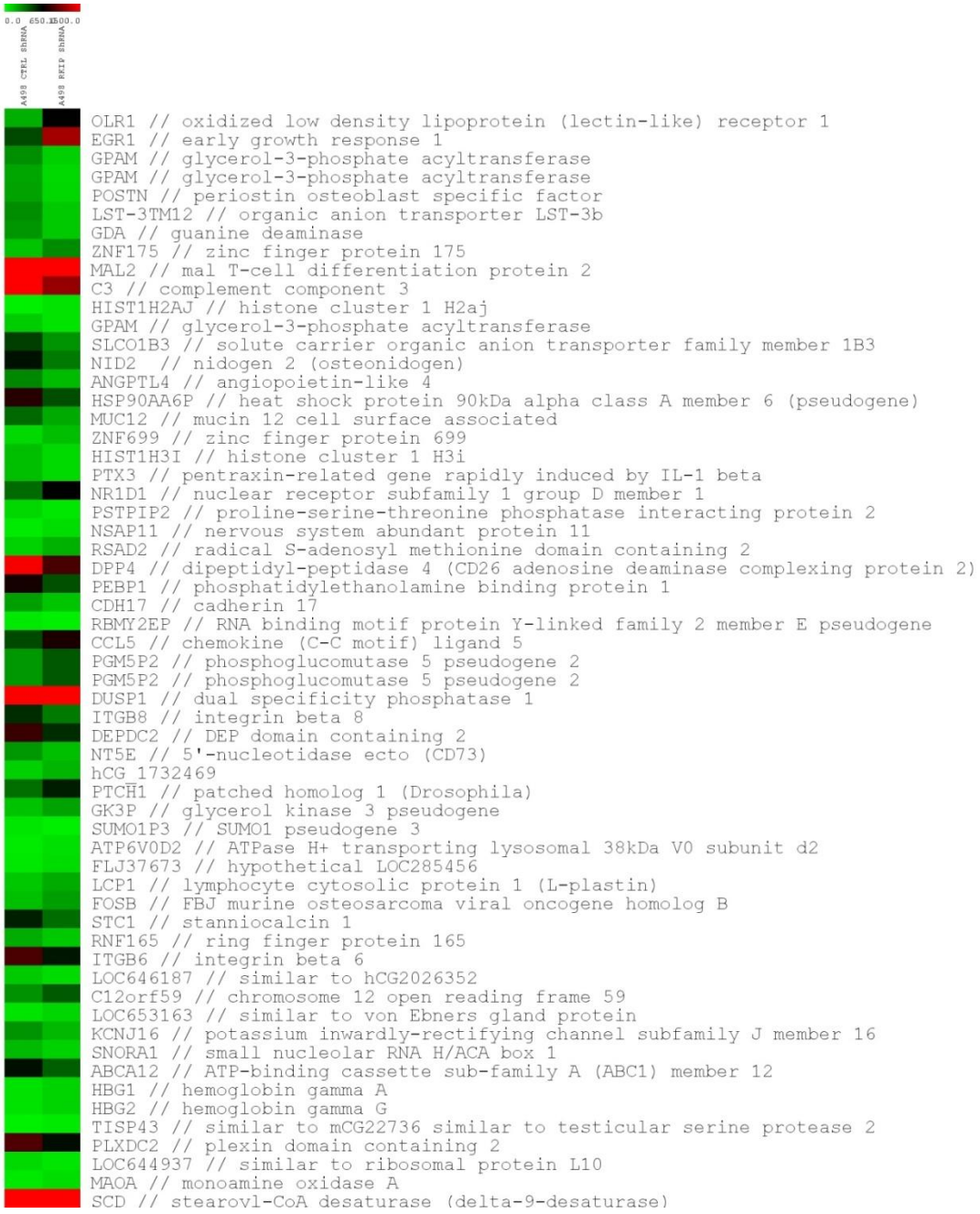

Figure 34: Heat map showing all changes in gene regulation between A498 CTRL ShRNA (left column) and A498 RKIP ShRNA (right column) with higher than 1.5 fold change difference. 59 genes were determined to have gene regulation changes. Expression intensity ranges from low (0, green) to medium (700, black) to high (1300.0, red).

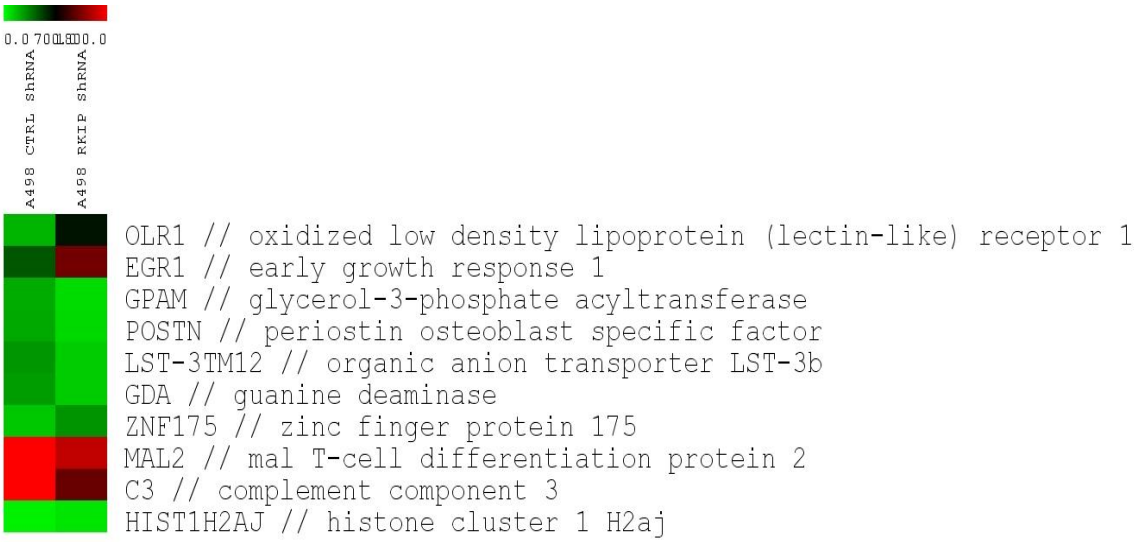

Figure 35: Heat map showing the top ten gene regulation changes between A498 CTRL ShRNA (left column) and A498 RKIP ShRNA (right column). Expression intensity ranges from low (0.0, green) to medium (700, black) to high (1800.0, red).

Table 9: Summary of Microarray Data

Gene	Gene Symbol	Fold Change (relative to CTRL)	Chromosome Location	Function
oxidized low density lipoprotein (lectin-like) receptor 1	OLR1	3.22 up	12	oxidatively modified low density lipoprotein regulator
early growth response 1	EGR1	2.62 up	5	transcription factor, tumour suppressor gene, involved in differentiation
glycerol-3-phosphate acyltransferase	GPAM	2.39 down	mitochondria	glycerolipid biosynthesis
glycerol-3-phosphate acyltransferase	GPAM	2.34 down	1	glycerolipid biosynthesis
periostin, osteoblast specific factor	POSTN	2.25 down	13	cell adhesion molecule for preosteoblasts
organic anion transporter LST-3b	LST-3TM12	2.09 down	12	exact function unknown
guanine deaminase	GDA	1.96 down	9	enzyme which converts guanine to xanthine and ammonia
zinc finger protein 175	ZNF175	1.96 up	19	DNA binding

mal, T-cell differentiation protein 2	MAL2	1.93 down	8	required for transcytosis
complement component 3	C3	1.93 down	19	immune system protein
histone cluster 1, H2aj	HIST1H2AJ	1.91 up	6	histone 2A family member, nucleosome component
glycerol-3-phosphate acyltransferase, mitochondrial	GPAM	1.88 down	5	glycerolipid biosynthesis
solute carrier organic anion transporter family, member 1B3	SLCO1B3	1.80 down	12	transporter
nidogen 2 (osteonidogen)	NID2	1.79 down	14	basement membrane protein, cell-adhesion protein
angiopoietin-like 4	ANGPTL4	1.77 down	19	regulates glucose homeostasis, lipid metabolism, and insulin sensitivity, potential role in tumour cell motility and invasiveness
heat shock protein 90kDa alpha (cytosolic), class A member 6 (pseudogene	HSP90AA6P	1.77 down	4	pseudogene
mucin 12, cell surface associated	MUC12	1.77 down	7	role in cell protection, adhesion and epithelial cell growth regulation, possible prognostic marker in colorectal metastasis

zinc finger protein 699	ZNF699	1.75 up	19	DNA binding
histone cluster 1, H3i	HIST1H3I	1.73 down	6	histone family member, nucleosome component
pentraxin-related gene, rapidly induced by IL-1 beta	PTX3	1.73 down	3	activates the classical pathway of complement
nuclear receptor subfamily 1, group D, member 1	NR1D1	1.72 up	17	gene transcription
proline-serine-threonine phosphatase interacting protein 2	PSTPIP2	1.72 down	18	regulates membrane-cytoskeletal interactions
nervous system abundant protein 11	NSAP11	1.71 up	8	unknown function
radical S-adenosyl methionine domain containing 2	RSAD2	1.67 up	2	anti-viral response
dipeptidyl-peptidase 4 (CD26, adenosine deaminase complexing protein 2)	DPP4	1.65 down	2	peptidase
phosphatidylethanolamine binding protein 1	PEBP1	1.65 down	12	metastasis suppressor, signaling modulator
cadherin 17, LI cadherin (liver-intestine)	CDH17	1.64 down	8	calcium-dependent glycoproteins mediates cell-cell adhesion

RNA binding motif protein, Y-linked, family 2, member E pseudogene	RBMY2EP	1.63 down	Y	pseudogene
chemokine (C-C motif) ligand 5	CCL5	1.62 up	17	immunoregulatory and inflammatory processes
phosphoglucomutase 5 pseudogene 2	PGM5P2	1.61up	9	pseudogene
phosphoglucomutase 5 pseudogene 2	PGM5P2	1.61 up	9	pseudogene
dual specificity phosphatase 1	DUSP1	1.60 up	5	role in cellular response to environmental stress, negative regulator of cell proliferation
integrin, beta 8	ITGB8	1.59 down	7	mediate cell-cell and cell-extracellular matrix interactions
DEP domain containing 2	DEPDC2	1.59 down	8	RAC1 guanine nucleotide exchange factor
5'-nucleotidase, ecto (CD73)	NT5E	1.58 down	6	catalyzes the conversion of extracellular nucleotides to membrane-permeable nucleosides.
hCG1732469	hCG_1732469	1.57 up	2	unknown function

patched homolog 1 (Drosophila)	PTCH1	1.57 up	9	sonic hedgehog receptor
glycerol kinase 3 pseudogene	GK3P	1.55 up	4	pseudogene
SUMO1 pseudogene 3	SUMO1P3	1.55 down	1	pseudogene
ATPase, H+ transporting, lysosomal 38kDa, V0 subunit d2	ATP6V0D2	1.55 up	8	proton pump
hypothetical LOC285456	FLJ37673, LOC285456	1.54 up	4	uncharacterized gene
lymphocyte cytosolic protein 1 (L-plastin)	LCP1	1.53 up	13	actin-binding protein
FBJ murine osteosarcoma viral oncogene homolog B	FOSB	1.53 up	19	regulators of cell proliferation, differentiation, and transformation
stanniocalcin 1	STC1	1.53 down	8	role in calcium and phosphate homoestasis
ring finger protein 165	RNF165	1.53 down	18	ubiquitination pathway
integrin, beta 6	ITGB6	1.53 down	2	mediate cell-cell and cell-extracellular matrix interactions
similar to hCG2026352	LOC646187	1.52 down	4	unknown function
chromosome 12 open reading frame 59	C12orf59	1.52 up	12	uncharacterized gene

similar to von Ebners gland protein	LOC653163	1.52 up	9	unknown function
potassium inwardly-rectifying channel, subfamily J, member 16	KCNJ16	1.52 down	17	potassium channel
small nucleolar RNA, H/ACA box 1	SNORA1	1.51 down	11	RNA processing
ATP-binding cassette, sub-family A (ABC1), member 12	ABCA12	1.51 down	2	transporter molecule
hemoglobin, gamma A	HBG1	1.51 up	11	oxygen transporter
hemoglobin, gamma G	HBG2	1.51 up	11	oxygen transporter
similar to mCG22736 | similar to testicular serine protease 2	TISP43|LOC 646743	1.51 up	2	uncharacterized gene
plexin domain containing 2	PLXDC2	1.50 down	10	57% identity to tumour endothelial marker, TEM7R
similar to ribosomal protein L10	LOC644937	1.50 down	5	potential ribosomal function
monoamine oxidase A	MAOA	1.50 up	X	degrades amine neurotransmitters
stearoyl-CoA desaturase (delta-9-desaturase)	SCD	1.50 up	10	unsaturated fatty acid synthesis

V. DISCUSSION

Clear cell RCC not only accounts for 75-85% of all RCC cases but also is one of the most aggressive forms of RCC (Motzer *et al.,* 1996; Lopez-Beltran *et al.,* 2009). Clear cell RCC thus contributes largely to RCC associated deaths (Kaelin, 2009). Two major contributing factors to ccRCC's lethality are the lack of effective means of diagnosis and our inability to treat the disease when ccRCC progresses to metastatic tumours. While the lack of warning signs for ccRCC tumours underlies the main reason as why a high proportion (40 to 45%) of patients present with locally advanced to metastatic ccRCC at diagnosis (Nelson *et al.,* 2007), ccRCCs are notoriously resistant to all current means of therapy (Motzer *et al.,* 1996; Brugarolas *et al.,* 2007). These current circumstances of ccRCC are largely attributable to our very limited understanding of the disease.

Accumulating evidence clearly demonstrates that loss of VHL is a critical event in ccRCC tumorigenesis. Patients with germline mutations of VHL are at risk of developing ccRCC with up to 600 tumours and 1100 cysts per kidney (Walther *et al.,* 1995). More importantly, biallellic inactivation of VHL by somatic mutations was detected in 60% - 70% of sporadic ccRCCs (Kim and Kaelin, 2004; Shuin *et al.,* 1994; Razorenova *et al.,* 2011). Due to our improving understanding of the critical role of VHL inactivation in ccRCC tumorigenesis, a set of small molecule inhibitors have been developed to systematically target the VHL pathway (Kaelin, 2009; Grandinetti and Goldspiel, 2007; Hudes, 2009). While these new therapies offer significant benefits to

patients with metastatic ccRCC in comparison to the classic standard care of interleukin 2 and interferon-α (Thompson Coon *et al.,* 2009; Grandinetti and Goldspiel, 2007), metastatic ccRCC remains incurable.

The issues discussed above therefore strongly suggest that some critical factors affecting ccRCC tumorigenesis remain to be identified. Supporting evidence to this notion is a well known understanding that while being critical, loss of VHL is not sufficient to induce ccRCC. Loss of VHL induces ccRCC that is often preceded by pre-neoplastic renal cysts (Neumann and Zbar, 1997) and mice deficient in VHL in the proximal tubule epithelium develop low levels of renal cysts only (Rankin *et al.,* 2006). We provided evidence that one of these unidentified factors is RKIP. Interestingly, a large body of evidence suggests RKIP being a tumour suppressor for ovarian cancer (Wang *et al.,* 2008), melanoma (Park *et al.,* 2005; Schuierer *et al.,* 2004) breast cancer (Hagan *et al.,* 2005) hepatocellular carcinoma (Schuierer *et al.,* 2006; Lee *et al.,* 2006a), prostate cancer (Fu *et al.,* 2003; Keller, 2004) and colorectal cancer (Al-Mulla *et al.,* 2006; Minoo *et al.,* 2007; Zlobec *et al.,* 2008a; Zlobec *et al.,* 2008b).

5.1. Reduction of RKIP in ccRCC

We collectively demonstrated reduction of RKIP using several approaches including both western blot and imunohistochemistry analysis. Upon examination of ccRCC patients in our small cohort, reduction of RKIP protein was observed in more than 90% of ccRCC, in comparison with the adjacent non-tumour kidney (ANK) tissues.

This observation was consolidated when using a large cohort containing 501 ccRCC patients. By using this cohort, we were able to show that in addition to comparison with ANK tissues, RKIP reduction was also observed when compared to kidney tissues of normal individuals. Taken together, by using both local and commercially available cohorts of ccRCC patients, we were able to show that decreases in RKIP expression are observed in ccRCC.

To our knowledge there have been no reports on RKIP protein expression in any other types of RCC including clear cell RCC. Our investigation reveals that RKIP expression is reduced in 92.3% (12 out of 13 patients) of papillary RCC cases in our small cohort of patients examined by western blot analysis (data not shown). Consistent with this finding, our TMA immunohisochemisty analysis revealed that 83.3% (10 out of 12 cores) of papillary tissue cores were considered negative for RKIP staining (data not shown). These results imply that reduction of RKIP is not limited to clear cell RCC but to other sub types of RCC as well.

5.2. Mechanism of RKIP decrease in ccRCC

While decreases in RKIP protein were observed in several human cancers, including tumours of the breast (Hagan *et al.*, 2005), prostate (Fu *et al.*, 2002; Keller, 2004), skin (Park *et al.*, 2005; Schuierer *et al.*, 2004) and colon (Al-Mulla *et al.*, 2006; Minoo *et al.*, 2007; Zlobec *et al.*, 2008a; Zlobec *et al.*, 2008b; Zeng *et al.*, 2008), the potential mechanisms responsible for reduction in RKIP expression are largely unknown.

The RKIP gene is located on the long arm of chromosome 12. Early research using microcell mediated chromosome transfer identified a novel metastasis suppressor region on chromosome 12 (Luu *et al.,* 1998). This 70cM portion on the chromosome contains two distinct regions that encode metastasis suppressor activity (Luu *et al.,* 1998). Mice that were injected with this section of the chromosome exhibited a 30 fold reduction in lung surface metastases then mice that lacked this region (Luu *et al.,* 1998). These regions were found to be located at q13 and q24 of chromosome 12. Interestingly, RKIP has been mapped to the q24.23 region on chromosome 12. Kilmura *et al,* 1998 identified two commonly deleted regions on the long arm of chromosome 12 in pancreatic cancer (Kilmura *et al.,* 1998). These regions were q21 and q22-q23.1, suggesting potential tumour suppressor genes at these locations (Kimura *et al.,* 1998). However, to date alterations in the genomic region containing RKIP and its adjacent areas have not been reported in human cancer (Schuierer *et al.,* 2004). Furthermore, research has revealed that there is no loss or mutation in the coding region of RKIP in melanoma cell lines and in acute myeloid leukemia (Schuierer *et al.,* 2004; Zebisch *et al.,* 2009). However, loss of the RKIP protein was commonly observed in prostate, breast, colon, gastrointestinal and ovarian tumours (Fu *et al.,* 2003; Keller *et al.,* 2005; Chatterjee *et al.,* 2004; Hagan *et al.,* 2005; Schuierer *et al.,* 2004; Martinho *et al.,* 2009; Wang *et al.,* 2008; Zlobec *et al.,* 2008a; Zlobec *et al.,* 2008b), suggesting that mechanisms in addition to alteration of the RKIP gene may be largely responsible for loss of RKIP function in human tumours. Consistent with this possibility, there have been no reports on chromosome 12 being mutated or lost in ccRCCs. The expression of the RKIP gene was further examined in

numerous human cancer tissues based on information derived from the Cancer Genome Anatomy Project (http://cgap/nci.nih.gov). This site compares gene expression in normal and cancer tissues. RKIP gene expression was found to be slightly decreased in brain, stomach, muscle and lymph node cancer tissues (Table 10). Interestingly RKIP expression was determined to be increased in cancerous tissues of the breast, colon, prostate and peritoneum (Table 10). This directly contrasts what has been reported in breast, prostate and colon cancers which show RKIP protein is dramatically reduced in tumours compared to normal tissue (Hagan *et al.,* 2005; Dangi-Garimella *et al.,* 2009; Fu *et al.,* 2003; Minoo *et al.,* 2007; Zlobec *et al.,* 2008a; Zlobec *et al.,* 2008b). No difference in RKIP expression was found in normal and cancer tissues of the kidney, consistent with there being no current investigations regarding RKIP expression in RCC. The observed discrepancies in RKIP gene expression profiles and its protein expression in human cancer tissues versus the respective non-cancerous tissues may be attributable to the complex composition of cell types in non-tumour tissues. Only specific types of cells in non-cancerous tissues are responsible for the generation of cancers. Alternatively, mechanisms instead of transcription regulation are responsible for the reduction of RKIP protein in human cancers.

Table 10: Expression profile of RKIP gene in cancer

Cancer Tissue	RKIP	Cancer Tissue	RKIP
Brain	++	Kidney	+++
Retina	++	Colon	++++
Thyroid	+++	Peritoneum	++++
Lung	+++	Prostate	++++
Breast	++++	Bone Marrow	+++
Stomach	++	Muscle	++
Pancreas	+	Skin	+++
Liver	+	Lymph Node	++

Note: The information was derived from the Cancer Genome Anatomy Project (http://cgap.nci.nih.gov). In comparison to normal tissues '+' and '++' represent expression levels that are dramatically lower and slightly lower, respectively; '+++' and '++++' represent expression levels that are comparable and higher in cancer tissue respectively.

Cancer cells often silence tumour suppressors through epigenetic mechanisms including DNA methylation (Baylin and Herman, 2000). Promoter methylation has been shown to repress RKIP transcription (Al-Mulla *et al.*, 2008). In line with these reports, we noticed that the levels of RKIP protein in ccRCC correlate with the abundance of RKIP mRNA. Additionally, inhibition of DNA methylation in the A498 ccRCC cell line increased RKIP mRNA. However, while inhibition of DNA methylation elevated RKIP protein abundance in A498 cells, RKIP protein was still significantly less than what is endogenous expressed in human proximal tubular epithelial cells (Figs 19, 20), revealing that additional mechanisms are also in place to regulate RKIP expression. These mechanisms may regulate the stability of RKIP mRNA or protein and need to be elucidated. It is also possible that translation efficiency of RKIP mRNA in ccRCC is reduced. This is consistent with the observations showing that the cellular translation

machinery is altered during tumourigenesis (Calkhoven *et al.,* 2002; Pandolf, 2004; Holland *et al.,* 2004).

5.3. RKIP mediated tumour suppression

RKIP has been suggested to be a metastasis inhibitor. This notion is largely based on several observations. Decreases in RKIP protein were observed in metastasized tumours of several human cancers (Hagan *et al.,* 2005; Fu *et al.,* 2003; Schuierer *et al.,* 2004; Keller *et al.,* 2005; Keller, 2004). Researchers have demonstrated that RKIP could be detected in non-cancerous prostate tissue and in primary prostate cancer but not in prostate metastases (Fu *et al.,* 2003). The expression levels of RKIP were highest for prostate tissue, decreased with increasing Gleason score and not present in prostate metastases (Keller *et al.,* 2004a; Keller *et al.,* 2004b). Research by Hagan *et al,* 2005 demonstrated that RKIP expression was present in primary breast cancer tumours but consistently lost in lymph node metastases (Hagan *et al.,* 2005). There is an inverse correlation reported between RKIP expression and tumour progression in melanoma (Schuierer *et al.,* 2004). RKIP protein expression was highest in benign tissue, decreased in primary melanoma and a further reduction was observed in metastatic melanomas (Schuierer *et al.,* 2004). The involvement of RKIP in suppression of metastasis is in line with our observations. In comparison to ccRCCs that did not metastasize, primary ccRCCs with distant metastasis expressed reduced levels of RKIP and ccRCC tissue harvested from metastasic sites expressed an even further reduction of RKIP protein.

Additionally, ccRCCs that metastasized to other organs (secondary tumour) expressed lower levels of RKIP than in their corresponding primary tumours located in the kidney. Overexpression of RKIP has no effect on the proliferation of breast and prostate cancer cells *in vitro* or on the formation of xenograft tumours in mice, but inhibits their ability to form metastases in immunocompromised mice (Fu *et al.,* 2003; Chatterjee *et al.,* 2004). Our results support this notion, as overexpression of RKIP did not affect the proliferation rate of A498 and 786-O cells *in vitro* and the formation of xenograft tumours *in vivo* (Fig 31). Similarly, knockdown of RKIP in these same cell lines (A498 and 786-O) had no effect on cell proliferation *in vitro* or tumour formation in mice (Fig 33). However, the impact of RKIP on tumourigenesis is a complex issue. Mice deficient for RKIP were found to display learning and olfactory defects and have reduced reproduction rates (Klysik *et al.,* 2008; Theroux *et al.,* 2007; Granovsky and Rosner, 2008). There have been no reports on enhanced tumour formation in these mice but $RKIP^{-/-}$ mice still contained the related genes PEBP2 and PEBP4 which could provide genetic compensation for PEBP1 (RKIP) absence (Zeng *et al.,* 2008). More research is needed to elucidate the role of RKIP in cancer development in these knockout mice.

It is possible that RKIP may also suppress tumourigenesis, as reduction of RKIP has been observed in organ-confined carcinomas of the breast and prostate (Fu *et al.,* 2003; Dangi-Garimella *et al.,* 2009). This is consistent with our observation showing that the levels of RKIP are commonly reduced in organ-confined (kidney) ccRCC. Furthermore, reduction of RKIP was observed when ccRCC progressed from tumour stage 2 to 3 and progressed from tumour grades 1 to 3 (Figs 12, 14). Advanced stage

ccRCC is associated with poor prognosis, few treatment options and a high rate of metastatic relapse (Motzer *et al.,* 1996; Brugarolas *et al.,* 2007; Grandinetti and Goldspiel, 2007). Advanced stage ccRCC was found to have lower RKIP protein expression then what is found in early stage RCC (Fig 13). This further confirms the significance of RKIP protein reduction in ccRCC progression.

5.4. Mechanism of RKIP mediated tumour suppression

Our research suggests that RKIP may suppress ccRCC metastasis by inhibiting ccRCC invasion. This was based on our observations that ectopic expression of RKIP in both A498 and 786-O ccRCC cells reduced the invasion abilities of both cell lines and that knockdown of endogenous RKIP enhanced this process (Figs 26-29). As changes in cytoskeleton are involved in cell migration and invasion (Guarino *et al.,* 2007, Yilmaz and Christofori, 2009; Fidler, 2003; Thiery, 2002; Leber and Efferth, 2009), our results are thus consistent with publications demonstrating that RKIP is implicated in cytoskeleton organization (Bodenstine and Welch, 2008; Kolch, 2005; Klymkowsky and Savagner, 2009).

A critical event in cancer metastasis is EMT in which epithelial cells modulate their phenotype and acquire mesenchymal properties (Guarino *et al.*, 2007; Vuoriluoto *et al.,* 2011). EMT is characterized by a loss in cell-cell adhesion and an increase in cell mobility (Yilmaz and Christofori, 2009; Guarino *et al.,* 2007). At the molecular level, EMT is associated with a cadherin switch; loss of E-cadherin (an epithelial cell-cell

adhesion molecule) is associated with increases in N-cadherin (a mesenchymal cell-cell adhesion molecule) (Yilmaz and Christofori, 2009; Thiery, 2002; Seidel *et al.*, 2004). This switch causes cells to lose affinity for epithelial neighbours and to gain affinity for mesenchymal cells (fibroblast and vascular endothelial cells) (Nieman *et al.*, 1999; Hulit *et al.*, 2007). N-cadherin expression allows for tumour cell binding to the stroma during invasion (Steeg, 2006). Commonly used molecular markers of EMT include loss of E-cadherin and gain of vimentin, N-cadherin, and fibromectin (Kalluri and Weinberg, 2009; Mendez *et al.*, 2010; Lee *et al.*, 2006b; Wu and Bonavida, 2009).

Consistent with the above discussions, RKIP has been reported to inhibit EMT (Beach *et al.*, 2007; Dangi-Garimella *et al.*, 2009). RKIP is able to inhibit the expression of Snail and Lin28 transcriptional factors which are involved in inducing EMT (Beach *et al.*, 2007; Dangi-Garimella *et al.*, 2009). Snail is involved in the initiation of EMT and is able to repress RKIP transcription (Beach *et al.*, 2008; Barbera *et al.*, 2004; Baritaki *et al.*, 2009). Consistent with this notion, RKIP inhibits the NFκB pathway and NFκB plays a major role in the upregulation of Snail and in turn metastasis formation (Wu and Bonavida, 2009; Tang *et al.*, 2010; Baritaki *et al.*, 2009; Yeung *et al.*, 2001). An interesting feedback loop has been proposed between Snail, RKIP and the NFκB pathway (Beshir *et al.*, 2010). In an abnormal state RKIP levels are decreased resulting in less inhibition on the NFκB pathway causing upregulation of Snail, enhancing metastasis (Beshir *et al.*, 2010; Wu and Bonavida, 2009).

RKIP may also inhibit EMT during ccRCC tumourigenesis. *In vitro*, ectopic expression of RKIP reduced the levels of N-cadherin and vimentin in A498 cells. Conversely, knockdown of endogenous RKIP up-regulated N-cadherin and vimentin in A498 cells (Figs 30, 31). However, we were unable to detect the impact of RKIP on E-cadherin expression *in vitro*, as A498 cells do not express detectable levels of E-cadherin protein. This is consistent with studies by Tani *et al,* 1995 which showed that A498 cells did not express E-cadherin (Tani *et al.*, 1995). Although loss of E-cadherin is the hallmark of EMT (Guarino *et al.*, 2007; Leber and Efferth, 2009; Wu and Bonavida, 2009; Gravdal *et al.*, 2007; Tran *et al.*, 1999; Christiansen and Rajasekaran, 2006; Kang and Massague, 2004; Mareel *et al.*, 1997), the presence of vimentin facilitates cell invasion in E-cadherin negative cells (Sommers *et al.*, 1991) and vimentin is known to increase cell motility (Mendez *et al.*, 2010; Gilles *et al.*, 2003). Furthermore, N-cadherin expression correlated with invasion, possibly owning to N-cadherin mediated interaction between cancerous cells and stromal cells (Hazan *et al.*, 1997). Taken together, our research supports the notion that RKIP inhibits EMT in ccRCC. However, further research is needed to examine the impact of RKIP on E-cadherin expression and whether RKIP correlates with EMT in primary ccRCC.

Another route to explain our observed RKIP mediated tumour invasion suppression not explored in the basis of this thesis includes the role of matrix metalloproteinases (MMPs). MMPs are zinc dependent enzymes capable of degrading extracellular matrix (ECM) proteins (Deryugina and Quigley, 2006; Stamenkovic, 2000). MMP expression is upregulated in most human cancers and MMPs are thought to be

active in all stages of tumour and metastasis development (Egebald and Werb, 2002). MMP-2 and MMP-9 play a major role in metastasis since these enzymes are able to degrade collagen IV which is a major component of basement membranes and both of these enzymes can promote angiogenesis (Stamenkovic, 2000). MMPs are also able to promote tumour growth and progression because these enzymes influence non-ECM components as well, including the release of chemokines, growth factors and receptors, adhesion molecules and apoptotic molecules (Yoon *et al.*, 2003). This results in critical and rapid cell response necessary for tumour growth to occur (Yoon *et al.*, 2003). Recently, Beshir *et al,* 2010 demonstrated that knockdown of RKIP resulted in increased expression of MMPs, with MMP-1 and MMP-2 being most upregulated (Beshir *et al.*, 2010).

5.5. Molecular pathways responsible for RKIP mediated tumour suppression

The major pathways regulated by RKIP include inhibition of the MAPK pathway and activation of G-protein signaling. When RKIP is phosphorylated at S153, RKIP loses its affinity for Raf-1 and thus its inhibition of the MAPK pathway. On the other hand, S153 phosphorylated RKIP is able to bind to GRK-2 and thereby activating the GPCR signaling pathway (Granovsky and Rosner, 2008, Zeng *et al.*, 2008).

Upon the examination of ERK activation in our patient cohort, we were unable to detect enhanced ERK activation in ccRCC. This is not consistent with current reports showing that ERK1 and ERK2 were activated in 48% of renal tumours and that

significant elevated levels of ERK2 were detected in clear cell RCC tissue samples (Oka *et al.,* 1995; Huang *et al.,* 2008). This inconsistency may result from different ccRCC populations being studied or the rather small size of our patient cohort. Additionally, our comparison was based on the ERK activation status in ANK and in ccRCC. As ccRCC originates from the proximal tubular epithelial cells, our comparison may therefore not truly reflect the activation status between proximal tubular epithelial cells and ccRCC. However, our results were consistent with the comparable level of RKIP S153 phosphorylation in ccRCC relative to ANK (Figs 5, 6). Nonetheless, additional research is needed to examine the relationship between RKIP reduction and changes in ERK activation status in ccRCC. Since no change in ERK activation was observed in our small cohort of ccRCC patients by western blot analysis, we elected not to purchase TMA slides to examine ERK activation in a large cohort of patients.

Our results may suggest that RKIP might suppress ccRCC tumourigenesis via ERK-independent pathways. While reduction of RKIP correlates with enhanced ERK activation in metastatic hepatoma (Lee *et al.,* 2006a), this correlation was not observed in metastatic breast cancer and melanoma (Hagan *et al.,* 2005; Houben *et al.,* 2008). This ERK-independent pathway, in the case of ccRCC, may involve factors whose expression is affected by RKIP. In an analysis of gene expression in A498 cells, in which RKIP was knocked down, we have noticed changes in several candidate genes, including early growth response 1 (EGR1), periostin (POSTN), nidogen 2 (NID2), angiopoietin-like 4 (ANGPTL4) and mucin 12 cell surface associated (MUC12) (Table 9). Changes in these candidates were reported in a variety of human cancers (Krones-Herzig *et al.,* 2005;

Adamson and Mercola, 2002; Ruan *et al.,* 2009; Bao *et al.,* 2004; Ulazzi *et al.,* 2007; Galaup *et al.,* 2006, Williams *et al.,* 1999). Specifically EGR1 can act as a tumour suppressor or tumour promoter and can stimulate tumour growth in prostate cancer (Krones-Herzig *et al.,* 2005; Adamson and Mercola, 2002). NID2, ANGPTL4 and MUC12 are involved in cell adhesion, invasion and motility (Ulazzi *et al.,* 2007; Galaup *et al.,* 2006; Williams *et al.,* 1999).

5.6. Significance and Future Directions

Clear cell RCC is unique in which loss of VHL commonly occurs in the disease, regardless of whether ccRCC is associated with germ line mutation of VHL or sporadically developed. However, loss of VHL is not sufficient to cause ccRCC. In our examination of more than 600 patients with ccRCC, we were able to show that reduction of RKIP occurs in more than 80% of tumours in comparison to either ANK or normal kidney tissues. The magnitude of decreases in RKIP thus matches to the level of reduction of VHL in ccRCC. Of note, this introduces a very intriguing concept that RKIP may be a second major tumour suppressor of ccRCC. Therefore, it will be interesting to examine whether loss of RKIP may substantially enhance ccRCC formation in mice in which RKIP is deficient specifically in the kidney. Another area of research that needs to be explored is the relationship between VHL and RKIP loss. Can the loss of either VHL or RKIP protein induce the loss of the other protein (VHL/RKIP)? Currently there is no evidence to support the notion that VHL loss can cause the loss of RKIP. Our

results demonstrate potential roles for RKIP in the suppression of metastasis formation and as a dominant tumour suppressor in ccRCC.

Although this thesis did make strides in characterizing the biochemical relationship between RKIP and ccRCC, some questions remain unanswered. Specifically, the ability of RKIP to inhibit metastasis needs to be addressed *in vivo*. In a preliminary trial, it was found when RKIP knockdown A498 cells were intravenous injected *in vivo* in mice, 1 in 5 mice formed tumours in the lungs. One possible reason for the low rate of metastasis is that this cell line isn't a metastatic cell line (Haviv *et al.*, 2004). Another possibility is that these cells were injected into the tail vein of the mice which by-passes the first stages of the metastatic process and only the postintravastion stage is modeled whereas, injection into the orthotopic location, in this case the kidney, would have been better (Steeg, 2006, Fidler, 2002). This would allow for the whole metastatic process to develop as it would in human ccRCC. Also the expression of RKIP protein in metastatic tissue needs to be examined in a larger patient population. Unfortunately our TMA slides only contained 8 ccRCC derived organ metastases and therefore an absolute determination of RKIP reduction in metastatic tissue could not be made.

VI. REFERENCES

Adamson, E.D. and Mercola, D. Egr1 transcription factor: multiple roles in prostate tumour cell growth and survival. *Tumor Biology*. **23,** 93-102 (2002).

Akaishi, J., Onda, M., Asaka, S., Okamoto, J., Miyamoto, S., Nagahama, M., Ito, K., Kawanami, O., and Shimizu, K. Growth-suppressive function of phosphatidylethanolamine-binding protein in anaplastic thyroid cancer. *Anticancer Research.* **26(6B),** 4437-4442 (2006).

Al-Mulla, F., Hagan, S., Behbehani, A.J., Bitar, M.S., George, S.S. Going, J.J., Garcia, J.J., Scott, L., Fyfe, N., Murray, G.I., and Kolch, W. Raf kinase inhibitor protein expression in a survival analysis of colorectal cancer patients. *Journal of Clinical Oncology*. **24,** 5672-5679 (2006).

Al-Mulla, F., Hagan, S., Al-Ai, W., Jacob, J.P., Behbehani, A.I., Bitar, M.S., Dallol, A., and Kolch, W. Raf kinase inhibitor protein: mechanism of loss of expression and association with genomic instability. *Journal of Clinical Pathology*. **61,** 524-529 (2008).

Banfield, M.J., and Brady, R.L. The structure of *Anterrhinum Centroradialis* protein (CEN) suggests a role as a kinase regulator. *The Journal of Molecular Biology*. **297,** 1159-1170 (2000).

Banfield, M.J., Barker, J.J., Perry A.C., and Brady, R.C. Function from structure? The crystal structure of human phosphatidylethanolamine-binding protein suggests a role in membrane signal transduction. *Structure*. **6(10),** 1245-1254 (1998).

Bao, S., Ouyang, G., Bai, X., Huang, Z., Ma, C., Liu, M., Shao, R., Anderson, R.M., Rich, J.N., and Wang, X.F. Periostin potently promotes metastatic growth of colon cancer by augmenting cell survival via the Akt/PKB pathway. *Cancer Cell*. **5,** 329-339 (2004).

Barberà, M.J., Puig, I., Domínguez, D., Julien-Grille, S., Guaita-Esteruelas, A., Peiró, S., Baulida, J., Francí, C., Dedhar, S., Larue, L., and García de Herreros, A. Regulation of Snail transcription during epithelial to mesenchymal transition of tumour cells. *Oncogene*. **23,** 7345-7354 (2004).

Baritaki, A., Chapman, A., Yeung, K., Spandidos, D.A., Palladino, M., and Bonavida, B. Inhibition of epithelial to mesenchymal transition in metastatic prostate cancer cells by the novel proteasome inhibitor, NPI-0052: pivotal roles of Snail repression and RKIP induction. *Oncogene.* **1,** 1-13 (2009).

Baylin, S.B., and Herman, J.G. DNA hypermethylation in tumorigenesis: epigenetics joins genetics. *Treads in Genetics.* **16,** 168-174 (2000).

Beach, S., Tang, H., Park, S., Dhillon, A.S., Keller, E.T., Kolch, W., and Yeung, K.C. Snail is a repressor of RKIP transcription in metastatic prostate cancer cells. *Oncogene.* **27,** 2243-2248 (2008).

Bernier, I., and Jolles, P. Purification and characterization of a basic 23kDa cytosolic protein from bovine brain. *Biochimica et Biophysica Acta.* **790,** 174-181 (1984).

Bernier, I., Tresca, J.P., and Jolles, P. Ligand binding studies with a 23kDa protein purified from bovine brain cytosol. *Biochimica et Biophysica Acta.* **871,** 19-23 (1986).

Beshir, A.B., Ren, G., Magpusao, A.N., Barone, L.M., yeung, K.C., and Fenteany, G. Raf kinase inhibitor protein suppresses nuclear factor-κB-dependent cancer cell invasion through negative regulation of matrix metalloproteinase expression. *Cancer Letters.* **299,** 137-149 (2010).

Bodenstine, T.M., and Welch, D.R. Metastasis Suppressors and the tumour microenvironment. *Cancer Microenvironment.* **1,** 1-11 (2008).

Bracarda, S., Caserta, C., Sordini, L., Rossi, M., Hamzay, A., and Crinò, L. Protein kinase inhibitors in the treatment of renal cell carcinoma: sorafenib. *Annals of Oncology.* **18(Suppl 6),** vi22-25 (2007).

Brugarolas, J. Renal cell carcinoma – molecular pathways and therapies. *The New England Journal of Medicine.* **356,** 185-187 (2007).

Calkhaven, C.F., Muller, C., and Leutz, A. Translational control of gene expression and disease. *TRENDs in Molecular Medicine.* **8,** 577-583 (2002).

Canadian Cancer Society's Steering Committee: **Canadian Cancer statistics 2010. Toronto: Canadian Cancer Society, 2010.**

Chatterjee, D., Bai, Y., Wang, Z., Beach, S., Mot, S., Roy, R., Braastad, C., Sun, Y., Mikhopadhyay, A., Aggarwal, B.B, Darnowski, J., Pantazis, P., Wyche, J., Fu, Z., Kitagwa, Y., Keller, E.T., Sedivy, J.M., and Yeung, K.C. RKIP sensitizes prostate and breast cancer cells to drug-induced apoptosis. *Journal of Biological Chemistry.* **279,** 17515-17523 (2004).

Chatterjee, D., Sabo, E., Tavares, R., and Resnick, M.B. Inverse association between raf kinase inhibitory protein and signal transducers and activators of transcription 3 expression in gastric adenocarcinoma patients: implications for clinical outcome. *Clinical Cancer Research.* **14,** 2994-3001 (2008).

Chen, Y., Ouyang, G.L., Yi, H., Li, M.Y., Zhang, P.F., Li, C., Li, J.L., Liu, Y.F., Chen, Z.C., and Xiao, Z.Q. Identification of RKIP as an invasion suppressor protein in nasopharyngeal carcinoma by proteomic analysis. *Journal of Proteome Research.* **7,** 5254-5262 (2008).

Choyke, P.L., Glenn, G.M., Walther, M.M., Zbar, B., and Linehan, W.M. Hereditary renal cancers. *Radiology.* **226,** 33-46 (2003).

Christiansen, J.J., and Rajasekaran, A.K. Reassessing epithelial to mesenchymal transition as a prerequisite for carcinoma invasion and metastasis. *Cancer Research.* **66,** 8319-8326 (2006).

Cohen, H.T. and McGovern F.J. Renal cell carcinoma. *The New England Journal of Medicine.* **353,** 2477-2490 (2005).

Coppin, C., Porzsolt, F., Awa, A., Kumpf, J., Coldman, A., and Wilt, T. Immunotherapy for advanced renal cell cancer. *Cochrane Database System Review Rev.1*. **CD001425**, 2005.

Corbit, K.C. Trakul, N., Eves, E.M., Diaz, B., Marshall, M., and Rosner, M.R. Activation of Raf-1 signaling by protein kinase C through a mechanism involving Raf kinase inhibitory protein. *The Journal of Biological Chemistry.* **278(15),** 13061-13068 (2003).

Costa, L.J. and Drabkin, H.A. Renal cell carcinoma: New developments in molecular biology and potential for targeted therapies. *The Oncologist.* **12,** 1404-1413 (2007).

Dangi- Garimela, S., Yun, J., Eves, E.M., Newman, M., Erkeland, S.J., Hamond, S.M., Minn, A.J., and Rosner, M.R. Raf kinase inhibitory protein suppresses a metastasis signalling cascade involving LIN28 and *let-7*. *The EMBO Journal.* **28(4),** 347-358 (2009).

Deryugina, E.I., and Quigley, J.P. Matrix malloproteinases and tumour metastasis. *Cancer Metastasis Review.* **25,** 9-34 (2006).

Drucker, B.J. Renal cell carcinoma: Current status and future prospects. *Cancer Treatment Reviews.* **31,** 536-545 (2005).

Egebald, M., and Werb, Z. New functions for the matrix metalloproteinases in cancer progression. *Nature Reviews Cancer.* **2,** 161-174 (2002).

Eves, E.M., Shapiro, P., Naik, K., Klein, U.R., Trakul, N., and Rosner, M.R. Raf kinase inhibitory protein regulates aurora B kinase and the spindle checkpoint. *Molecular Cell.* **23,** 1561-1574 (2006).

Fidler, I.J. The pathogenesis of cancer metastasis: the 'seed and soil' hypothesis revisited. *Nature Reviews Cancer.* **3,** 1-6 (2002).

Fletcher, C.D.M. Diagnostic Histopathology of Tumors. Volume 1 2nd ed. Churchill Livingstone Harcourt Publishers limited: London. (2000).

Foster, K., Prowse, A., van den Berg, A., Fleming, S., Hulsbeek, M.M.F., Crossey, P.A., Richards, F.M., Cairns, P., Affara, N.A., Ferguson-Smith, M.A., Buys, C., and Maher, E.R. Somatic mutations of the von Hippel-Lindau disease tumour suppressor gene in non-familial clear cell renal carcinoma. *Human Molecular Genetics.* **3,** 2169-2173 (1994).

Frayne, J., McMillen, A., Love, S., and Hall, L. Expression of phosphatidylethanolamine-binding protein in the male reproductive tract: immunolocalisation and expression in prepubertal and adult rat testes and epididymides. *Molecular Reproduction and Development.* **49(4),** 454-460 (1998).

Frayne, J., Ingram, C., Love, S., and Hall, L. Localisation of phosphatidylethanolamine-binding protein in the brain and other tissues of the rat. *Cell and Tissue Research.* **298(3),** 415-423 (1999).

Fu, Z., Dozmorov, I., and Keller, E. Osteoblasts produce soluble factors that induced a gene expression pattern in non metastatic prostate cells similar to that found in bone metastatic cancer cells. *Prostate.* **51,** 10-20 (2002).

Fu, Z., Kitagawa, Y., Shen, R., Mehra, R., Rhodes, D., Keller, P.S., Mizokami, A., Dunn, R., Chinnaiyan, A.M., Yao, Z., and Keller, E.T. Metastasis suppressor gene Raf kinse inhibitory protein (RKIP) is a novel prognostic marker in prostate cancer. *Prostate.* **66(3),** 248-256 (2006).

Fu, Z., Smith, P.C., Zhang, L., Rubin, M.A., Dunn, R.L.,Yau, Z., and Keller, E.T. Effects of Raf kinase inhibitor protein expression on suppression of prostate cancer metastasis. *Journal of the National Cancer Institute.* **95(12),** 878-889 (2003).

Fuhrman, S.A., Lasky, L.C., and Limas, C. Prognostic significance of morphologic parameters in renal call carcinoma. *American Journal of Surgical Pathology.* **6,** 655-663 (1982).

Galaup, A., Cazes, A., Le Jan, S., Philippe, J., Connault, E., Le Coz, E., Mekid, H., Mir, L.M., Opolon, P., Corvol, P., Mannot, C., and German, S. Angiopoietin-like 4 prevents metastasis through inhibition of vascular permeability and tumour cell motility and invasiveness. *PNAS.* **103(49),** 18721-18726 (2006).

Gilles, C., Polette, M., Mestdagt, M., Nawrocki, R.B., Ruggeri, P., Birembaut, P., and Foidart, J.M. Transactivation of vimentin by beta-catenin in human breast cancer cells. *Cancer Research.* **63,** 2658-2664 (2003).

Gnarra, J.R., Tory, K., Weng, Y., Schmidt, L., Wei, M.H., li, H., Latif, F., Liu, S., Chen, F., Duh, F.M., Lubensky, I., Duan, D.R., Florence, C., Pozzatti, R., Walther, M.M., Bander, N.H., Grossman, H.B., Brauch, H., Pomer, S., Brooks, J.D., Isaacs, W.B., Lerman. M.I., Zbar, B., and Linehan, W.M. Mutations of the VHL tumour suppressor gene in renal carcinoma. *Nature Genetics.* **7,** 85-90 (1994).

Gollob, J.A., Wilhelm, S., Carter, C., and Kelly, S.L. Role of raf kinase in cancer: therapeutic potential of targeting the raf/MEK/ERK signal transduction pathway. *Seminars in Oncology.* **33,** 392-406 (2006).

Grandineti, C.A., and Goldspiel, B.R. Sorafenib and sunitinib: novel targeted therapies for renal cell cancer. *Pharmacotherapy.* **27,** 1125-1144 (2007).

Granovsky, A.E. and Rosner, M.R. Raf kinase inhibitory protein: a signal transduction modulator and metastasis suppressor. *Cell Research.* **18,** 452-457 (2008).

Gravdal, K., Halvorsen, O.J., Haukaas, S.A., and Akslen, L.A. A switch from E-cadherin to N-cadherin expression indicates epithelial to mesenchymal transition and is of strong and independent importance for the progress of prostate cancer. *Clinical Cancer Research.* **13(23),** 7003-7011 (2007).

Guarino, M., Rbuino, B., and Ballabio, G. The role of epithelial-mesenchymal transition in cancer pathology. *Pathology.* **39,** 305-318 (2007).

Hagan, S., Al-Mulla, F., Mallon, E., Oien, K., Ferrier, R., Gusterson, B., Garcia, J.J., and Kolch, W. Reduction of Raf-1 kinase inhibitor protein expression correlates with breast cancer metastasis. *Clinical Cancer Research.* **11,** 7392-7397 (2005).

Haviv, Y.S., van Houdt, W.J., Lu, B., Curiel, D.J., and Zhu, Z.B. Transcriptional targeting in renal cancer cell lines via the human CXCR4 promoter. *Molecular Cancer Therapeutics.* **3,** 687-691 (2004).

Hazan, R.B., Kang, L., Whooley, B.P., and Borgen, P.I. N-cadherin promotes adhesion between invasive breast cancer cell and the stroma. *Cell Adhesion and Communication.* **4,** 399-411 (1997).

He, L., Fan, C., Kapoor, A., Ingram, A.J., Rybak, A.P., Austin, R.C., Dickhout, J., Cutz, J.C., Scholey, J., and Tang, D. α-Mannosidase 2C1 attenuates PTEN function in prostate cancer cells. *Nature Communications.* **2,** 307 (2011).

He, L., Ingram, A., Rybak, A.P., and Tang, D. Shank-interacting protein-like 1 promotes tumourigenesis via PTEN inhibition in human tumour cells. *Journal of Clinical Investigation.* **120,** 2094-2108 (2010).

Holland , E.C., Sonenberg, N., Pandolfi, P.P., and Thomas, G. Signaling control of mRNA translation in cancer pathogenesis. *Oncogene.* **23,** 3138-3144 (2004).

Hoshino, R., Chatani, Y., Yamori, T., Tsuro, T., Oka, H., Yoshida, O., Shimada, Y., Ari-i, S., Wada, H., Fujimoto, J., and Kohno, M. Constitutive activation of the 41-/43-kDa mitogen-activated protein kinase signaling pathway in human tumours. *Oncogene.* **18,** 813-822 (1999).

Houben, R., Vetter-Kauczok, C.S., Ortmann, S., Rapp, U.R., Broecker, E.B., and Becker, J.C. Phospho-ERK staining is a poor indicator of the mutational status of BRAF and NRAS in human melanoma. *Journal of Investigative Dermatology.* **128,** 2003-2012 (2008).

Huang, D., Ding, Y., Luo, W.M., Bender, S., Qian, C.N., Kort, E., Zhang, Z.F., VandenBeldt, K., Duesbery, N.S., Rasau, J.H., and Teh, B.T. Inhibition of MAPK kinase signaling pathways suppressed renal cell carcinoma growth and angiogenesis in vivo. *Cancer Research.* **68(1),** 81-88 (2008).

Hudes, G.R. Targeting mTOR in renal cell carcinoma. *Cancer.* **115 (Suppl. 10),** 2313-2320 (2009).

Hulit, J., Suyama,K., Chung, S., Keren, R.,. Agiostratidou, G., Shan, W., and Dong, X. N-cadherin signaling potentiates mammary tumour metastasis via enhanced extracellular signal-regulated kinase activation. *Cancer Research.* **67,** 3106-3116 (2007).

Jemal, A., Siegel, R., Xu, J., and Ward, E. Cancer Statistics, 2010. *CA A Cancer Journal for Clinicians.* **60,** 277-300 (2010).

Kaelin, W.G. Treatment of kidney cancer: insights provided by the VHL tumour-suppressor protein. *Cancer.* **115(Suppl. 10),** 2262-2272 (2009).

Kalluri, R., and Weinberg, R. A. The basics of epithelial-mesenchymal transition. *Journal of Clinical Investigation.* **119(6),** 1420-1428 (2009).

Kang, Y., and Massague, J. Epithelial-mesenchymal transitions: twist in development and metastasis. *Cell.* **118,** 277-279 (2004).

Karp, G. Cell and Molecular Biology. 4th ed. John Wiley & Sons Inc: New Jersey. (2005).

Keller, E.T. Metastasis suppressor genes: a role for Raf kinase inhibitory protein (RKIP). *Anti-Cancer Drugs.* **15,** 663-669 (2004).

Keller, E.T., Fu, Z., and Brennan, M. The role of Raf kinase inhibitor protein (RKIP) in heath and disease. *Biochemical Pharmacology.* **68,** 1049-1053 (2004a).

Keller, E.T., Fu, Z., Yeung, K., and Brennan, M. Raf kinase inhibitor protein: a prostate cancer metastasis suppressor gene. *Cancer Letters.* **207,** 131-137 (2004b).

Keller, E.T., Fu, Z., and Brennan, M. The biology of a prostate cancer metastasis suppressor protein: raf kinase inhibitor protein. *Journal of Cellular Biochemistry.* **94,** 273-278 (2005).

Kim, H.J., and Kaelin, W.G. Role of VHL gene mutation in human cancer. *Journal of Clinical Oncology.* **22,** 4991-5004 (2004).

Kim, D.H., and Rossi, J.J. Strategies for silencing human disease using RNA interference. *Nature Reviews Genetics.* **8,** 173-184 (2007).

Kimura, M., Furukawa, T., Abe, T., Yatsuoka, T., Youssef, E.M., Yokoyama, T., Ouyang, H., Ohnishi, Y., Sunamura, M., Kobari, M., Matsuno,S., and Horii, A. Identification of two common regions of allelic loss in chromosome arm 12q in human pancreatic cancer. *Cancer Research.* **58,** 2456-2460 (1998).

Klumkowsky, M.W., and Savagner, P. Epithelial-mesenchymal transition. A cancer's researcher's conceptual friend and foe. *American Journal of Pathology.* **174,** 1588-1593 (2009).

Klysik, J., Theroux, S.J., Sedivy, J.M., Moffit, J.S. and Boekelheide, K. Signaling crossroads: the function of Raf kinase inhibitory protein in cancer, the central nervous system and reproduction. *Cellular Signalling.* **20,** 1-9 (2008).

Kolch, W. Coordinating ERK/MAPK signalling through scaffolds and inhibitors. *Nature Reviews Molecular Cell Biology.* **6,** 827-838 (2005).

Kondo, K., and Kaelin, W.G. Jr. The von Hippel-Lindau tumor suppressor gene. *Experimental Cell Research.* **264,** 117-125 (2001).

Krones-Herzig, A., Mittal, S., Yule, K., Liang, H., English, C., Urcis, R., Soni, T., Adamson E.D., and Mercola, D. Early growth response 1 acts as a tumour suppressor *in vivo* and *in vitro* via regulation of p53. *Cancer Research.* **65,** 5133-5143 (2005).

Leber, M.F., and Efferth, T. Molecular principles of cancer invasion and metastasis. *International Journal of Oncology.* **34,** 881-895 (2009).

Lee, H.C., Tian, B., Sedivy, J.M., Wands, J.R., and Kim, M. Loss of Raf kinase inhibitor protein promotes cell proliferation and migration of human hepatoma cells. *Gastroenterology.* **131,** 1208-1217 (2006).

Lee, J.M., Dedar, S., Kalluri, R., and Thompson, E.W. The epithelial-mesenchymal transition: new insights in signaling, development, and disease. *The Journal of Cell Biology.* **172(7),** 973-981 (2006).

Li, H.Z., Wang, Y., Gau, Y., Shao, J., Zhao, X.L., Deng, W.M., Liu, Y.X., Yang, J., and Yau, Z. Effects of Raf kinase inhibitor protein expression on metastasis and progression of human epithelial ovarian cancer. *Molecular Cancer Research.* **6,** 917-928 (2008).

Linehan, W.M. Identification of the genes of kidney cancer. *Cancer Biology and Therapy.* **5,** 696-699 (2006).

Linehan, W.M., Pinto, P.A., Srinivasan, R., Merino, M., Choyke, P., Choyke, L., Coleman, J., Toro, J., Glenn, G., Vocke, C., Zbar, B., Schmidt, L.S., Bottaro, D., and Neckers, L. Identification of the genes for kidney cancer: opportunity for disease-specific targeted therapeutics. *Clinical Cancer Research.* **13,** 671s-679s (2007).

Linehan, W.M., and Zbar, B. The genetic basis of cacner of the kidney. *The Journal of Urology.* **170,** 2163-2172 (2003).

Lopez-Beltran, A., Carrasco, J.C., Cheng, L., Scarpelli, M., Kirkali, Z., and Montironi, R. 2009 update on the classification of renal epithelial tumours in adults. *International Journal of Urology.* **16,** 432-443 (2009).

Lorenz, K., Lohse, M.J., and Quitterer U. Protein kinase C switches the Raf kinase inhibitor from Raf-1 to GRK-2. *Nature.* **426(6966),** 574-579 (2003).

Luu, H.H., Zagaja, G.P., Dubauskas, Z., Chen, S.L., Smith, R.C., Watabe, K., Ichikawa, Y., Ichikawa, T., Davis, E.M., Le Beau, M.M., and Rinker-Schaeffer, C.W. Identification of a novel metastasis-suppressor region on human chromosome 12. *Cancer Research.* **58,** 3561-3565 (1998).

Maher, E.R., and Kaelin, W.G. von Hippel-Lindau disease. *Medicine.* **76,** 381-391 (1997).

Mandell, J.W., Hussaini, I.M., Zecevic, M., Weber, M.J., VandenBerg, S.R., In situ visualization of intratumor growth factor signaling: immunohistochemical localization of activated ERK/MAP kinase in glial neoplasms. *American Journal of Pathology.* **153,** 1411-1423 (1998).

Mareel, M., Boterberg, T., Noe, V., Van Hoorde, L., Vermeulen, S., Bruyneel, E., and Bracke, M. E-cadherin/catenin/cytoskeleton complex: a regulator of cancer invasion. *Journal of Cellular Physiology.* **173,** 271-274 (1997).

Martinho, O., Gouveia, A., Silva, P., Pimenta, A., Reis, R.M., and Lopes, J.M. Loss of RKIP expression is associated with poor survival in GISTs. *Virchows Archiv.* **455,** 227-284 (2009).

Mendez, M.G., Kojima, S.I., and Goldman, R.D. Vimentin induces changes in cell shape, motility, and adhesion during the epithelial to mesenchymal transition. *The FASEB Journal.* **24,** 1838-1851 (2010).

Minoo, P., Zlobec, K., Baker, K., Tornillo, L., Terracciano, L., Jass, J.R., and Lugli, A. Loss of Raf-1 kinase inhibitor protein expression is associated with tumor progression and metastasis in colorectal cancer. *American Journal of Clinical Pathology.* **127,** 820-827 (2007).

Motzer, R.J., Bander, N.H., and Nanus, D.M. Renal cell carcinoma. *The New England Journal of Medicine.* **335(12),** 865-875 (1996).

Nelson E.C., Evans, C.P., and Lara, P.N. Renal cell carcinoma: Current status and emerging therapies. *Cancer Treatment Reviews.* **33,** 299-313 (2007).

Neumann, H.P., and Zbar, B. Renal cysts, renal cancer and von Hippel-Lindau disease. *Kidney International.* **51,** 16-26 (1997).

Nieman, M.T., Prudoff, R.S., Johnson, K.R., and Wheelock, M.J. N-cadherin promotes motility in human breast cancer cells regardless of their E-cadherin expression. *Journal of Cell Biology.* **147,** 631-644 (1999).

Odabaei, G., Chatterjee, D., Jazirehi, A.R., Goodglick, L., Yeung, K., and Bonavida, B. Raf-1 kinase inhibitor protein: structure, function, regulation of cell signaling and pivotal role in apoptosis. *Advances in Cancer Research.* **91,** 169-200 (2004).

Oka, H., Chatani, Y., Hoshino, R, Ogawa, O., Kakehi, Y., terachi, T., Okada, Y., Kawaichi, M., Kohno, M., and Yoshida, O. Constitutive Activation of mitogen-activated protein (MAP) kinases in human renal cell carcinoma. *Cancer Research.* **55,** 4182-4187 (1995).

Pandolfi, P.P. Aberrant mRNA translation in cancer pathogenesis: an old concept revisited come finally of age. *Oncogene.* **23,** 3134-3137 (2004).

Pantuck, A.J., Zisman, A., and Belldegrum, A.S. The changing natural history of renal cell carcinoma. *The Journal of Urology.* **166(5),** 1611-1623 (2001).

Park, S., Rath, O., Beach, S., Xiang, X., Kelly, S.M., Luo, Z., Kolch, W., and Yeung, K. Regulation of RKIP binding to the N-region of the Raf-1 kinase. *FEBS Letters.* **580,** 6405-6412 (2006).

Park, S., Yeung, M.L., Beach, S., Shields, J.M., and Yeung, K.C. RKIP downregulates B-Raf kinase activity in melanoma cancer cells. *Oncogene.* **24(21),** 3534-3540 (2005).

Rankin, E.B., Tomaszewski, J.E., and Haase, V.H. Renal cyst development in mice with conditional inactivation of the von Hippel-Lindau tumour suppressor. *Cancer Research.* **66,** 2576-2583 (2006).

Rath, O., Park, A., Tang, H., Banfield, M.J., Brady, R.L., Lee, Y.C., Dignam, J.D., Sedivy, J.M., Kolch, W., and Yeung, K. The RKIP (Raf-1 kinase inhibitory protein) conserved pocket binds to the phosphorylated N-region of Raf-1 and inhibits the Raf-1-mediated activated phosphorylation of MEK. *Cellular Signalling.* **20,** 935-941 (2008).

Razorenova, O.V., Finger, E.C., Colavitti, R., Chernikova, S.B., Boiko, A.D., Chan, C.K.F., Krieg, A., Bedogni, B., LaGory E., Weissman, I.L., Broome-Powell, M., and Giaccia, A.J. VHL loss in renal cell carcinoma leads to upregulation of CUB domain-containing protein 1 to stimulate PKCδ-driven migration. *PNAS.* **108,** 1931-1936 (2011).

Reddy, K.B., Nabha, S.M., and Atanaskova, N. Role of MAP kinase in tumour progression and invasion. *Cancer Metastasis Review.* **22,** 395-403 (2003).

Rini, B.I., Campbell, S.C. and Escudier, B. Renal cell carcinoma. *Lancet.* **373,** 1119-1132 (2009).

Ruan, K., Bao, S., and Ouyang, G. The multifaceted role of periostin in tumourigenesis. *Cellular and Molecular Life Sciences.* **66,** 2219-2230 (2009).

Salh, B., Marotta, A., Matthewson, C., Ahluwalia, M., Flint, J., Owen, D., and Pelech, S. Investigation of the Mek-MAP kinase-Rsk pathway in human breast cancer. *Anticancer Research.* **19,** 731-740 (1999).

Schuierer, M.M., Bataille, F., Hagan, S., Kolch, W., and Bosserhoff, A.K. Reductionin Raf kinase inhibitor protein expression is associated with increased ras-extracellular signal-regulated kinase signalling in melanoma cell lines. *Cancer Research.* **64,** 5186-5192 (2004).

Schuierer, M.M., Bataille, F., Weiss, T.S., Hellerbrand, C., and Bosserhoff, A.K. Raf kinase inhibitor protein is downregulated in hepatocellular carcinoma. *Oncology Reports.* **16(3),** 451-456 (2006).

Seidel, B., Braeg, S., Adler, G., Wedlich, D., and Menke, A. E- and N-cadherin differ with respect to their associated $p120^{ctn}$ isoforms and their ability to suppress invasive growth in pancreatic cancer cells. *Oncogene.* **23,** 5532-5542 (2004).

Shuin, T., Kondo, K., Torigoe, S., Kishida, T., Kubota, Y., Hosaka, M., Nagashima, Y., Kitamra, H., Latif, F., Zbar, B., Lerman, M.I., and Yao, M. Frequent somatic mutations and loss of heterozygosity of the von Hippel-lindau tumour suppressor gene in primary human renal cell carcinomas. *Cancer Research.* **54,** 2852-2855 (1994).

Sivaraman, V.S., Wang, H., Nuovo, G.J., and Malbon, C.C. Hyperexpression of mitogen-activated protein kinase in human breast cancer. *Journal of Clinical Investigation.* **99,** 1478-1483 (1997).

Sloan, K.A., Marquez, H.A., Li, J., Cao, Y., Hinds, A., O`Hara, C.J., Kathuria, S., Ramirez, M.I., Williams, M.C. and Kathuria, H. Increased PEA3/E1AF and decreased Net/Elk-3, both ETS proteins, characterize human NSCLC progression and regulate caveolin-1 transcription in Calu-1 and NCI-H23 NSCLC cell lines. *Carcinogenesis.* **30,** 1433-1442 (2009).

Sommers, C.L., Thompson, E.W., Torri, J.A., Kemler, R., Gelmann, E.P., and Byers, S.W. Cell adhesion molecule uvomorulin expression in human breast cancer cell lines: relationship to morphology and invasive capacities. *Cell Growth and Differentiation.* **2,** 365-372 (1991).

Stamenkovic, I. Matrix metalloproteinases in tumor invasion and metastasis. *Seminars in Cancer Biology.* **10,** 415-433 (2000).

Steeg, P.S. Tumour metastasis: mechanistic insights and clinical challenges. *Nature Medicine.* **12(8),** 895-904 (2006).

Tang, H., Park, S., Sun, S.C., Trumbly, R., Ren, G., Tsung, E., and Yeung, K.C. RKIP inhibits NF-κB in cancer cells by regulating upstream signalling components of the IκB kinase complex. *FEBS Letters.* **584,** 662-668 (2010).

Tani, T., Laitinen, L., Kangas, L., Lehto, V.P., and Virtanen, I. Expression of E- and N-cadherin in renal cell carcinomas, in renal cell carcinoma cell lines *in vitro* and in their xenografts. *International Journal of Cancer.* **64,** 407-414 (1995).

Theroux, S., Pereira, M., Casten, K.S., Burwell, R.D., Yeung, K.C., Sedivy, J.M., and Klysik, J. Raf kinase inhibitory protein knockout mice: expression in the brain and olfaction deficit. *Brain Research Bulletin.* **71,** 559-576 (2007).

Thiery, J.P. Epithelial-Mesenchymal transitions in tumour progression. *Nature Reviews Cancer.* **2,** 442-454 (2002).

Thijssen,V., Brandwijk, R., Dings, R., and Griffioen, A. Angiogenesis gene expression profiling in xenograft models to study cellular interactions. *Experimental Cell Research.* **299,** 286-293 (2004).

Thompson Coon, J.S., Liu, A., Hoyle, M., Rogers, G., Green, C., Moxham, T., Welch, K., and Stein, K. Sunitinib and bevacizumab for first-line treatment of metastatic renal cell carcinoma: a systematic review and indirect comparison of clinical effectiveness. *British Journal of Cancer.* **101,** 238-243 (2009).

Trakul, N., Menard, R.E., Schades, G.R., Qian, Z., and Rosner, M.R. Raf kinase inhibitory protein regulates Raf-1 but not B-Raf kinase activation. *The Journal of Biological Chemistry.* **280(26),** 24931-24940 (2005).

Trakul, N., and Rosner, M.R. Modulation of the MAP kinase signaling cascade by Raf kinase inhibitory protein. *Cell Research.* **15(1),** 19-23 (2005).

Tran, N.L., Nagle, R.B., Cress, A.E., and Heimark, R.L. N-cadherin expression in human prostate carcinoma cell lines. An epithelial-mesenchymal transformation mediating adhesion with stromal cells. *American Journal of Pathology.* **155,** 787-798 (1999).

Ulazzi, L., Sabbioni, S., Miotto, E., Veronese, A., Angusti, A., Gafa, R., Manfredini, S., Farinati, F., Sasaki, T., Laza, G., and Negrini, M. Nidogen 1 and 2 gene promoters are aberrantly methylated in human gastrointestinal cancer. *Molecular Cancer.* **6,** 17-25 (2007).

Vuoriluoto, K., Haugen, H., Kiviluoto, S., Mpindi, J.P., Nevo, J., Gjerdrum, C., Tiron, C., Lorens, J.B., and Ivaska, J. Vimentin regulated EMT induction by Slug and oncogenic H-Ras and migration by governing Axl expression in breast cancer. *Oncogene.* **30,** 1436-1448 (2011).

Walther, M.M., Lubensky, I.A., Venzon, D., Zbar, B., and Linehan, W.M. Prevalence of microscopic lesions in grossly normal renal parenchyma from patients with von Hippel-Lindau disease, sporadic renal cell carcinoma and no renal disease: clinical implications. *Journal of Urology.* **154,** 2010-2014 (1995).

Wang, Y., Gao, Y., Shao, J., Zhao, X.L., Deng, W.M., Liu, Y.X., Yang, J., and Yao, Z. Effects of raf kinase inhibitor protein expression on metastasis and progression of human epithelial ovarian cancer. *Molecular Cancer Research.* **6,** 917-928 (2008).

Williams, S.J., McGuckin, M.A., Gotley, D.C., Eyre, H.J., Sutherland, G.R., and Antalis T.M. Two novel mucin genes down-regulated in colorectal cancer identified by differential display. *Cancer Research.* **59,** 4083-4089 (1999).

Weinberg, R.A. The Biology of Cancer. Garland Science: New York. (2007).

Wu, K., and Bonavida, B. The activated NF-kappaB-snail-RKIP circuitry in cancer regulates both the metastatic cascade and resistance to apoptosis by cytotoxic drugs. *Critical Reviews in Immunology.* **29,** 241-254 (2009).

Yang, J.C., Haworth, L., Sherry, R.M., Hwu, P., Schwartzentruber, D.J., Topalian, S.L., Steinberg, S.M., Chen, H.X., and Rosenberg, S.A. A randomized trial of bevacizumab, an anti-vascular endothelial growth factor antibody, for metastatic renal cancer. *The New England Journal of Medicine.* **349,** 427-434 (2003).

Yeung, K., Jonosch, P., McFerran, B., Rose D.W., Mischak, H., Sedivy, J.M., and Kolch, W. Mechanism of suppression of the Raf/MEK/Extracellular signal-regulated kinase pathway by the Raf kinase inhibitor protein. *Molecular and Cellular Biology.* **20(9),** 3079-3085 (2000).

Yeung, K., Seitz, T., Li, S., Janosch, P., McFerran, B., Kaiser, C., Fee, F., Katsnakis, K.D., Rose, D.W., Mischak, H., Sedivy, J.M., and Kolch, W. Suppression of Raf-1 kinase activity and MAP kinase signalling by RKIP. *Nature.* **401,** 173-177 (1999).

Yeung, K.C., Rose, D.W., Dhillon, A.S., Yaros, D., Gustafsson, M., Chatterjee, D., McHerran, B., Wyche, J., Kolch, W., and Sedivy, J.M. Raf kinase inhibitor protein interacts with NF-κB-inducing kinase and TAK1 and inhibits NF-κB activation. *Molecular and Cellular Biology.* **21,** 7207-7217 (2001).

Yilmaz, M., and Christofori, G. EMT, the cytoskeleton, and cancer cell invasion. *Cancer Metastasis Review.* **28,** 15-33 (2009).

Yoon, S.O., Park, S.J., Yun, C.H., and Chung, A.S. Roles of matrix metalloproteinases in tumour metastasis and angiogenesis. *Journal of Biochemistry and Molecular Biology.* **36,** 128-137 (2003).

Zaravinos, A., Bizakis, J., and Spandidoe, D.A. RKIP and BRAF aberrations in human nasal polyps and the adjacent turbinate mucosae. *Cancer Letters.* **264,** 288-298 (2008).

Zebisch, A., Haller, M., Hiden, K., Goebal, T., Hoefler, G., Troppmair, J., and Sill, H. Loss of RAF kinase inhibitor protein is a somatic even in the pathogenesis of therapy-related acute myeloid leukemias with C-RAF germline mutations. *Leukemia.* **23,** 1049-1052 (2009).

Zhang, L., Fu, Z., Binkley, C., Giordano, T., Burant, C.F., Logsdon, C.D., and Simeone, D.M. Raf kinase inhibitory protein inhibits β-cell proliferation. *Surgery.* **136(3),** 708-715 (2004).

Zeng, L., Imamoto, A., and Rosner, M.R. Raf kinase inhibitory protein (RKIP): A physiological regulator ad future therapeutic target. *Expert Opinion on Therapeutic Targets.* **12(10),** 1275-1287 (2008).

Zlobec, I., Baker, K., Minoo, P., Jass, J.R., Terracciano, L., and Lugli, A. Node-negative colorectal cancer at high risk of distant metastasis identified by combined analysis of lymph node status, vascular invasion and Raf-1 kinase inhibitor protein expression. *Clinical Cancer Research.* **14,** 143-148 (2008a).

Zlobec, I., Baker, K., Terracciano, L., Peter, S., Degen, L., Beglinger, C., and Lugli, A. Two-marker protein profile predicts poor prognosis in patients with early rectal cancer. *British Journal of Cancer.* **99,** 1712-1717 (2008b).